ACRIDINE ORANGE FLUORESCENCE MICROSPECTROPHOTOMETRY IN THE ANALYSIS OF NUCLEIC ACIDS IN DIFFERENT MICROENVIRONMENTS AND IN SINGLE NEURONS

Thesis for the Degree of M. S. MICHIGAN STATE UNIVERSITY ROBERT GENE CANADA 1976



This is to certify that the

thesis entitled
ACRIDINE ORANGE FLUORESCENCE
MICROSPECTROPHOTOMETRY IN THE ANALYSIS OF
NUCLEIC ACIDS IN DIFFERENT MICROENVIRONMENTS AND
IN SINGLE NEURONS

presented by

ROBERT GENE CANADA

has been accepted towards fulfillment of the requirements for

M. S. degree in BIOPHYSICS

Major professor

Date 15 MARCH 1976

O-7639

ABSTRACT

ACRIDINE ORANGE FLUORESCENCE MICROSPECTROPHOTOMETRY IN THE ANALYSIS OF NUCLEIC ACIDS IN DIFFERENT MICROENVIRONMENTS AND IN SINGLE NEURONS

Bv

Robert Gene Canada

The application of biophysical cytochemistry to single neurons in culture represents a model system whereby inferences, anent the structure and functions of a biopolymer engaged in neuronal interactions, may be devised by studying the interactions of a fluorescent molecular probe and the macromolecule under question. A large segment of this investigation was concerned with the binding and structure characterization of acridine orange--nucleic acid complexes embedded in gelatin microdroplets, exposed to various microenvironmental conditions. This investigation affirms that acridine orange (AO) has the same binding mode and a specific affinity for each nucleic acid (NA) conformation investigated (rRNA, DNA, Poly U, and denatured rRNA), where each AO-NA complex has a green fluorescence maximum at 536 nm. and a prominent shoulder towards the longer wavelengths at 604 nm. The alteration of the NA microenvironment altered the binding of AO to the NA, whereby increasing the AO-NA interaction time, NA denaturation, pH, and dye concentration increased the binding of AO to the NA. In addition, the binding of AO to the NA was enhanced in the presence of NaCl. More importantly, there was a

linearity between the AO-NA emission and the amount of NA available for binding an unchanging AO concentration. Fluorescence coefficients for specific staining conditions were procured and employed in the calculation of the NA content inside the soma of single neurons identified in dissociated cell cultures of the rat brain. The NA content per neuron was found to depend more upon neuronal type and maturity than size. The binding of AO to the NA in the neurons and microdroplets is predominantly in the monomer form with a small degree of aggregation.

ACRIDINE ORANGE FLUORESCENCE MICROSPECTROPHOTOMETRY IN THE ANALYSIS OF NUCLEIC ACIDS IN DIFFERENT MICROENVIRONMENTS AND IN SINGLE NEURONS

Ву

Robert Gene Canada

A THESIS

Submitted to
Michigan State University
in partial fulfillment of the requirements
for the degree of

MASTER OF SCIENCE

Department of Biophysics

1976

Copyright by ROBERT GENE CANADA 1976

DEDICATION

To Donna

I thank whatever God there be,
For the Love, Peace, and Happiness You have given Me.

ACKNOWLEDGMENTS

I wish to communicate my profound appreciation to: Dr. John I. Johnson, Jr., for his services, advice and support as chairman of my Masters Thesis research committee and my primary adviser; Dr. Eloise Kuntz, who gave me my start in Biophysics and who acquainted me with quantitative scientific techniques of superior quality and served as a committee member. I gratefully extend my special thanks to Dr. Richard W. Wagner who introduced me to his dissociated cell culture techniques and who provided assistance and encouragement throughout the course of this work; Mrs. Donna Maria Trotter Canada who supplied the necessary ingredients to make my research a success.

This research was supported by funds from NIH Research Grants No. NSO5982, NIH Training Grant No. GM-01422, the College of Osteopathic Medicine, the College of Natural Science, and the College of Human Medicine of Michigan State University.

TABLE OF CONTENTS

	Pa	ge
List of 1	Tables	vi
List of F	Figures	ii
I. INTRO	DDUCTION	1
B. 1 C. 7	Biophysical Cytochemistry	3
A	Activities	9
D. N	Neuron Cultures	16
II. EXPE	ERIMENTAL DETAILS	23
A. M		23
B. M	Methods	24
_		24 26
C. I	Instrumentation	29
III. RES	SULTS AND DISCUSSION	33
A. I	Introduction	33
B. M	Microdroplet Analysis	37
1	. The fluorescence changes of AO-NA complexes as a	
2	2. The fluorescence changes of AO-NA complexes as a	39
3	function of acridine orange staining time	45
	function of acridine orange staining solution pH .	50
4	I. The fluorescence intensity changes of AO-NA com- plexes as a function of NaCl content	58
5	The fluorescence intensities of AO-rRNA complexes at various microdroplet forming solution	၁၀
6		64
_	gelatin-protein complexes during continuous	65

																											Page
		7.	con	fli mple: ntrai	xes tio	a: n,	s a aı	a 1 nd	fui tl	nc he	tio q	on uai	of nti	f 1 ita	the ati	i ve	nuc	ale det	eio ter	m	aci ina	id ati	i OI		•		
				/iro																				•	•		69
	C.	Neur	ron	Ana	lys	is	•	•	•	•	•	•	•	•	•	•	•	•	•	•	•	•	•	•	•	•	79
IV.	CO	NCLUS	OIS	IS		•	•	•	•	•	•			•	•	•	•	•	•	•	•	•	•	•	•	•	125
LIST	OF	REFE	EREN	ICES													•	•									134

LIST OF TABLES

Table		Page
1	The relative fluorescence intensity of AO-NA complexes at 536 nm. and 604 nm	36
2	The average relative fluorescence intensities of AO-3% purified pigskin only and AO-NA complexes in 3% pf. pgsk. at 536 nm. and 604 nm. for different acridine orange staining concentrations (expressed in molarities), pH 4.1, staining time 15 minutes	41
3	The average relative fluorescence intensities of AO-NA complexes in 3% pf. pgsk. at 536 nm. and 604 nm. for different staining times (expressed in minutes), acridine orange staining concentration, 5 x 10-5M, pH 4.1	46
4	The average relative fluorescence intensities of 1.0 pg. DNA-AO and 1.0 pg. rRNA-AO complexes in 3% pf. pgsk., and gelatin protein-AO complexes of 3% purified pigskin only, at 536 nm. and 604 nm., for different acridine orange staining solution pH, AO staining concentration 5 x 10^{-5} M, staining time 30 mins	51
5	The average relative fluorescence intensities of 0.5 pg. DNA-AO complexes and 1.0 pg. rRNA-AO complexes in 3% pf. pgsk., at 536 nm. and 604 nm., for various NaCl contents expressed in picograms, AO staining concentration 5 x 10^{-5} M, staining time 30 mins., pH 4.1	60
6	The average relative fluorescence intensities of 1.0 pg. rRNA-AO complexes in 3% pf. pgsk., at 536 nm. and 604 nm., for various microdroplet forming solution temperatures, AO staining concentration $5 \times 10^{-5} M$, at pH 4.1, staining time 30 mins	65
7	The average relative fluorescence intensities of AO bound to DNA or rRNA, at 536 nm. and 604 nm., in 3% pf. pgsk. for various DNA and rRNA concentrations, AO staining concentration 5 x 10 ⁻⁵ M, staining time 30 minutes, pH 4.1	70

Table	Page
8	The nucleic acid content of 3% purified pigskin microdroplets, derived from the sum of the embedded pg. rRNA + 4.63 (pg. DNA) on the left side of equation (4), is compared to its value on the right side of the equation, obtained from [(log F_{536} - log b)/f.c. $_{536}$]. The fluorescence spectrum and intensity, at 536 nm., of each microdroplet was obtained with the microspectrophotometer while irradiating at 400 nm. The average relative fluorescence intensity of 3% pf. pgsk. microdroplets, containing no NA, at 536 nm. is equal to 54.5. The microdroplets were stained for 30 mins., with 5 x 10^{-5} M AO, at pH 4.1
9	The R + γ D content in the cell bodies of Canada, II, and Canada, bipolar neurons, at 67 da. and 99 da. old, as determined microspectrophotometrically using equation (4), R + γ D = (log F ₅₃₆ - log b)/ f.c.rgNA , where γ is equal to 4.63 and f.c.rgNA is equal to 0.272. Cells #1 through 7 were stained with 1 x 10 ⁻⁴ M AO, and neurons #8 through 12 were stained with 5 x 10 ⁻⁵ M AO for 30 mins. at a pH 4.1. All of the cells were taken from the cerebral cortex of a 3 da. old albino female rat and maintained in dissociated cell cultures. Neurons #8 through 12 are from the somatic sensory cortex I and II. 93

LIST OF FIGURES

Figure		Page
1	Absorption spectra of acridine orange in aqueous solution. Solvent: citrate-phosphate buffer, pH 6.0, 20°C (from Zanker, 1952)	6
2	Fluorescence spectra of acridine orange in aqueous solution. Solvent: citrate-phosphate buffer, pH 6.0, 20°C (from Zanker, 1952)	6
3	Acridine orange molecular configuration and schematic molecular configurations of AO-NA complexes in the monomer form (AO to nucleotide phosphorus = 1:6) and aggregate form (AO to nucleotide phosphorus = 1:1.5)	7
4	Diagram of the principle of the LEITZ fluorescence vertical illuminator	31
5	Diagram of the microspectrophotometer	32
6	The normalized fluorescence spectra of AO molecules bound to different NA conformations and gelatin proteins, AO staining concentration 5×10^{-5} M, staining time 30 mins., pH 4.1	35
7	The average relative fluorescence intensities of AO-3% purified pigskin only and AO-NA complexes in 3% pf. pgsk. at 536 nm. and 604 nm. for different acridine orange staining concentrations (expressed in molarities), pH 4.1, staining time 15 minutes	40
8	The degree of aggregation of AO onto 1.0 pg. DNA or rRNA in 3% pf. pgsk. for different acridine orange staining concentrations (expressed in molarities), pH 4.1, staining time 15 minutes	43
9	The average relative fluorescence intensities of AO-NA complexes in 3% pf. pgsk. at 536 nm. and 604 nm. for different staining times, AO staining concentration $5 \times 10^{-5} M$, pH 4.1	47

Figure		Page
10	The average relative fluorescence intensities of 1.0 pg. DNA-AO and 1.0 pg. rRNA-AO complexes in 3% pf. pgsk., and gelatin protein-AO complexes of 3% pf. pgsk. only, at 536 nm. and 604 nm., for different acridine orange staining solution pH, AO staining concentration 5 x 10 ⁻⁵ M, staining time 30 mins	52
11	The degree of aggregation of AO onto 1.0 pg. DNA or rRNA in 3% pf. pgsk. for different acridine orange staining solution pH, AO staining concentrations 5 x 10^{-5} M, staining time 30 mins	56
12	The average relative fluorescence intensities of 0.5 pg. DNA-AO and 1.0 pg. rRNA-AO complexes in 3% pf. pgsk. and gelatin protein-AO complexes of 3% pf. pgsk. only, at 536 nm. and 604 nm., for various NaCl contents (expressed in picograms), AO staining concentration 5 x 10 ⁻⁵ M, staining time 30 mins., pH 4.1	59
13	The degree of aggregation of AO onto 0.5 pg. DNA or 1.0 pg. rRNA in 3% pf. pgsk. for various NaCl contents, AO staining concentration 5 x 10^{-5} M, staining time 30 mins., pH 4.1	62
14	Fluorescence decay of AO-NA complexes at 536 nm. and 604 nm., as function of the irradiation time, AO concentration 5 x 10^{-5} M, pH 4.1, staining time 30 mins., excitation wavelength 400 nm	67
15	The average relative fluorescence intensities of AO bound to DNA or rRNA, at 536 nm. and 604 nm., in 3% pf. pgsk. for various DNA or rRNA concentrations, AO staining concentration 5 x 10^{-5} M, staining time 30 mins., pH 4.1	71
16	The average relative fluorescence intensities of AO bound to rRNA, at 536 nm. and 604 nm., in 3% pf. pgsk. for various rRNA concentrations, AO staining concentration 5 x 10^{-5} M, staining time 30 mins., pH 4.1	74
17	The degree of aggregation of AO onto DNA or rRNA in 3% pf. pgsk. for different NA concentrations, AO staining concentrations 5 x 10 ⁻⁵ M, staining time 30 mins., pH 4.1	76

Figure		Page
18	A photomicrograph of a living brain cell found in a dissociated monolayer cell culture, taken from the somatic sensory cortex I and II, of a 3 days old female albino rat. The cell was maintained 23 days in culture; at the time of photo, it has a diamond shape with a length of 13- microns and a width of 96 microns. The nucleus of the cell is centrally located, having an oval shape 30 microns long and 18 microns wide, with several nucleoli. This cell has been designated the Canada, Type I neuron. The scale for the photomicrograph is 14.4 microns per centimeter	82
19	A photomicrograph of a living Canada, bipolar neuron (right of center) found in a dissociated monolayer cell culture, taken from the somatic sensory cortex I and II, of a 3 days old female albino rat. The cell was maintained 32 days in culture. The cell body is spherical, with a length of 26 microns and a width of 17 microns. Note the fibrous astrocyte above the center of the photomicrograph. The Canada, bipolar neuron is making a contact with a Canada, Type II neuron (bottom of center). The scale for the photomicrograph is 14.4 microns per centimeter	84
20	A photomicrograph of a Canada, Type II neuron found in a dissociated monolayer cell culture, taken from the brain of a 3 days old female albino rat. The neuron was maintained 96 days in culture, stained with 1 x 10 ⁻⁴ M acridine orange, at 22°C, for 30 minutes, at a pH of 4.1, and irradiated with 400 nm. light. The cytoplasm of the neuron is full of orange granules and the nucleus has a yellow-orange color, indicating that under these conditions the degree of aggregation of AO onto the NA macromolecules in the neuroplasm is very high and greater than that for the NA macromolecules in the neucleoplasm. The average soma area of the Canada, Type II neurons found in this culture was 179 sq. microns. Note that the processes of the cell in the bottom right corner appears to be making contacts with the soma and processes of the Canada, Type II neuron; the cell has an orange cytoplasm with a yellow-orange nucleus and its ratio of the nucleus to soma areas is greater than that for the Canada, Type II neuron	85

Figure		Page
21	A photomicrograph of two Canada, bipolar neurons, found in a dissociated monolayer cell culture, taken from the brain of a 3 days old female albino rat. The cells were maintained 96 days in culture, stained with 1 x 10 ⁻⁴ M acridine orange at 22°C, for 30 minutes at a pH of 4.1, and irradiated with 400 nm. light. The average area of their somas is 112 sq. microns, having two processes at opposite poles, with a bifurcation in one of the processes. Both of their nuclei are large and round, taking up most of the soma while stained a yellow-orange color. Their cytoplasm is orange in color. One of the Canada, bipolar neurons, with its bifurcated process, is making contact with a process of the other neuron	86
22	A photomicrograph of living fibrous astrocytes during redifferentiation. The cells were maintained 23 days in a dissociated monolayer cell culture, and were taken from the somatic sensory cortex, I and II, of a 3 days old female albino rat. As it happens with cells in brain sections, these cells in culture may be confused with neurons	88
23	A photomicrograph of three living neurons redifferentiating, the cells were taken from the somatic sensory cortex, I and II, of a 3 days old female albino rat. They were grown 23 days in a dissociated monolayer cell culture. Note that there is a soma-somatic contact between two of the neurons. The nucleus of each cell conforms with the general shape of the cell body, having one or two nucleoli. The cytoplasm of each cell is dense with Nissl bodies. The cells in the surrounding environment are glia or connective tissue	90
24	A photomicrograph of a single Canada, bipolar neuron found in the same culture and subjected to the same conditions as those in Figure 21. The average area of the soma is 112 sq. microns. The other large oval-shaped yellow-green objects are the nuclei of glia cells. Note the local accumulation of dye molecules at the orange thickenings in the bifurcated process, before and at the bifurcation, due to an increased aggregation of AO	95

Figure		Page
25	A photomicrograph of a Canada, bipolar neuron found in a dissociated monolayer cell culture, taken from the brain of a 3 days old female albino rat. The cell was maintained 96 days in culture, stained with 1 x 10 ⁻⁴ M acridine orange, at 22°C, for 30 minutes at a pH of 4.1, and irradiated with 400 nm. light. The average area of the soma is 112 sq. microns, having two processes at opposite poles, with a bifurcation in one of the processes. Note that the neuron at the bottom of the photomicrograph is sending its process towards the bifurcated process of the Canada, bipolar neuron	96
26	These two cells are Canada, Type II neurons. Canada, Type II neurons occur in polymorphic form, with 3 to 4 processes, in dissociated monolayer cell cultures of 3 days old female albino rat brains. Note that there is one contact between the two neurons and a contact with a common body. The cells were maintained 96 days in culture, stained with 1 x 10 ⁻⁴ M acridine orange, at 22°C for 30 minutes at pH 4.1. The photomicrograph was taken while exciting the cell with 400 nm. light. The average area of their soma is 179 sq. microns. The cytoplasm is stained orange. The yellow-orange nucleus is usually round or oval in shape, comprising about hal the area of their somas	
27	A Canada, Type II neuron, in upper section, found in the same culture and subjected to the same conditions as those in Figure 26. Notice the extensive network of fibers between this cell and the cell in the lower section. Two of the processes of the Canada, Type II neuron are making several contacts with the processes of other cells	98
28	The [rRNA + $\gamma(DNA)$] content, in picograms, per neuronal type for different neuronal ages	100
29	The [rRNA + γ (DNA)] content, in picograms, per neuronal age for different soma areas of the neurons	101
30	Fthidium Ryamida	102

I. INTRODUCTION

In recent years neuroscientists have gained valuable information anent the structure and function of macromolecules involved in neuronal systems during behavioral responses. However, this information is inadequate to fully understand the molecular interactions between the central nervous system and the mind. Our knowledge of molecular mechanisms for behavior can be characterized as being in the infant phase. This suggests that neuroscientists are confronted with many challenging problems that require a variety of innovative and incisive techniques for their solution. An application of biophysical cytochemistry to single neurons in culture is one method that may provide salient answers concerning the molecular events engaged in neuron to neuron interactions.

A. Biophysical Cytochemistry

In 1972, Seymour S. West and Andrew E. Lorincz [West and Lorincz, 1973] introduced the term "biophysical cytochemistry" to the conference on "Quantitative Fluorescence Techniques as Applied to Cell Biology."

The term suggested the application of biophysical techniques and theories to cytology: in particular, the use of fluorescent molecular probes as cytochemical tools to study the behavior of complex biopolymers. Fluorescent molecular probes are small planar dye molecules, with emission properties that respond to alterations within their near and distant environment. Fluorescent probes bind to unique locations on biological macromolecules without appreciably disturbing those features of the macromolecule desired for investigation [Stryer, 1968]. Inferences

about the structure and function of the macromolecule can be formulated by studying behavioral variations of the bound probe. This reduces the problem of investigating a complex macromolecule to a simple dye molecule. Consequently, the extent to which we understand the behavior of biological macromolecules will depend upon our knowledge of the dye, macromolecule, and dye-macromolecule interations.

Fluorescence microspectrophotometry is an invaluable technique for applying quantitative cytochemistry to cellular components and their functions. It allows for the investigation of biopolymers within individual cells by fluorescent molecular probes. Acridine orange (AO) is a fluorescent probe used in microspectrophotometry for analysis of various intracellular macromolecules. Because of its high quantum efficiency and metachromasy, Rigler [1966] used acridine orange to study the nucleic acids and nucleoproteins in single cells from fixed microscopic preparations. He found that the orthochromatic green fluorescence is due to AO binding to helical molecular configurations in a monomer molecular form (having a low AO content), and the metachromatic red fluorescence is the result of the dye binding to random coil molecular configurations in an associated molecular fashion (having a high AO content). West [1969, 1973] utilized acridine orange in television fluorescence microspectrophotometry to examine the nucleic acids and mucopolysaccharides in living cells. He related the emission properties of the dye-biopolymer complex to the intracellular dye content within the cell. A low intracellular dye content produced a green fluorescence with an emission maximum between 530-540 nm. A high intracellular dye content elicited a red fluorescence with a long wavelength emission peak at 690 nm. He also noted that as the intracellular

		,
		1
		1
		:
		Ì
		{
		ļ
		!
		1
		1
		1
		İ
)
		1
		1
		,
		i
		1
		1
·		1
		!
		1
		1
		!
		,
)
		:

dye content increased, the fluorescence of the cells cytoplasm progressively changed from green to yellow, yellow to orange, and orange to red, with each color depending upon the present intracellular dye content.

The application, by Rigler [1966] and West [1969, 1973], of acridine orange fluorescence microspectrophotometry to nucleic acids in single cells successfully demonstrated its utility for fixed and living microscopic preparations. This allows for a possible direct comparison of in situ results with those obtained from in vitro model systems. Neuroscientists should note that most biophysical cytochemistry is performed on non-neural material, such as leukocytes, lymphocytes, bacteriophages, spermatozoa or fibroblasts. A beginning researcher in this area should acquaint himself with the techniques for fixed nervous material before attempting living tissue. This will enable him to conquer the many difficulties in using living nervous tissue. As an example, under certain experimental conditions acridine orange can be used as a vital stain for nervous tissue [Zieger and Harders. 1951], and under other experimental conditions it becomes a neurotoxin [West, 1969]. Learning the techniques for fixed single neurons will provide the novice with enough knowledge to overcome the basic problems involved in fluorescence microspectrophotometry in conjunction with dissociated neurons in culture.

B. The Metachromasy of Acridine Orange

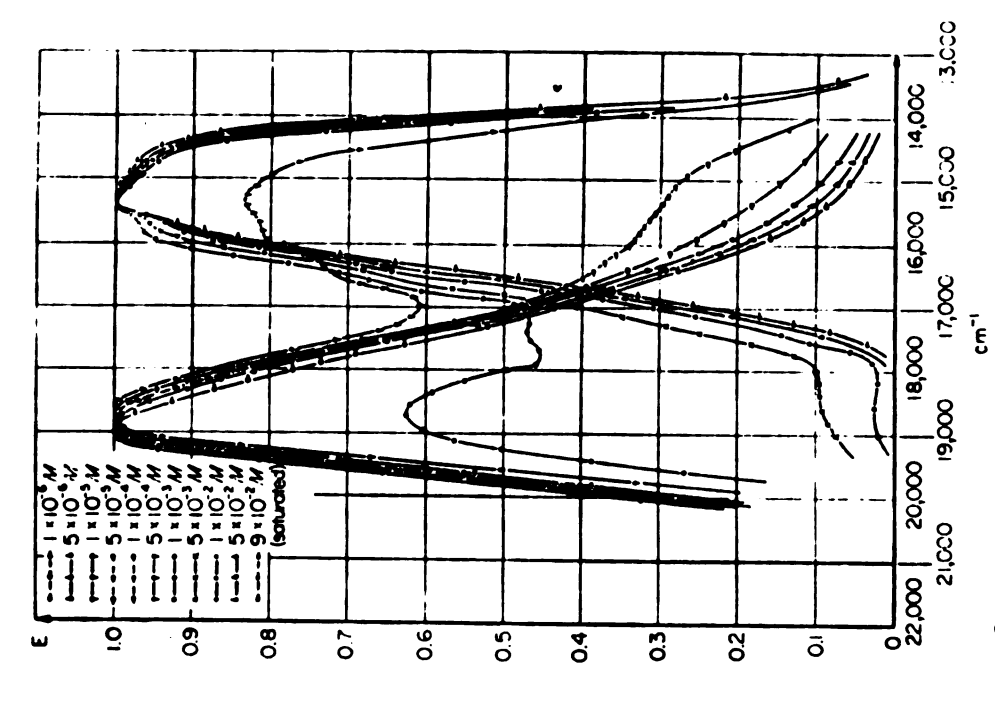
Acridine orange has been established as a fluorescent dye for vital staining of nervous tissue and vital studies on the function of the kidney and liver [West, 1969]. The fluorescence colors of cells stained with AO is different from the fluorescence color of the dye in dilute solution. Further, the various intracellular structures themselves fluoresce with different colors when stained with acridine orange.

Ehrlich [1879; West, 1969] termed this effect "metachromasy" and the color that was different from the dye in dilute solution "metachromatic." The wavelength shift (change in color) produced by a metachromatic dye is due to aggregation of the dye molecules. This association results in the dye's deviation from Beer's law [West, 1969].

Zanker [1952] provided the first explanation of the metachromatic behavior of acridine orange in aqueous solutions. He related the metachromatic shifts of the absorption and emission spectra towards lower and higher wavelengths, respectively, to the increased association of the dye molecules at increasing dye concentrations. At low concentrations, acridine orange is a monomer with an absorption maximum of 490 nm. and a fluorescence peak at 535 nm.. AO is a polymer at high concentrations with an absorption peak at 455 nm. and a fluorescence maximum at 660 nm. The absorption peak of the polymer shifts with dilution, however the absorption maximum for monomer AO does not change. There were only slight changes in maxima for the corresponding fluorescence spectra. Zanker [1952b, 1959; Rigler, 1966] proposed that the long wavelength absorption band of 490 nm. was caused by electronic transitions from the zero vibrational level of the ground state to the zero vibrational level of the excited electronic state (0-0 transition band). This absorption band elicits the short wavelength fluorescence peak at 535 nm.. On the other hand, the electronic transitions for the AO polymer is slightly different. The short wavelength absorption band of 455 nm. was interpreted to be due to electronic transitions from the zero vibrational level of the ground state to the first or second vibrational level of the excited electronic state (0— 1 and 0—2 transition bands), yielding the long wavelength fluorescence peak at 660 nm.. The short

and long wavelength fluorescence bands are the result of electronic transitions from the zero vibrational level of the excited electronic state to the zero, first and second vibrational levels of the ground state. Zanker [1952; West, 1969] suggested a stacked-coin model for the structural configuration of the acridine orange polymer. The absorption and fluorescence spectra from Zanker's investigation are shown in Figures 1 and 2; the wavelengths are expressed in wave numbers.

A number of investigators have studied the metachromatic behavior of acridine orange in solution with nucleic acids (NA), [Bradley and Wolf, 1960; Loeser et al, 1969; West, 1969; Rigler, 1966]. They found that two distinct molecular complexes are formed when AO binds to NA in solution. The first complex, relatively stable, is formed at low dye-to-nucleotide ratios, absorbing at 502 nm. and emitting at 540 nm... The absorption and fluorescence spectral characteristics of this complex resemble those of the monomer dye alone at low concentrations in aqueous solutions. A second, less stable complex is formed at high dye-to-nucleotide ratios, with spectral characteristics similar to that of the polymer dye alone in solution, absorbing at 465 nm. and emitting at 660 nm. More importantly, the absorption and fluorescence characteristics of the two complexes do not distinguish between RNA and DNA in solution. However, Lerman [1961, 1963, 1964] and Rigler [1966] proposed a molecular configuration for the two binding modes of acridine orange to nucleic acids, see Figure 3. The mode of binding of AO to a helical configuration, when the dye-to-nucleotide ratio is low, is by intercalation. The planar AO cations are sandwiched between two adjacent base pairs inside the helix. The dimethylamino groups of the dye form ionic bonds with the negatively charged $P0_{4}^{-}$ groups of the nucleotides.



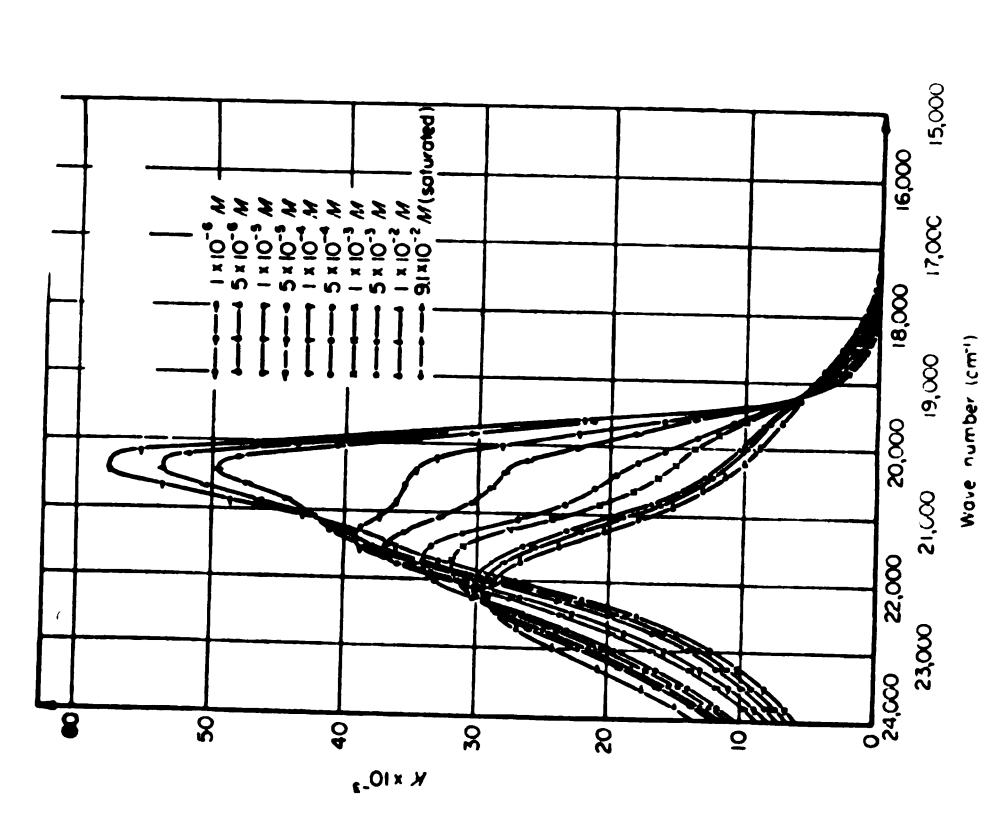


Figure 1. Absorption spectra of acridine orange in aqueous solution. Solvent: citrate-phosphate buffer, the 6.0, 20 C. (From Zanker, 1952.)

Figure 2. Fluorescence spectra of acridine orange in aqueous solution. Solvent: citrate-phosphate buffer, pH 6.0, 20 C. (From Zanker, 1952.)

		i
		1

Figure 3. Acridine orange molecular configuration, and schematic molecular configurations of AO-NA complexes in the monomer form (AO to nucleotide phosphorus ratio = 1:6) and aggregate form (AO to nucleotide phosphorus ratio = 1:1.5).



A0 bound in the, double stranded, helical regions of the NA conformation, via intercalation.



AO bound along the single strand of the NA conformation, via aggregation. This complex is not only stabilized by the hydrophobic interactions between the AO ring structure and the hydrophobic interior of the helix, and the ionic bonds, but also by the dipole-dipole interactions between the acridine ring and the purine-pyrimidine rings of the upper and lower base pairs [Rigler, 1966]. Acridine orange is a monomer in this form, because the distance between two dye molecules is large enough to prevent any dye-dye interaction. Note that the second NA-AO complex appears when the dye-to-nucleotide ratio is high; the dye is now considered bound by almost every nucleotide unit. The AO molecules are stacked along the outside of helical configurations or along the single strand of random coil configurations. The close association of AO molecules results in a dye-dye interaction that produces a long wavelength emission (660 nm.) and less stability. The second complex is considered the aggregated form of NA-AO complexes. In both binding complexes, the planes of the acridine rings are parallel to the planes of the purine-pyrimidine rings [MacInnes and Uretz, 1966; Rigler, 1966].

The metachromatic phenomenon is caused by the aggregation of dye molecules on a given macromolecule. Bradley and Wolf [1959; West, 1969] reported that the aggregation of AO on a biopolymer can be described in terms of its "stacking coefficient." A biopolymer's stacking coefficient is proportional to the free energy of interaction between a pair of neighboring dye molecules and its value is related to the conformation of the biopolymer. A highly ordered biopolymer has a small stacking coefficient. Native DNA has a stacking coefficient of 1.25 and upon denaturation it increases to 6.2. RNA has a slightly higher stacking coefficient of 3. However, some polysaccharides have a stacking coefficient greater than 800 [West, 1969]. This means that if a biopolymer

has a large stacking coefficient, then the aggregation of the dye will occur at low dye-to-biopolymer ratios. On this basis, at a low intracellular dye content macromolecules in an AO-stained cell will fluoresce red (660 nm.-690 nm.) if their stacking coefficients are very high, or green (500 nm.-540 nm.) if their stacking coefficients are low [West, 1969].

Forster [1951] and Rigler [1966] attributed the metachromatic behavior of aggregated acridine orange molecules to the existence of an intermediate metastable state. They theorized that two associated dye molecules are elevated to an excited state with both of their electronic oscillators vibrating in phase, $\frac{1}{2}$, along their long axis. The excited AO dimer makes a radiationless transition to an intermediate metastable state of lower energy, with both electronic oscillators vibrating out of phase, $\frac{1}{1}$. Since the probability of a transition from a metastable to a ground state is low, this intermediate state is preserved for a certain period. The metastable dimer reaches the ground state by a radiationless transition or by a prolonged long wave fluorescence and lifetime. A sustained phosphorescence at room temperature can be ruled out since the emission wavelengths have lifetimes of less than 10^{-3} seconds. Therefore, the dimerization of AO results in a long wave fluorescence, involving a radiationless transition from the excited state over an intermediate metastable state to the ground state, with an additional loss of vibrational energy.

C. The Relationship Between Nucleic Acids and Neuronal Activities

The nucleus is the principal morphological feature within the soma of neurons. The entire nucleus is surrounded by a perinuclear envelope

containing large pores. The nucleoplasm is primarily composed of chromatin and contains at least one nucleolus rich in ribonucleic acids (RNA). The nucleolus manufactures the ribosomal RNA used in the formation of ribosomes for protein synthesis [Lehninger, 1971, p. 33]. Deoxyribonucleic acid (DNA) molecules, in association with histones and other proteins, form the genes, which are arranged into the chromosomal material of chromatin. Chromosomes are pre-programmed with the genetic information necessary for the development and maintenance of a neuron. The genetic message, contained in the sequences of DNA nucleotides, is transcribed and translated by ribonucleic acids for conversion into proteins. The mitochrondria of neurons also contain small amounts of DNA that code for the synthesis of a few specific proteins which are located in the mitochrondria membrane. The DNA content per neuron is constant for a given species and it cannot be altered by internal or external environmental circumstances [Lehninger, 1971, chap. 28-30].

The rapid accumulation of DNA in the brain, i.e., the replication of DNA molecules, occurs during the proliferation of neuroblasts and spongioblasts, which are the embryonic precursors of differentiated neurons and neuroglia, with the proliferation of the neuroblasts, preceding that of the spongioblasts [Benjamins and McKhann, 1972]. At some appropriate time the induction and/or repression of specific chromosomal genes initiates the differentiation of a neuroblast into a specific neuronal type (Betz, Deiters, granule, mitral, Purkinje, etc.) and a spongioblast into a specific neuroglia (fibrous astrocyte, oligodendroglia, protoplasmic astrocyte, etc.). Before differentiation and the appearance of Nissl substance, neuroblast division ends. The DNA in differentiated macroneurons (long-axoned, input-output neurons) and

most microneurons (short-axoned, modulating interneurons) lack self-replication; therefore, in most cases a differentiated nerve cell loses its capacity to divide. However, the DNA in differentiated neuroglia, and microneurons in certain brain regions, e.g., the outer granular layer of the hippocampus, olfactory lobe, cerebellar cortex, and the ventral cochlear nucleus, can self-replicate, resulting in further accumulation of brain DNA and multiplication of cells [Mahler, 1972]. The total brain DNA, in most species, accumulates in a linear manner as a function of time until the adult level is reached. As the accumulation of DNA ends, the ratio of RNA to DNA increases [Benjamins and McKhann, 1972].

As indicated by the measurements of brain DNA levels, the human brain has two major periods of cell proliferation [Dobbins, and Sands, 1970; Benjamins and McKhann, 1972]. The first period corresponds to the proliferation of neuroblasts and begins at 15 to 20 weeks of gestation. In the second period the multiplication of neuroglia occurs, in addition to a second wave of neurogenesis restricted to microneurons in the granular layer of the olfactory lobe, cerebellar cortex, and hippocampus. This second period begins at 25 weeks of gestation and continues into the second year of postnatal life [Dobbins and Sands, 1970; Benjamins and McKhann, 1972].

Nissl bodies are considered a prime characteristic of neurons. Except for the axon hillock and axoplasm, Nissl bodies are found within the neuroplasm of the soma and the dendrites. The neuroplasm is the cytoplasm in neurons and should not be confused with nucleoplasm [Jenkins, 1972, p. 47]. Nissl bodies are basophilic granules consisting primarily of ribosomal RNA. Nissl bodies are involved in protein synthesis and

are the ribosomes that stud the rough endoplasmic reticulum of other cells. Nissl bodies (ribosomes) may even participate in conformational changes during protein synthesis, where both the polypeptide chain and the translated mRNA are translocated along the granules [Lehninger, 1970, p. 698]. The amount of Nissl substance contained in the soma of neurons can be correlated with the physiological and functional activity of the neuron. They may increase or decrease, depending upon the rate of neuronal stimulation and development as well as the behavioral and metabolic changes of the neuron. Nissl bodies reflect the neuronal RNA content, thus indicating the level of protein synthesis.

Injury to a mammalian neuron results in a decrease in its neuronal RNA content. In most vertebrate neurons injury is accompanied by a dilation of the soma, and the shrinkage and deformation of the nucleus, with its displacement toward the periphery of the cell body [Jenkins, 1972, p. 121]. There can be an incomplete chromatolysis if the insult (nerve fiber injury) is distal to the soma; here the Nissl bodies partially dissolve and the residual neuroplasm becomes vacuolated. Complete chromatolysis occurs when the insult is proximal to the soma, causing total disintegration of the Nissl bodies. The interruption of protein synthesis initiates the dissipation of the perikaryon with all organelles, and is suggestive of impending neuronal death. However, under suitable conditions, there can be a restoration of the Nissl bodies and protein synthesis, and the subsequent regeneration of the fiber.

A distinction of neurons is the characteristic possession of a high RNA content. The RNA level in a neuron changes during the neuron's lifecycle. A connection between the RNA content and neuronal activities was reported in retinal ganglion neurons as a function of light stimulation

[John, 1967, p. 95]. The RNA levels of the cells were found to be proportional to the total light stimulation received by the cells. In addition, light deprivation caused a dramatic decrease in the RNA concentration of the retinal ganglion neurons. This suggests that there is a positive relationship between the RNA content and neural activity, as reflected in the neuron's RNA level. In another experiment, analysis on the nuclear and ribosomal fractions of centrifuged homogenates taken from brains of animals trained to perform a conditioned avoidance response displayed greater incorporation of radioactively labelled RNA precursors than the identical fractions taken from untrained animals [John, 1967, p. 97]. This demonstrated that synthesis of RNA by a neuron increases during increased neural activity, e.g. learning situations, thereby establishing more directly a positive relationship between the RNA content and neuronal activity. This suggests that the high RNA levels and changes during the life of a neuron are attributed to the functional activity of that neuron.

The classic works by Hyden [1967, p. 200] demonstrated that the RNA content per neuron increases and the nuclear RNA base ratios change during a learning experience. In two different experiments, he determined the amount and base composition of the RNA manufactured by vestibular and cortical neurons. The nuclear RNA of cortical neurons exhibited a slight increase during the early and acute stages of a learning situation (right handed rats were induced to use their left hand in retrieving food from far down a narrow glass tube). The nuclear RNA formed had a high adenine-uracil value. As learning increases and performance improves, the nuclear RNA of the cortical neurons is enhanced significantly, and the adenine-uracil rich RNA base ratio changes to a

composition similar to ribosomal RNA. Thus, a differentiated formation of nuclear RNA occurs in cortical neurons engaged in a learning experience, reflecting a genic stimulation. After physiological stimulation and work requiring memorization (young rats learn how to balance on thin wire strung 45° between the floor and a small platform with food in order to eat), the RNA content of Deiter neurons from the lateral vestibular nucleus of rats was analyzed. Hyden [1967, p. 200] found that the RNA content per neuron increased during learning and physiological stimulation. The nuclear RNA formed during physiological stimulation had the base characteristics of a ribosomal RNA. In contrast, the nuclear RNA formed during learning was an asymmetric, adenine-rich RNA of the chromosomal type, signify that the increase in the adenine-to-uracil ratio was specific for learning. The cytoplasmic RNA of the Deiter neurons increased during learning but did not change in base composition. Hyden also reported that there occurs a transfer of RNA between glia and neurons. The two cells communicate during neuronal functions, whereby an increase or decrease in the RNA content and enzyme activities of the neuron causes an opposite response in the surrounding glia.

The priceless contribution of Hyden [1967] and others [Cameron et al, 1970; Rosenblatt, 1970; Unger, 1970] coincides with the author's proposition that there exists a direct functional relationship between the ribonucleoprotein (RNA) characteristics of a neuronal complex and the maintenance of memory and learning, and that this relationship is manifested in the form of a proportional change. This may be evidenced when a change in the concentration, composition and/or conformation of ribonucleoproteins results during the facilitation or inhibition of behavioral processes.

At present the Edstrom [1953, 1958, 1964] method is widely used for the determination and analysis of nucleic acids in isolated subcellular units and cell samples. The Edstrom method has some advantages and disadvantages in comparison to absorption and fluorescence microspectrophotometry. One of the positive aspects of the Edstrom method is its ability to determine the base composition for the nucleic acids. However, the sensitivity of this method is only good for about 25 picograms of material, and the extraction and isolation procedures could result in leaving portions of the nucleic acids undetected. In addition, the method [Edstrom, 1953, 1958, 1964] is unable to detect any molecular activities within the whole neuron, due to internal or external environmental circumstances. At this interim, the aforementioned method [Edstrom, 1953, 1958, 1964] is not recommended or used by this author for more than one reason. Not only do its negative aspects outweigh its positive elements, but it is time-consuming and tedious.

A number of investigators [Haltia, 1970; Sobkowicz et al, 1973] have noted that changes in metabolic activities (aging) can result in changes in the RNA content of neurons. A piece of work presented by Haltia [1970] was concerned with the RNA content of spinal anterior horn neurons during the postnatal development of rats (in vivo). The neurons were isolated from the other cells, but the Edstrom [1953, 1958, 1964] method was employed for determination of the RNA content as a function of age. A rapid acceleration in the neuronal RNA content was observed between the ages of 1 and 15 days. At 15 days, a deceleration in the RNA content occurred and almost reached adulthood values at 30 days of age. No significant change in the RNA content was observed after 90 days of age. These results were interpeted by Haltia [1970] to represent a differential growth rate, a growth-curve relationship between

the RNA content and the age of the developing neuron, evidenced by a sigmoid curve (S-shape curve) for the RNA content (ordinate) plotted against the age (abscissa) of the neuron. This relationship was further substantiated by Sobkowicz et al [1973]. They displayed a growth-curve correlation compatible to Haltia's [1970] results. The RNA content of normal and cultured cells from fetal rat spinal ganglia was determined, again by the Edstrom [1953, 1958, 1964] method, as a function of age. Both the in vitro and in vivo neurons demonstrated a differential growth rate. The RNA content of the cells rapidly increased during the first stages of normal neuronal development. Sobkowicz et al [1973] suggested that the increase in neuronal RNA content was associated with the formation and differentiation of Nissl material. Also, it was noted that the cells in the explant cultures develop at a much slower pace than in vivo. This may be the result of a change in environment or trauma from explanation. In any case, it is evident that there exists a differential growth rate during the maturation of neurons. A growth-curve relationship, in the RNA content, as a function of age, is found for neurons in culture as well as in vivo. This particular relationship is an excellent test situation, in respect to the author's proposed techniques, which involves the utilization of acridine orange fluorescence microscopy in the analysis of nucleic acids in single neurons maintained in dissociated cell cultures.

D. Neuron Cultures

The ability to grow nervous tissues in cultures can greatly enhance our knowledge in the neurosciences. It has been demonstrated that the morphological, biochemical, organizational and functional developments of neurons in culture are similar to neurons in the natural situation.

The experimental control over neurons in cultures can be utilized to study the activities of macromolecules under given conditions. Neurons grown in culture provide an excellent model system to probe the macromolecular mechanisms involved in neuronal interactions. The following paragraphs exemplify some of the similarities between neurons maintained in culture and neurons grown in vivo.

Vatter and Seeds [1971] demonstrated that the morphological development of cells from an embryonic mouse brain in culture is quite similar to cells in vivo. They observed that dissociated cells reassociated into highly organized aggregates in a basal Eagle's medium with 10% fetal calf serum. Vatter and Seeds [1971] reported that the cells differentiated and formed myelinated axons after five weeks in culture. The cells arranged themselves in the same cytoarchitectural design that exists in vivo. In addition, synapses matured and increased in number during this period. These morphological results were correlated to be identical to the in vivo cytoarchitectural development of the embryonic mouse brain.

In an earlier paper, Seeds [1971] established that the development of enzymatic activities related to chemical transmission in the reaggregating cell culture are similar to the <u>in vivo</u> situation. Seeds dissociated neurons from an embryonic mouse brain and allowed them to reassociate in a rotation culture to form aggregates. The specific activities of choline acetyltransferase (ChAT), acetylcholinesterase (AChE), and glutamate decarboxylase (Gluase) were obtained from the aggregates as a function of time in culture. The results, displayed by their activity/time curves in culture, were analogous to the typical S-shape patterns found in the brain. Further, it was observed that at the curve's maxima, the ChAT activity has a greater propinguity toward the

<u>in vivo</u> levels than the AChE. One possible explanation for this involves the difference in the rate of development between axons and dendrites. In the aggregates, axon development proceeds at a faster rate than does dendrite maturation. Because ChAT is found in the synaptic bouton of the axon, whereas the AChE activity is largely in the postsynaptic membrane of the dendrite, it seems plausible that the peak levels reached by the enzymes would be affected by these circumstances [Seeds, 1971].

Nelson and Peacock [1972] provided evidence that substantiated the equivalence between the electrophysiological experiences of L cells in culture and experiences of L cells in vivo. Utilizing iontophoretic techniques, they applied acetylcholine to L cells in culture. The affected cells evoked a prolonged active membrane hyperpolarization; and the administration of atropine was found to block this response. Plus, a cell to cell functional interaction was demonstrated in culture, whereby a hyperpolarizing activiation response was recorded in cells adjacent to cells stimulated with acetylcholine. The sensitivity to this neurotransmitter suggests that L cells in culture are capable of generating electrophysiological responses similar to L cells in the natural environment.

The onset and development of functional interneuronal connections in cultures were described by Crain and Peterson [1967]. They reported that the complex bioelectrical activities evoked by nervous tissue in cultures resembles, to a high degree, the functional organization of synaptic networks <u>in vivo</u>. Crain and Peterson performed their recordings on rat spinal cord ganglia explants. Their results exhibited that 14-15 days old fetal rat explants in culture for 2-3 days elicited either a simple spike potential or no bioelectrical transmission

whatsoever from one neuron to another. However, 3-4 days in culture demonstrated complex bioelectric activities. Facilitation was observed with paired stimuli at long test intervals. Also brief tetanic stimulation produced slow waves and a long lasting spike barrage. These results correlated closely with in vivo conditions, in that they indicated that polysynaptic networks are beginning to function in the culture. Furthermore, electron micrographs of these explants illustrated that morphological parameters associated with sequential development of bioelectric functions increased during culture maturation. Crain and Peterson [1967] digested their results and concluded that nervous tissue, grown under suitable cultural conditions, have smiliar morphological, biochemical and functional characteristics as the in vivo state.

In reiteration, it has thus far been demonstrated that the development of a neuronal complex in a cell culture is analogous in function to its development in vivo. It has not yet been established that the mental behavior of neurons maintained in culture exhibits the same characteristics as the natural state--or, in fact, that there exists a mental behavior in neurons in culture. Whether or not a behavior is localized in neuronal complexes or encompasses the entire brain is, indeed, a controversial issue. However, regardless of the conclusions one may draw, it must be acknowledged that neuron-to-neuron molecular interactions are significant in a behavioral process. The complex molecular interactions of these neurons are the consequence of neuronal metabolic activities whose functions are related to behavior. Therefore, the parameters that reflect metabolic functions can be intimately associated to behavior. It is for these reasons that this author submits that a thorough understanding of the neuronal molecular interactions of

nucleic acids and proteins will eventually lead to the elucidation of the molecular mechanisms involved in the functioning neuron.

A number of investigators [Chignell, 1973; Kohen et al, 1973; Rigler, 1966; West and Lorinez, 1973] have used fluorescent probes in conjunction with cell cultures to study various cellular macromolecules. Rigler [1966] and West and Lorinez [1973] have used the fluorescent probe, acridine orange, to study, respectively, nucleic acids and mucopolysaccharides in cell cultures. Kohen et al [1973] have used rapid microfluorometry to examine enzyme reactions and transport mechanisms in single living cells maintained in cultures. Neurons maintained in cell culture have a number of advantages for use with fluorescent probes. The dissociated cell cultures can provide individual neurons: the macromolecules can be analyzed in non-mutilated neurons (fixed or living). The neurons are maintained in an environment that can be controlled and easily manipulated. In addition, they are readily accessible to diffusible materials and any unbound excess probe can be washed off freely. Furthermore, neurons and neuronal contacts in a monolayer cell culture are simple to observe and their fluorescence easily analyzed with microspectrophotometry. It is evidenced that cell cultures in combination with fluorescent probes furnish a valuable model system to study the molecular interactions of neuronal activities.

The objective of this investigation is to survey and increase the information about the use of fluorescent molecular probes in the study of macromolecular interactions involved in the functional activities of neurons in culture. Specifically, the author intends to obtain the fluorescence characteristics of the binding of acridine orange to nucleic acids in different microenvironments, by examining: 1. The fluorescence

changes of AO-NA complexes, at 536 nm. and 604 nm., in gelatin microdroplets as a function of the AO concentration in the microenvironment of the NA. This is to determine whether the fluorescence intensities of AO molecules bound to 1.0 pg. DNA or rRNA in the monomer and/or aggregated forms are proportional to the amount of AO permitted to bind to the NA macromolecules, 2. The fluorescence changes of AO-NA complexes at 536 nm. in gelatin microdroplets as a function of the AO staining time. This is to find out the optimum interaction time for the binding of AO to the monomer binding sites in the DNA or rRNA conformations. 3. The fluorescence variations of AO-NA complexes at 536 nm. and 604 nm. in gelatin microdroplets as a function of the hydrogen ion concentration in the micro environment of the NA. This is to determine the effects of ionization on the binding of AO to 1.0 pg. of DNA or rRNA in the monomer and aggregated forms, 4. The fluorescence intensity changes of AO-NA complexes at 536 nm. and 604 nm. in gelatin microdroplets as a function of the NaCl concentration in the microenvironment of the NA. This is to ascertain the effects of the environmental ionic strength on the binding of AO molecules to the DNA or rRNA conformations in the monomer and aggregated forms, 5. The fluorescence intensities of AO-rRNA complexes at 536 nm. and 604 nm. in gelatin microdroplets at various temperatures. This is to resolve whether the denatured conformations of rRNA binds AO in different modes, 6. The fluorescence intensity changes at 536 nm. and at 604 nm. of AO-NA complexes in gelatin microdroplets during continuous irradiation. This is to determine if the fluorescence of AO molecules bound to DNA macromolecules decay differently than that of AO molecules bound to rRNA macromolecules, and if the

fluorescence of AO molecules bound to NA in the monomer form decay differently compared to those bound in the aggregated form, 7. The fluorescence intensity changes of AO-NA complexes as a function of the NA concentration in the microenvironment of gelatin microdroplets, for the quantitative determination of DNA or rRNA contained in a given microenvironment. The author intends to answer the question—If the nucleic acid (RNA) content of neurons varied as a result of neuronal activity, what, then, is the nucleic acid content of specific neuronal types grown in culture, at two different ages? In addition, another purpose of this inquiry is to acquaint the author and novice with the basic techniques involved in the combined use of fluorescence microscopy and the methods of dissociated neuron cultures.

II. EXPERIMENTAL DETAILS

A. Materials

The nucleic acids used in studying the binding behavior of acridine orange were obtained from Sigma Chemical Company. The deoxyribonucleic acid (Type I: sodium salt) was in highly polymerized form isolated from calf thymus. The rRNA (Type XI) was purified by Sigma from Baker's Yeast ribosomes after Crestfield et al [1955] and the Polyuridylic acid was Type II: potassium salt. The nucleic acids were suspended in gelatin solutions of 3% purified pigskin in bidistilled water. The purified pigskin was obtained from Sargent-Welch Scientific Company. The gelatin microdroplets served as inert carriers, the protein matrix of the microdroplets prevented the elution of the nucleic acids during the staining procedures.

Punified acridine orange (3,6-bis-dimethylamino-acridinium chloride) was secured from Sigma Chemical Company. Stock solutions of AO $(1\times10^{-3}\text{M})$ were made up in bidistilled H_2O and stored at 4°C in glass-stoppered low-actinic glass flasks. Aliquots of the acridine orange stock solutions were diluted to a desired concentration by McIlvanine's citric acid-phosphate buffer. Other than the experiment involving the fluorescence intensity changes of AO-NA complexes, as a function of pH, the citrate-phosphate buffer was always buffered to pH 4.1 by the same procedure, permitting the ionic strength of each buffer solution to remain constant. All reagents were of analytical quality and were used without further purification.

Dissociated cells from the cerebral cortex of 3 days old female

albino rats were used. The rats were purchased from Spartan Research Animals Company. The dissociated neurons were cultivated in Culturstat MEM Eagle's medium (Earle's base without serum) with 17% Fetal calf serum, incubated at 37°C, as monolayers on glass slides in sterilized plastic culture dishes. The medium and serum were obtained from Bio Quest Company, Cockeyville, Maryland. The incubator was a Napco 322 from the National Appliance Company, with a temperature variation of ± 0.5 °C. The internal environment of the incubator was $\rm CO_2$ -air (5:95) and humid with bidistilled water. All culture glassware was autoclaved for 30 minutes. The surgical instruments were sterilized by the flame.

B. Methods

1. Microdroplet procedures.

Specific amounts of DNA, rRNA or Poly U stock solutions were mixed with enough bidistilled water to make a maximum liquid content of 9.7 ml. (see the example on the following p.26), and added to 0.3 gm. of purified pigskin in a 25 ml. Erlenmeyer flask. The flasks were sealed with paraffin papers, and the solutions were stirred (using a stirring bar and magnetic stirrer) at temperatures around 37°C. A mixing temperature of 37°C would avoid denaturation of the nucleic acids. After equilibrium was reached, 0.1 microliter droplets of each solution were delicately placed on a clean glass slide with a microsyringe, in a micromanipulator, at an angle of 90°. A maximum amount of space between each microdroplet was allowed to prevent adjacent droplets from being indirectly irradiated by stray excitation light. The microdroplets were fixed in formaldehyde gas for 12 to 48 hours. The formaldehyde gas fixation stops the loss of NA when the gelatin swells in water.

The glass slides were attached to a holder, and immersed vertically into the reaction solutions. The reaction vessels were matched, each containing 100 ml. of reaction solution. The reaction solutions stood 12 to 48 hours in a 22°C water bath, until equilibrium. The staining process was carried out in the dark, and obeys Fick's diffusion law for reproducibility. The following is the basic staining procedure employed, unless stated otherwise:

- 1. Citric acid Na₂HPO₄ buffer, pH 4.1 5 mins.
- 2. $5 \times 10^{-5} M$ AO in buffer solution, pH 4.1 30 mins.
- 3. Rediffusion of AO into buffer, pH 4.1 5 mins.
- 4. Rediffusion of AO into buffer, pH 4.1 5 mins.
- 5. Rediffusion of AO into buffer, pH 4.1 5 mins.

The rediffusion process removes the excess, unbound AO molecules from the microdroplets. The microdroplets were placed 12 hours to 13 days under formaldehyde gas in the dark, after rediffusion. The length of fixation, before or after staining, has no appreciable effect on the fluorescence of the AO-NA complexes in the microdroplets. After fixation, the diameter of each microdroplet measured 1.0 ± 0.1 millimeters, and the thickness at the center of the microdroplet was 5 microns. Focused at its center, the microdroplet was irradiated at 400 nm. by the Fluorescence Vertical Illuminator.

An aperture, 22 microns in diameter, is situated in front of the monochromator housing. Because of the aperture, the fluorescence detected by the photomultiplier was restricted to a finite volume in the center of the microdroplet. The volume was cylindrical in shape, and equal to 1.9×10^{-9} cubic centimeters. The fluorescence spectra of the AO-NA complexes in the micro-cylinder were recorded during

continuous irradiation. Depending upon the NA concentration of the microdroplet forming solution, the NA content in the gelatin microcylinder can be accurately calculated. As an example:

DNA stock solution, 5.3×10^{-4} gm. DNA/ml.

Sample Number	ml. of stock sol'n used	ml. of H ₂ O added	gm. of pf. pgsk. in Erlyms.
1. 2. 3. 4. 5. 6. 7.	9.7 7.7 5.7 3.7 1.7 0.85	- 2 4 6 8 8.85 9.7	0.3 0.3 0.3 0.3 0.3 0.3 0.3
Sample Number	DNA conc. in microd forming solution	DNA cont 1.9x10 ⁻⁹ micro-cy	cm ³
1. 2. 3. 4. 5. 6.	5.3x10-4gm./ml. 4.2x10-4gm./ml. 3.1x10-4gm./ml. 2.0x10-5gm./ml. 9.3x10-5gm./ml. 4.6x10-5gm./ml.	1.00 pg. 0.80 pg. 0.59 pg. 0.38 pg. 0.18 pg. 0.09 pg. 0.00 pg.	
	10		

Note: $1.0 \text{ pg.} = 1.0 \times 10^{-12} \text{ gm.}$

2. <u>Neuron Culture procedures</u>.

The nature of this endeavor suggest that there may exist a variety of factors that, if left uncorrected, may lead to erroneous results and conclusions. For example, the location and condition of the area to be utilized in the preparation and growing of the neurons are critical. The entire working area should be sterilized; if not, germs may invade the cell culture and disrupt the neuronal development. A mixture of mineral oil and xylene can serve this purpose. The fetal calf serum is inactivated in a constant temperature water bath at 56°C for 40 min.

before use. After the MEM Eagle's Culturstat Preparation a mixture of 17% fetal calf serum in MEM Eagle's Culturstat is prepared and labelled neuron medium. The excess serum and culturstat is stored at -4°C. The neuron medium is kept sealed at room temperature. The entire culture preparation procedures require aseptic techniques.

Before brain removal, the animals were anesthetized with ether and were sterilized in 70% ethanol and iodine - 70% ethanol. The surgical instruments were rinsed in ethanol from water, before flaming with a blue flame. The whole brains from 3 day old female albino rats were removed via a calvarium dislocation. The brains were placed in culture dishes containing neuron medium. An attempt was made to dissect the somatic sensory cortex, I and II according to the location and external limiting boundaries described by Welker and Sinha [1972]. These sections and the entire cerebral cortex were mechanically dissociated without the utilization of trypsin to reduce unwanted chemical interferences. The dissociated tissue and neuron medium were intimately associated in a test tube with a vortex. This mixture was agitated for 5 mins. and allowed to settle (by gravity) for 30 mins. at room temperature. 2.0 ml. of the supernatant from the test tube were diffused on a glass slide in a culture dish, and incubated for 24 hours. The next day, 10 ml. of neuron medium were added to each dish. The cultures were incubated at 37°C with a humid CO_2 -air (5:95) environment. Two weeks after the cultures were set up, 2 ml. of fresh neuron medium were added to each culture. Three weeks later, the old medium was poured off and 12 ml. of fresh medium were added to each culture. This neuron feeding procedure was continued to allow the cultures to develop satisfactorily. The age of the neurons in culture equaled the age in days at the time of sacrifice

plus the number of days spent in culture. The cultures met a morphological criterion (axonal and dendritic redifferentiation) before rinsing and fixation. The glass slide was removed from the cultures and rinsed, at 22°C, by gently placing in a dish of 0.87% physiological saline. The glass slide (with cells attached) was fixed for 3 hours at room temperature in 1:1 ethanol and acetone. The entire staining process was performed, in the dark, at a constant temperature of 22°C, to maintain a diffusion equilibrium with the solution:

- 1. Acetylation of amino groups. The amino groups of the protein fraction in the nucleoproteins were blocked with acetic acid anhydride in pyridine:
 - (a) Pyridine, water-free

5 mins.

(b) Acetic acid anhydride:pyridine (2:3)

15 mins.

- Purification and rehydration. The cells were purified from acetic acid anhydride, and transferred into an aqueous medium:
 - (a) Ethanol 100 percent

5 mins.

(b) Ethanol 95 percent

5 mins.

(c) Ethanol 60 percent

5 mins.

(d) Ethanol 30 percent

5 mins.

(e) bidistilled H₂0

5 mins.

- 3. Staining process. $5 \times 10^{-5} M$ AO in Citric acid Na_2HPO_4 buffer, pH 4.1:
 - (a) Citric acid Na₂HPO₄ buffer

5 mins.

(b) A0 in citrate-phosphate buffer

30 mins.

- 4. Rediffusion process. Washing away of unbound AO with citrate-phosphate buffer, pH 4.1:
 - (a) Citric acid Na_2HPO_4 buffer

5 mins.

(b) Citric acid - Na₂HPO₄ buffer

5 mins.

(c) Citric acid - Na₂HPO₄ buffer

5 mins.

The reaction vessels were matched and each contained 100 ml of reaction solution. The solutions were allowed to reach equilibrium in the thermostatic waterbath for 24 hours. After the rediffusion process, the excess buffer solution was drained off. The cells were sealed in the same citric acid - Na₂HPO₄ buffer solution, pH 4.1, with a coverslip and paraffin. The areas of the cell bodies were determined by projecting and tracing the cell outlines on paper. A planimeter was used to measure the areas of the cells' profiles.

C. Instrumentation

The observations and emission spectra were registered with a microspectrophotometer constructed from commercially available components. The microscope was a Leitz Ortholux, with fluorescence equipment.

The light source was a Xenon arc lamp, type XBO 150, housed in a Universal Lamp housing model #250. A blue filter, #GS 5-56 (Corning Glass Works), was placed in front of the light exit aperture on the Lamp housing. The Xenon lamp was powered by a power supply which produces a constant current that maintains the light output within \pm 1% (E. Leitz, New York).

For fluorescence excitation of samples, in incident light, the energy source was focused into the entrance slit of a Leitz Fluorescence Vertical Illuminator (according to Ploem). The fluorescence excitation was produced by exciting filters, 4 mm BG 38 and 5 mm BG 12, in the lamp housing. A dichroic beam-splitting mirror, TK495, was also used. The fluorescence of the samples was filtered through a built-in suppression filter, K495, and a Sharp-Cut filter, 3-70 (Corning Glass Works),

contained in the suppression filter slide (see Figure 4). The radiation emitted from the irradiated sample was collected and projected into a 4 in. diameter, 180°, wedge interference filter (linear from 400 nm. to 700 nm.). The monochromator was motorized, and powered by a Heathkit IP32 regulated power supply (see Figure 5).

The monochromatic radiation was focused onto a R 446S (200 nm. to 800 nm.) potted photomultiplier tube (American Instrument Company). The phototube high voltage electrical power was manufactured by two Heathkit IP32 regulated power supplies. The electrical responses were amplified by an instrument modelled after the Aminco Solid-State Blank-Substract Photomultiplier Microphotometer 10-180 [St. Pierre, 1972]. The emission spectra were recorded on a 135C X-Y Recorder (Hewlett Packard, Mosely Division) (see Figure 5).

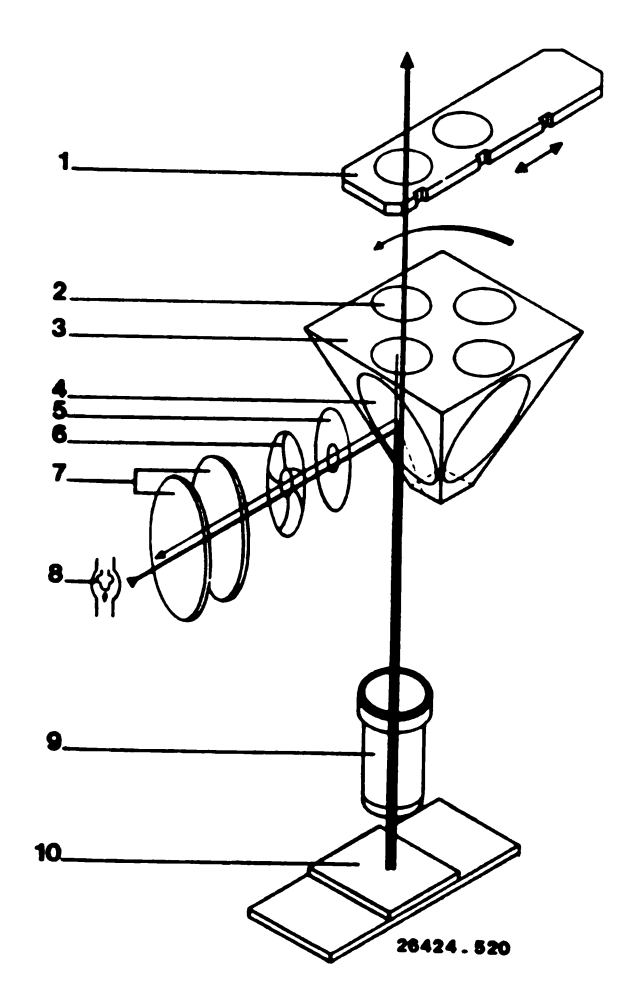


Figure 4. Diagram of the principle of the LEITZ fluorescence vertical illuminator

- 1. suppression filter slide
- 2. suppression filter
- turret with suppression filters and beam-splitting mirror
- 4. beam-splitting mirror
- 5. stray light stop
- 6. field diaphragm
- 7. exciting-filter combination (in the lamp housing)
- 8. ultra-high-pressure Xenon arc lamp
- 9. objective
- 10. object

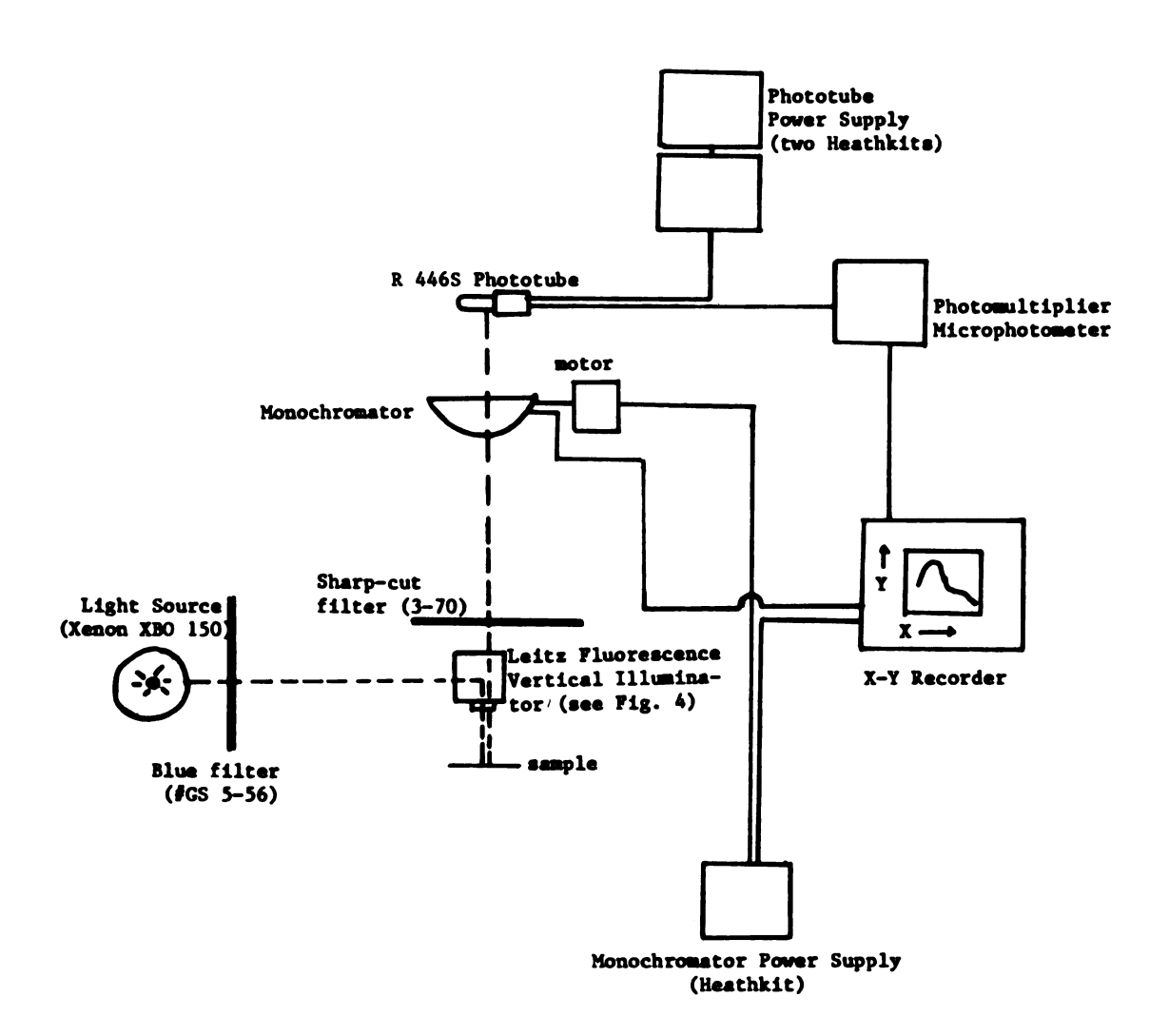


Figure 5. Diagram of the microspectrophotometer.

III. RESULTS AND DISCUSSION

A. Introduction

The extent to which we understand the behavior of biological macromolecules will depend upon our knowledge of the dye molecule, and dyemacromolecule interaction. Acridine orange (AO), a small planar dye molecule, is a fluorescent molecular probe used in the investigation of nucleic acids (NA). Zanker [1952; West, 1969] has studied the nature of AO alone in aqueous solutions, while other investigators have examined the conduct of AO and NA together, in aqueous solutions and in gelatin microdroplets, under various environmental conditions [Bradley and Wolf, 1959, 1960; Loeser et al, 1960; Rigler, 1966]. Under certain conditions the spectral characteristics of the acridine orange-nucleic acid complexes can be employed in determining the AO and/or NA content, as well as to delineate the nucleic acids within individual fixed or living cells [Rigler, 1966; West, 1969]. Inferences about the structure and function of macromolecules that are involved in neuronal phenomena, such as plasticity (memory), energy transduction, specificity and aging, may be devised by studying the interactions of the fluorescent probe and macromolecule. Biophysical cytochemistry provides the neurobiophysicist with valuable tools to investigate the salient features of various neuronal phenomena.

A large segment of my research was concentrated on the binding and structure characterization of AO-NA complexes embedded in gelatin microdroplets exposed to various microenvironmental conditions. The spectral distribution of the emission of different AO-NA complexes subjected to

the same staining conditions is displayed in Figure 6. Notice that equivalent amounts of different AO-NA complexes (AO-DNA, AO-RNA, AO-Poly U) have identical spectral patterns, with a green fluorescence maximum at 536 nm. and a prominent shoulder toward the longer wavelengths at 604 nm. Table 1 displays the relative fluorescence intensities for the various AO-NA complexes under the same conditions. The differences in the intensities suggest that AO has a specific binding affinity for each of the NA; this theme is observed in all of the microdroplet experiments.

In summary, my research on other gelatin microdroplet systems revealed a considerable amount of information about the binding of acridine orange to nucleic acids. It affirms that no significant difference in the aggregation of AO on the various NA exists, as evidenced by only minute variations in the degree of aggregation for each nucleic acid. The degree of aggregation, α , is a measure of the degree of dye association of AO on a particular nucleic acid configuration [Rigler, 1966]. and can be calculated from the ratio of the emission intensity at the longer wavelength (604 nm., associated AO) to the short wavelength (536 nm., monomer AO) fluorescence maximum intensity. In the presence of an increasing dye concentration, the degree of aggregation and binding of the dye molecules onto the nucleic acid in both the monomer and associated forms intensified linearly within a specific AO concentration range. Increasing the interaction time of the acridine orange molecules with the biopolymers enhanced the binding of the dye molecules to the nucleic acids. My results also showed that the binding of AO to the nucleic acids increased as the pH increased from 4.0 to 8.4. The degree of aggregation for rRNA decreased slightly as the pH increased. No significant change in the degree of aggregation for DNA was noticed,

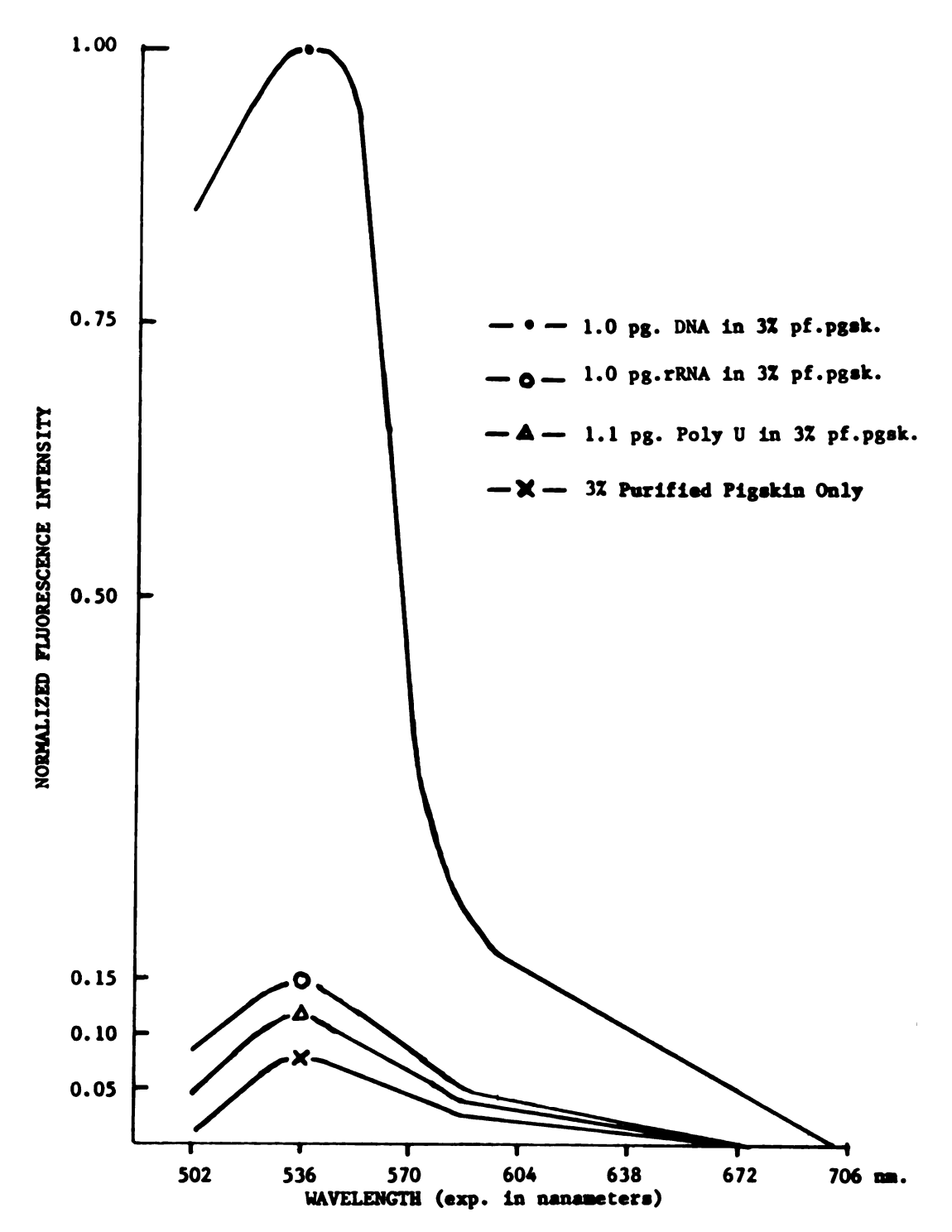


Figure 6. The normalised fluorescence spectra of AO molecules bound to different NA conformations and gelatin proteins, AO staining concentration 5 x 10^{-5} M, staining time 30 mins., pH 4.1.

TABLE 1.

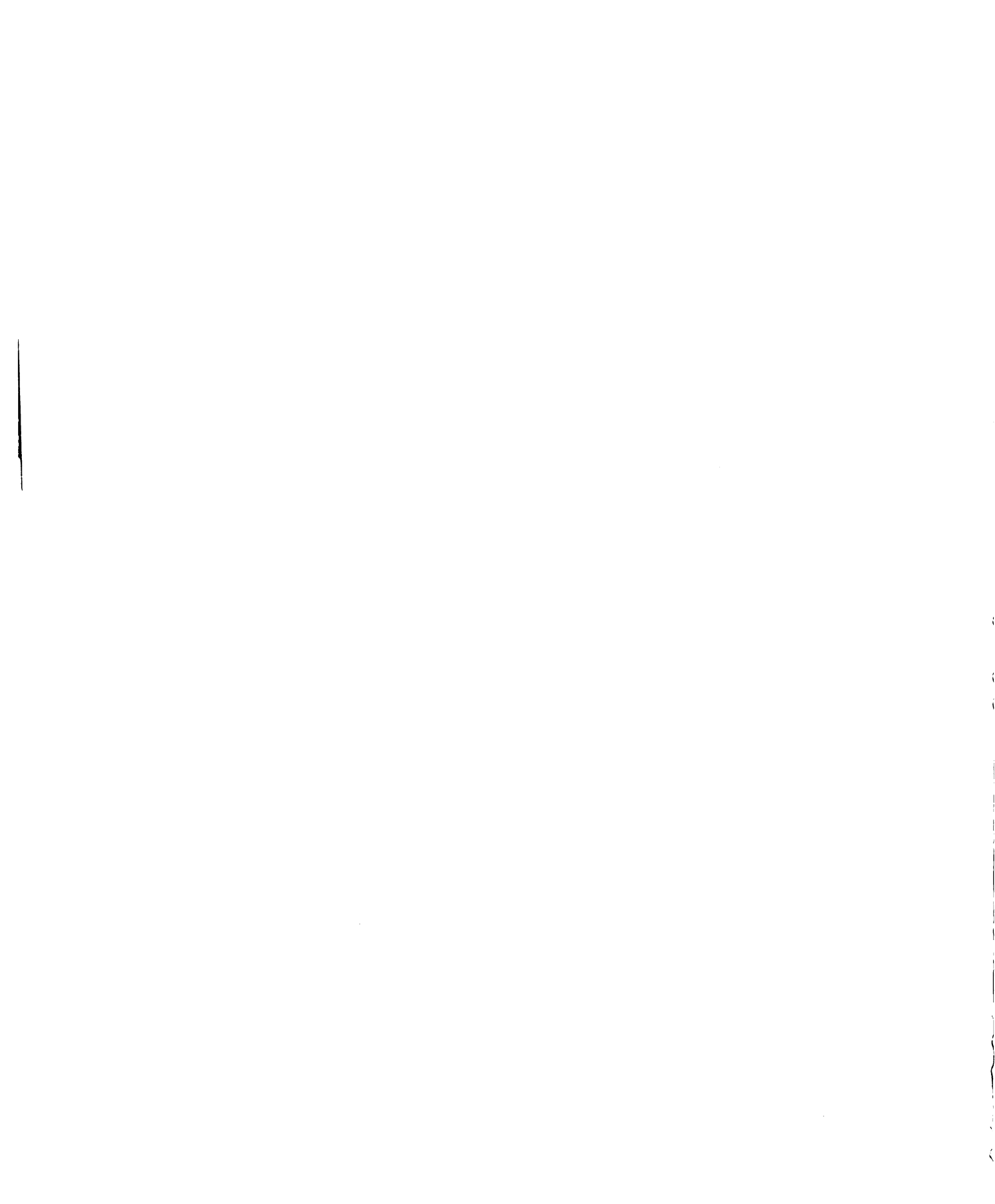
The relative fluorescence intensity of AO-NA complexes at 536 nm. and 604 nm.

Staining Condition: 5 x 10⁻⁵M Acridine Orange, 30 minutes staining time, pH 4.1 + 0.1, at 22°C.

		536 nm.	604 nm.
1.	1.0 pg. DNA in 3% pf. pgsk.	822	135
2.	1.0 pg. rRNA in 3% pf. pgsk.	122	30.1
3.	1.1 pg. Poly U in 3% pf. pgsk.	98.1	23
4.	3% purified pigskin only	64.3	17.9

indicating that the binding of AO to nucleic acids in the monomer fashion is preferred at high pH levels or at low hydrogen ion concentrations. More importantly a linearity between the emission of the AO-NA complexes and the amount of NA available for binding was established, whereby increasing the amount of NA proportionately increased the amount of AO bound by the NA. Under the proper micro-environmental conditions, the degree of aggregation for DNA and rRNA are tantamount and stable as the NA content increases. Increasing the ions in the NA micro-environment increases the binding of AO and decreases its degree of aggregation onto the NA, suggesting that a high ion content favors the binding of AO to NA in a monomer formation. The denaturation of rRNA does not appreciably affect the degree of aggregation of AO or rRNA, however, the binding of AO to rRNA increases slightly with increasing temperature. These results affirm that AO has the <u>same</u> binding modes with different affinities for different NA conformations.

Another segment of my research involved the microspectrophotometric analysis of AO-NA complexes within individual neurons identified in



dissociated cell cultures of specific and nonspecific areas of the rat brain. From the microdroplet inquiry, fluorescence coefficients for specific staining conditions were procured and used to calculate the NA content inside the soma of single neurons. The nucleic acid content of two neuronal types was determined at two ages, and the NA content per neuron was found to depend more upon neuronal type and maturity than size. The average value of the NA content of each neuronal type was 28% greater at the older age than at the younger age. The NA content of one neuronal type always averaged 8% greater than the NA content of the other type. However, the NA content per neuron, as a function of neuronal soma area. presented no definite pattern. Under the same staining conditions, the spectral patterns of AO-NA complex emissions in single neurons were found to be analogous to AO-NA complex emissions embedded in gelatin microdroplets. The fluorescence characteristic of the AO-NA complexes in neurons and in microdroplets are attributed to the binding of AO to the NA predominantly in the monomer conformation, with a small degree of aggregation.

B. Microdroplet Analysis

Inasmuch as the main thrust of this inquiry was to develop and apply a microspectrophotometric technique to the qualitative and quantitative determination of intrasomatic nucleic acids in single neurons, the binding mechanisms of acridine orange to nucleic acids were examined in a protein carrier system, in hopes of understanding, in detail, the nature of AO-NA complexes within various microenvironments. In view of the fact that neurons have cell and nuclear membranes, organelles, and other biopolymers, the interactions of acridine orange and nucleic acids

within living and even fixed cells are more complicated than that within simple protein microdroplet systems.

In each of the subsequent results, an average of three microdroplets was analyzed per relative fluorescence intensity value (these being actual experimental values without mathematical manipulations). The use of an average of three microdroplets proves to be a sufficient quantity since, on numerous occasions, different microdroplets with identical contents yield tantamount fluorescence intensities and spectra, when treated to the same conditions. In calculating the degree of aggregation, defined earlier, necessary mathematical corrections were made, since the fluorescence of AO fades during excitation and the protein environment interacts with the dye molecules. Because the scanning speed of the X-Y recorder is slow in the X direction (0.14 cm/sec) the fluorescence intensities at the 604 nm. wavelength were the result of a longer irradiation time than that of the 536 nm. wavelength. The relative fluorescence intensity values for the 536 nm. wavelength had to be multiplied by a 0.76 correction factor, making the fluorescence intensity equal to the intensity values if irradiated the same length of time as the 604 nm. wavelength (see the Fluorescence Decay during Continuous Irradiation section, p. 65). Before calculating the degree of aggregation for a given condition, the relative fluorescence intensity values for 3% purified pigskin (pf. pgsk.) only (containing no nucleic acids) were used to eliminate any environmental influences of the AO-protein (gelatin) complexes from the AO-DNA and AO-rRNA complexes in the microdroplets. This was accomplished by subtracting the values for 3% pf. pgsk. only from that of AO-DNA and AO-rRNA in 3% pf. pgsk. at each wavelength. An example of the calculations of the degree of aggregation of AO onto DNA for a specific staining condition is as follows:

$$\alpha = \frac{1}{0.76} \cdot \frac{(F_{604} \text{ of DNA in } 3\% \text{ pf. pgsk.}) - (F_{604} \text{ of } 3\% \text{ pf. pgsk. only})}{(F_{536} \text{ of DNA in } 3\% \text{ pf. pgsk.}) - (F_{536} \text{ of } 3\% \text{ pf. pgsk. only})}$$

1. The fluorescence changes of AO-NA complexes as a function of acridine orange staining concentration.

The relative fluorescence intensities of the AO-NA complexes at 536 nm. and 604 nm. reflect the amount of AO bound to the NA in the monomer formation and in the aggregated structure, respectively. In this experiment, groups of microdroplets were subjected to a different AO staining solution concentration, while the rRNA or DNA contents, analyzed within each microdroplet, were held constant over the entire AO staining concentration range (5x10⁻⁶M to 5x10⁻⁴M). The microdroplets were stained for 15 minutes each, and all of their reaction solutions had pH 4.1. With the microspectrophotometer, the fluorescence spectra of the AO-DNA, AO-rRNA, or AO-gelatin protein complexes were recorded from each microdroplet while excited at 400 nm. The average relative fluorescence intensities of the AO-DNA, AO-rRNA, and AO-gelatin protein complexes, at 536 nm. and 604 nm. for each AO staining concentration are tabulated in Table 2 and graphically displayed in a semilogarithmic plot in Figure 7.

In Figure 7, the relative fluorescence intensities, at 536 nm. and 604 nm., for AO bound to 1.0 pg. rRNA and 1.0 pg. DNA in 3% pf. pgsk., and to 3% purified pigskin only were found to increase linearly as the AO staining concentration increased from 5 x 10^{-6} M to 5 x 10^{-4} M. This indicates that the total amount of AO bound to the NA and gelatin proteins, in both the monomer and aggregated forms, depends proportionately on the quantity of free dye initially available for binding a NA or protein macromolecule. The slope (m) for 1.0 pg. DNA in 3% pf. pgsk. at 536 nm.,

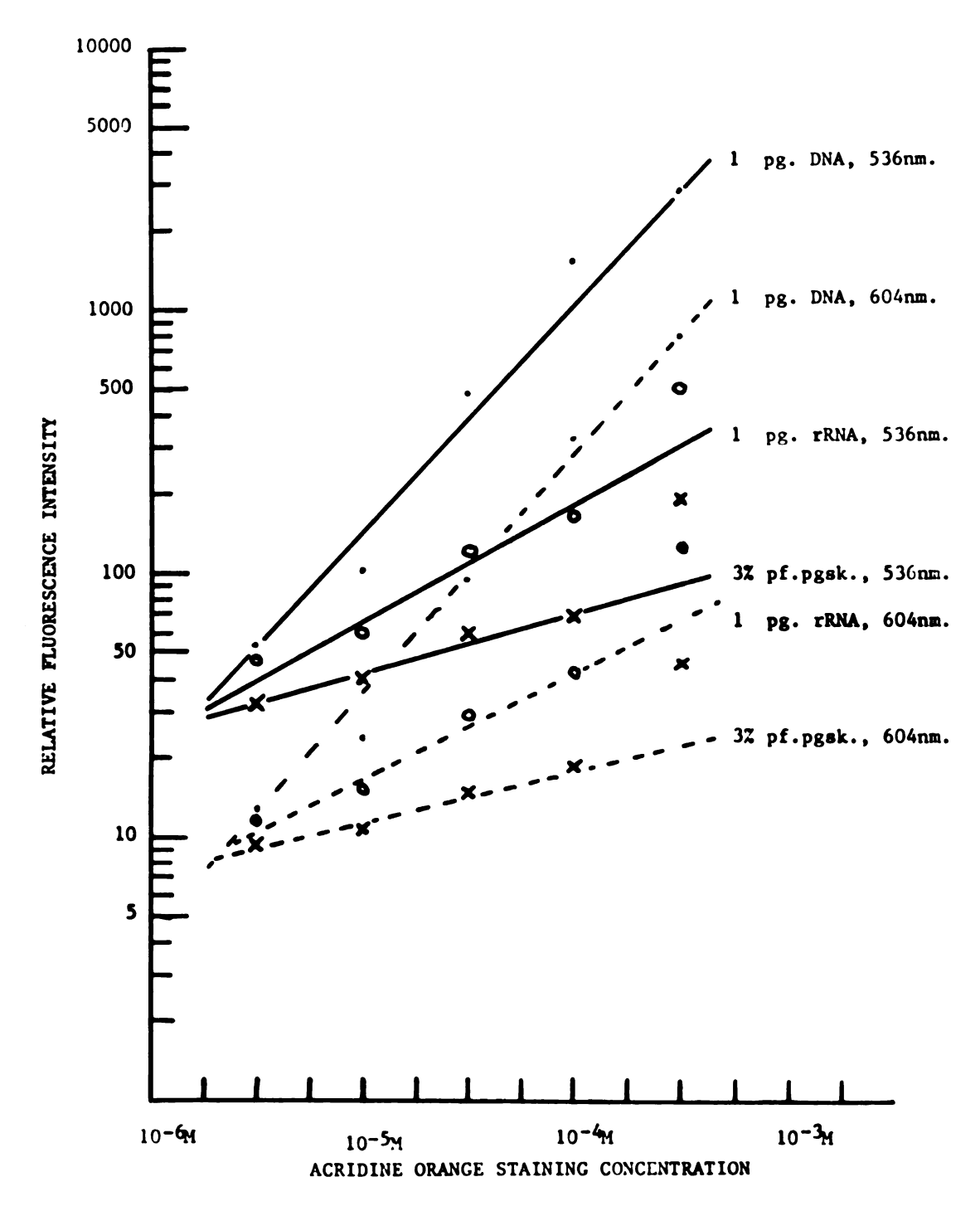


Figure 7. The average relative fluorescence intensities of AO-3% purified pigskin only and AO-NA complexes in 3% pf. pgsk. at 536 nm. and 604 nm. for different acridine orange staining concentrations (expressed in molarities), pH 4.1, staining time 15 minutes.

TABLE 2

The average relative fluorescence intensities of AO-3% purified pigskin only and AO-NA complexes in 3% pf. pgsk. at 536 nm. and 604 nm. for different acridine orange staining concentrations (expressed in molarities), pH 4.1, staining time 15 minutes.

Acridine	Orange	Concentrations
----------	--------	----------------

	5x10 ⁻⁶ M	1x10 ⁻⁵ M	5x10 ⁻⁵ M	1x10 ⁻⁴ M	5×10 ⁻⁴ M
3% pf. pgsk 536 nm. 604 nm.	32.5	40.3	59.2	69	194
	9.5	10.8	14.7	18.5	45.5
1.0 pg. rRNA - 536 nm.	47.3	59.5	122	165	503
604 nm.	11.8	15.3	29	42	127
1.0 pg. DNA - 536 nm.	54	102	480	1540	2825
604 nm.	13	24	95	325	790

where $m = 9.5 \times 10^3 / M$ AO, was 1.9 times the value of the slope for 1.0 pg. rRNA in 3% pf. pgsk. at the same wavelength. Further, the slope for 1.0 pg, rRNA in 3% pf, pgsk, $(m = 5.0 \times 10^3/M \text{ AO})$ was 2.2 times higher than the slope for 3% purified pigskin only at 536 nm., whose m equals 2.3 x 10^3 /M AO. At AO staining concentrations between 1 x 10^{-5} M and 5 x 10^{-4} M, the relative fluorescence intensities, at 536 nm. and at 604 nm., of 1.0 pg. DNA in 3% pf. pgsk, are greater than the corresponding intensities for 1.0 pg. rRNA in 3% pf. pgsk. However, at lower dye concentrations, the amount of AO bound to 1.0 pg. DNA in the monomer and aggregated form are equivalent to the amount of AO bound to 1.0 pg. rRNA, as indicated by the intersection of the lines for 1.0 pg. DNA and 1.0 pg. rRNA in 3% pf. pgsk. around 5 x 10^{-6} M AO. This suggests that certain regions within the DNA and rRNA conformations have equal capabilities for binding AO, and these regions are probably located on the surface or outer portions of the NA macromolecule. For each AO staining concentration, the relative fluorescence intensities, at 604 nm., of

each AO-NA complex, were sizeably less than their intensities at 536 nm., suggesting that within this AO staining concentration range (5 x 10^{-6} M - 5 x 10^{-4} M) AO binds to NA and to gelatin proteins preferentially in the monomer conformation. Although the results in Figure 7 are not enough to calculate binding constants for DNA and rRNA, they do suggest that the constant for each biopolymer may be different, such that the binding constant for a DNA macromolecule is greater than a rRNA macromolecule and, due to a greater number of binding sites and/or regions, the DNA macromolecule has the capacity to bind more AO molecules than has the rRNA macromolecule.

Figure 8 displays the degree of aggregation of AO on 1.0 pg. DNA and on 1.0 pg. rRNA as a function of the acridine orange staining concentration. This figure demonstrates that the degree of dye aggregation for DNA and rRNA depends upon the AO staining concentration, whereby increasing the amount of dve available for binding the NA augments the association of AO on the NA conformations. The degree of aggregation at $5 \times 10^{-4} M$ AO, for both DNA and rRNA, is only 1.7 times larger than their degrees of aggregation at $5 \times 10^{-6} M$. Therefore, to produce a small change (2x) in the degree of aggregation requires a large change in the staining concentration (100-fold). This implies that each DNA and rRNA macromolecule must contain a large amount of AO molecules to secure at least a degree of aggregation equal to 1, and, in order to evoke a red fluorescence, the degree of aggregation and the AO content per NA biopolymer must be tremendous. Therefore, for all practical purposes at an AO staining concentration between 5 x 10^{-6} M and 5 x 10^{-4} M, the degree of aggregation for rRNA (from 0.204 to 0.347) is equivalent to the degree of aggregation for DNA (from 0.214 to 0.372),

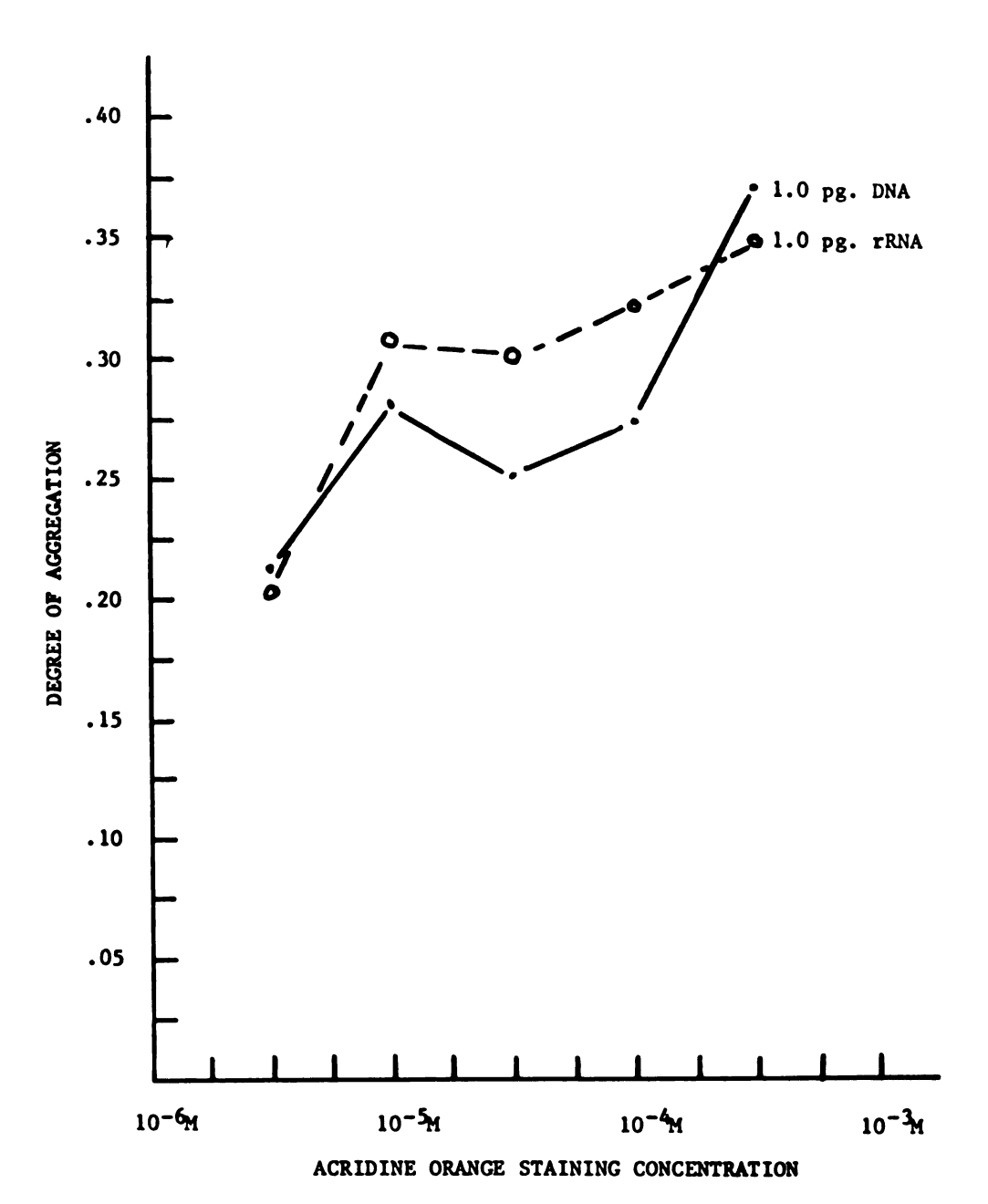


Figure 8. The degree of aggregation of AO onto 1.0 pg. DNA or rRNA in 3% pf. pgsk. for different acridine orange staining concentrations (expressed in molarities), pH 4.1, staining time 15 minutes.

and as the AO staining concentration increases, they both follow the same pattern. The author proposes that there are sites or regions within the DNA and rRNA conformations, specific for binding AO in the aggregated form, with similar binding behaviors as a function of the dye concentration.

Utilizing a fluorometer, West [1969; Zanker, 1952] measured the fluorescence of monomer acridine orange as a function of dye concentration. He found that in aqueous solutions (0.154M NaCl, pH 7) the fluorescence emission at 538 nm. is linear up to an AO concentration of 1×10^{-6} M. The slope was approximately equal to unity. More significantly, the emission at 538 nm. deviates from linearity (i.e., decreases) at higher AO concentrations, due to the formation of AO polymers. My results indicate that in gelatin microdroplets the fluorescence emission of monomer AO-NA complexes, as a function of dye concentration, is linear up to $5 \times 10^{-4} M$ AO, with a slope nearly equal to 1 x 10^4 /M for 1.0 pg. DNA and 0.5 x 10^4 /M for 1.0 pg. rRNA. Because of the rediffusion process (removal of free dye molecules) the reader should note that, within gelatin microdroplets, the actual AO concentration bound per NA macromolecule is much less than the AO staining concentration; this confines the interactions to dye molecules primarily bound by a macromolecule. In comparison, AO molecules free in aqueous solutions have greater diffusion rates than AO molecules bound and unbound to NA in gelatin microdroplets. Therefore, due to the lack of mobility and the medium. the collision rates of AO molecules bound to the inflexible NA macromolecules are negligible. This lowers the interaction between AO molecules considerably, thus limiting the formation of unbound AO polymers, i.e., free aggregates are washed away during

rediffusion. In addition, the results from Figures 7 and 8 indicate that within gelatin microdroplets the aggregation of AO onto a NA macromolecule may be proportional to the AO staining concentration. This suggests that there are specific binding sites on the DNA and rRNA macromolecule for independently binding AO in either the monomer or aggregated formations.

Rigler [1966] measured the degree of aggregation and the fluorescence of monomer AO at 530 nm. in a fixed tetraploid mouse fibroblast cell, as a function of AO staining concentration. He published results showing that the degree of aggregation increased to 0.53, while the fluorescence intensity at 530 nm. decreased by 25%, as the AO staining concentration increased from $1 \times 10^{-4} \text{M}$ to $1 \times 10^{-3} \text{M}$. As one might expect, unlike the simple gelatin microdroplet systems, the nuclear and cell membranes, along with other intracellular structures, served to concentrate the AO content within the fixed cell by obstructing the diffusion of excesses outside the cell. This increases the quantity of AO molecules per NA macromolecule which enhances aggregation. The quenching of the monomer AO fluorescence suggests an increased formation of unbound AO polymers. In the opinion of this author, the monomer AO formation is the primary mode of binding onto the NA biopolymers, and the disposition of each AO formation depends heavily upon microenvironmental conditions, such as the dye concentration.

2. The fluorescence changes of AO-NA complexes as a function of acridine orange staining time.

In this experiment, groups of microdroplets were subjected to different reaction intervals, while the rRNA or DNA contents analyzed

within each microdroplet, and the acridine orange concentration $(5 \times 10^{-5} \text{M})$ were held constant over the entire range of staining times (5 minutes to 120 minutes). The staining solutions and all other reaction solutions had a pH 4.1. The fluorescence spectra of the AO-DNA and AO-rRNA complexes were recorded from each microdroplet while irradiating at 400 nm. The average relative fluorescence intensities of AO bound to 1.0 pg. DNA or 1.0 pg. rRNA in 3% pf. pgsk., at 536 nm. and 604 nm. for each staining time are tabulated in Table 3 and graphically displayed, in a semilogarithmic plot, in Figure 9.

TABLE 3 The average relative fluorescence intensities of AO-NA complexes in 3% pf. pgsk. at 536 nm. and 604 nm. for different staining times (expressed in minutes), acridine orange staining concentration, $5 \times 10^{-5} M$, pH 4.1.

	Statisting stille								
	5m	1 Om	15m	30m	45m	60m	90m	120m	
3% pf. pgsk. -536 nm. -604 nm.	-	-	53.3 13.8	61.3 16	-	-	-	•	
1.0 pg. rRNA -536 nm. -604 nm.		71.3 21.8	68.3 17.5	81.5 22	98.5 22.5	96.5 24.5	131.5 28.5	145 30.5	
1.0 pg. DNA -536 nm. -604 nm.	366 74.5	400 88	435 80	634 124	715 153	-	825 190	990 255	

Staining Time

In Figure 9, the relative fluorescence intensities, at 536 nm. and 604 nm., for AO bound to 1.0 pg. DNA and 1.0 pg. rRNA in 3% pf. pgsk., demonstrated an enhancement along with prolonged reaction intervals. The relative fluorescence intensities of AO-rRNA complexes in 3% pf. pgsk. increased linearly, at 536 nm. and 604 nm., as a function

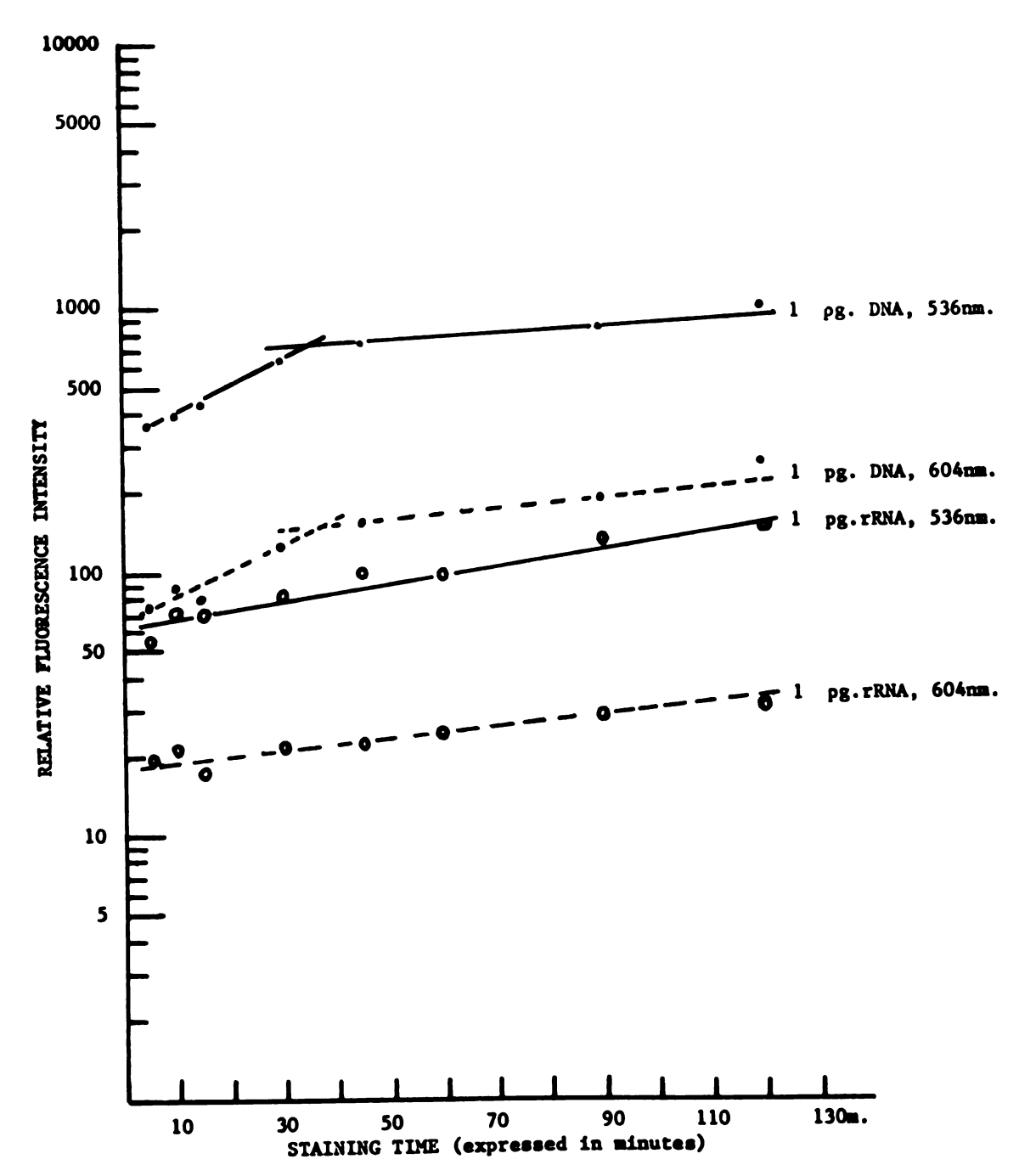


Figure 9. The average relative fluorescence intensities of AO-NA complexes in 3% pf. pgsk. at 536 nm. and 604 nm. for different staining times, AO staining concentration $5 \times 10^{-5} \, \text{M}$, pH 4.1.

of staining time, whereas the amount of AO bound to rRNA in the monomer and aggregated forms were proportional to the length of time, in minutes, the dye molecules were allowed to bind to the rRNA macromolecules. The slope of the line for AO bound to rRNA in the monomer form, at 536 nm., is equal to 2.9 x 10^{-3} /mins. of staining and is a little larger than the slope for AO bound to rRNA in the aggregated form at 604 nm. Contrarily, the relative fluorescence intensities of AO-DNA complexes, at 536 nm., rapidly doubled between 5 minutes and 35 minutes staining times with a slope equal to 9.8×10^{-3} /mins. of staining. Prolonging the staining time above 35 mins. changed the slope, such that the slope significantly decreased 86% of its original value, to 1.4 \times 10⁻³/mins. where, at the 120 mins. staining interval, the fluorescence intensity had only increased 1.3 times greater than its value at 35 mins. staining time. Clearly, two phases are involved in the binding of AO molecules to DNA macromolecules: during the first 35 mins. of staining, there is a rapid uptake of dye molecules by the DNA macromolecules; later, the rate of uptake of the dye molecules substantially decreases by more than 80% of the initial value. This suggests that there exist highly seductive binding sites within unique regions inside the DNA biopolymer, which promptly bind AO molecules in the monomer form; these sites, as a result of such binding, are capable of being completely filled within 35 mins. There are other regions, with hindered binding sites, that secure the dye molecules at a much slower rate. The slopes for DNA as compared to rRNA, infer that initially the binding rate for AO molecules onto the DNA macromolecules is approximately 3.4 times faster than the rate for rRNA--the binding rate is taken to be the quantity of AO molecules bound per minute in a specific conformation

per NA macromolecule. In addition, for each reaction interval, the fluorescence intensities of AO - 1.0 pg. rRNA and AO - 1.0 pg. DNA complexes at 536 nm. averaged 3.9 and 4.6 times greater, respectively, than the intensities at 604 nm.; and the fluorescence intensities of AO-DNA complexes averaged 6.2 times larger than the intensities of AO-rRNA complexes. These results conclude that AO molecules selectively bind to NA in the monomer form and the dye molecules preferentially bind to the DNA macromolecule rather than the rRNA macromolecule.

In comparison, the relative fluorescence intensity changes of AO-DNA complexes in gelatin microdroplets, as a function of staining time, in this study are similar to the results of AO-NA complexes in a tetraploid cell. Rigler [1966] published the fluorescence intensity changes of AO-NA complexes, in a fixed tetraploid mouse fibroblast cell, at 530 nm., as a function of staining time. He found that the average fluorescence intensity increased as the staining time increased from 15 mins. to 30 mins., having a slope equal to 1 x 10^{-2} /mins. Prolonging the staining time above 30 mins. to 100 mins. substantially decreased the fluorescence intensity, with a line having a negative slope equal to -2×10^{-3} /mins. During the initial 30 mins. of staining, the A0 molecules are quickly bound by all of the available monomer binding sites on the NA macromolecules. Above 30 mins. further uptake of the dye molecules increases the degree of aggregation, thus decreasing the monomer fluorescence at 530 mn. The graphic pattern for AO-NA complexes, as a function of staining time in tetraploid cells, is primarily due to the AO molecules binding to chromosomal DNA macromolecules in the monomer form, whereby the dye molecules readily bind to specific regions of high affinity inside the DNA conformation in less than 35 mins. The

binding rates of AO molecules in the monomer form to a DNA macromolecule are greater in a fixed teraploid mouse fibroblast cell than in a gelatin microdroplet. This elevation, reflected by different corresponding slopes in each of the environments, is principally due to the nuclear and cell membranes concentrating the intracellular AO content within the cell. This serves to increase the collision rates between the molecules, whereby the binding of the dye molecules onto the NA macromolecules in the monomer and aggregated forms is intensified considerably. Therefore, the amount of dye molecules bound to a DNA macromolecule depend more on the microenvironmental circumstances (specifically, the AO content per NA macromolecule in the intracellular environment versus that of a gelatin microdroplet) than the interaction time between the dye molecules and the DNA macromolecule.

3. The fluorescence changes of AO-NA complexes as a function of acridine orange staining solution pH.

Undoubtedly, the pH of the reaction solutions, i.e. the degree of ionization of the acridine orange and nucleic acid molecules, affect the binding of acridine orange onto the nucleic acids. In this experiment, groups of microdroplets were exposed to a variety of acridine orange staining solution pH. The rRNA or DNA contents analyzed within each microdroplet were held at 1.0 picograms. The AO staining concentration was held constant at 5 x 10^{-5} M, and the microdroplets were each stained for 30 mins. apiece. The pH of the rediffusion solutions were the same as the staining solution. After rediffusion, the emission spectrum of each microdroplet was recorded, with the microspectrophotometer, during irradiation at 400 nm. The average relative fluorescence

intensities of AO-DNA, AO-rRNA, and AO-gelatin protein complexes, at 536 nm. and 604 nm., for each AO staining solution pH, are tabulated in Table 4 and graphically displayed in a semilogarithmic plot in Figure 10.

TABLE 4

The average relative fluorescence intensities of 1.0 pg. DNA-AO and 1.0 pg. rRNA-AO complexes in 3% pf. pgsk., and gelatin protein-AO complexes of 3% purified pigskin only, at 536 nm. and 604 nm., for different acridine orange staining solution pH, AO staining concentration $5 \times 10^{-5} M$, staining time 30 mins.

		Staining Solution pH				
	pH 4.0	pH 5.7	pH 7.2	pH 8.4		
3% pf. pgsk 536 nm.		297 56.5	675 98	790 115		
1.0 pg. rRNA - 536 nm - 604 nm		943 133	3050 450	1990 240		
1.0 pg. DNA - 536 nm - 604 nm		3075 615	4170 850	7050 1150		

The relative fluorescence intensities of AO bound to NA and gelatin protein, at 536 nm. and 604 nm., exhibited an enlargement as a function of pH; see Figure 10. The fluorescence intensities of AO - 1.0 pg. DNA complexes in 3% pf. pgsk., at 536 nm., increased by 5.3 times, from a pH of 4.0 to 5.7, with a slope equal to 3.8×10^{-1} /pH. Above pH 5.7, the slope decreased by more than 65% (m = 1.2 x 10^{-1} /pH), while the fluorescence increased another 140% at pH 7.2, and over 200% at pH 8.4. The graphic pattern of the fluorescence intensities, at 604 nm., of AO-DNA complexes as a function of pH, is tantamount to the pattern at 536 nm.; however, at each pH unit, the fluorescence intensities at 604 nm. averaged 19% of the intensities at 536 nm. In addition, the relative fluorescence intensities for AO bound to 1.0 pg. rRNA in 3% pf.

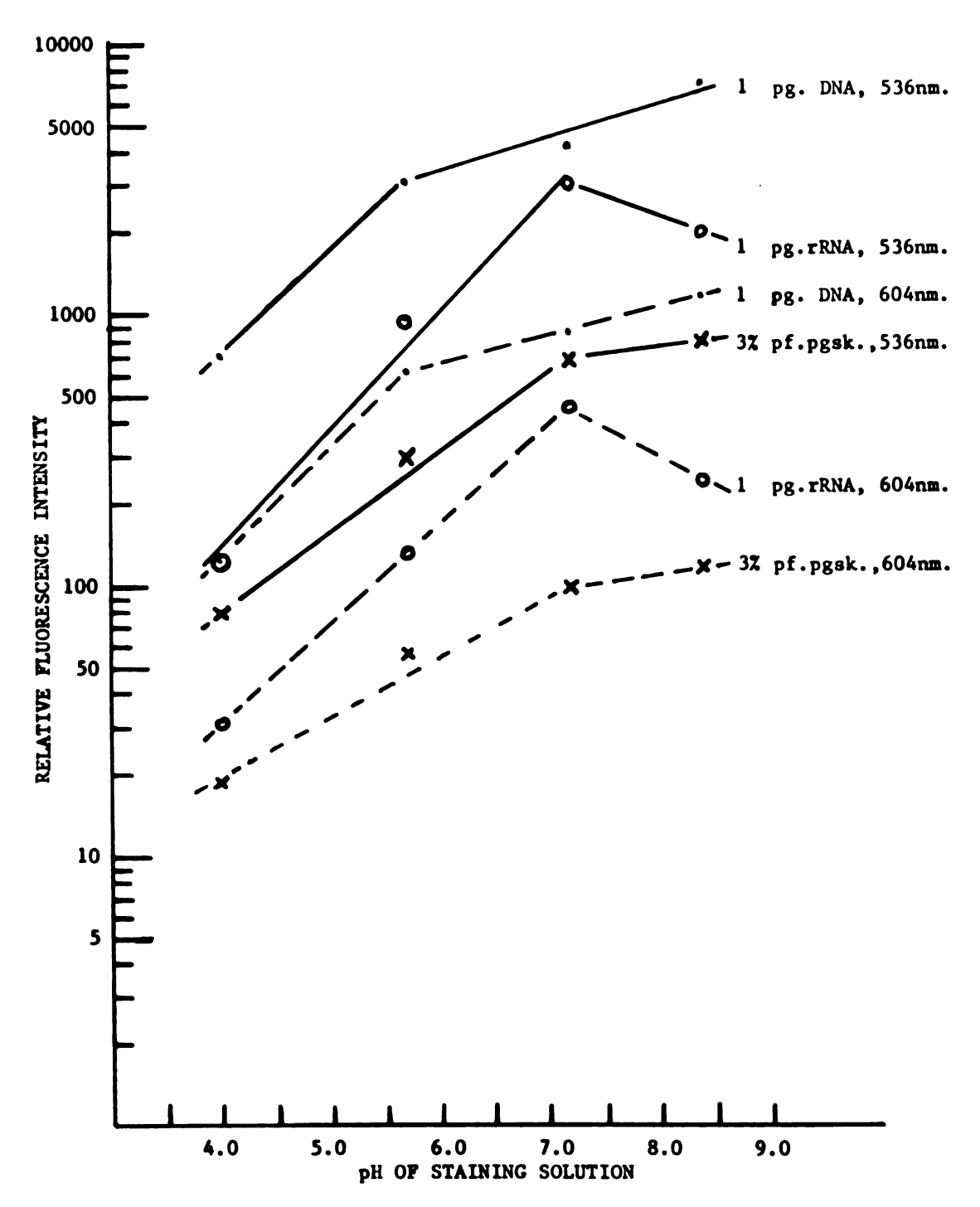


Figure 10. The average relative fluorescence intensities of 1.0 pg. DNA-AO and 1.0 pg. rRNA-AO complexes in 3% pf. pgsk., and gelatin protein-AO complexes of 3% pf. pgsk. only, at 536 nm. and 604 nm., for different acridine orange staining solution pH, AO staining concentration 5 x 10^{-5} M, staining time 30 mins..

pgsk., at 536 nm., itensified by 24.4 times, from pH 4.0 to 7.2, having a slope equal to 4.2×10^{-1} /pH. At pH 8.4 the fluorescence intensity decreased to 65% of it value at pH 7.2 and the slope changed its value to -1.8×10^{-1} /pH. The fluorescence intensity changes at 604 nm. for A0-rRNA complexes as a function of pH were the same as the changes at 536 nm., except the slopes were slightly lower and the fluorescence intensities at each pH were 12 to 25% of the 536 nm. values. It has been reported that AO exists as a cation completely ionized at pH 7 with a pK of 10.45 [Zanker, 1952; West, 1969]. The lower fluorescence intensities for AO-DNA and AO-rRNA complexes in 3% pf. pgsk. at acid pH are due to an augmented positive charge on the AO molecules and on the negative phosphoric acid residues of the NA nucleotides. This leads to an enhanced molecular repulsion, suppression of the NA dye binding sites, along with a slight denaturation of the NA macromolecule, thereby decreasing the binding of AO molecules to a NA macromolecule. Decreasing the positive charge concentration to neutral pH values maintains a relatively stable NA conformation and permits the phosphoric acid residues to become ionized [Levene and Simons, 1925]. This favors the molecular attraction and hydrophobic interactions of the NA nucleotides and AO molecules, thus increasing the binding of AO to the NA macromolecule. The dye molecules can readily form molecular complexes with the monomer and aggregated binding sites on the NA macromolecule, as hinted by an intensification of fluorescence for AO-DNA and AO-rRNA complexes in 3% pf. pgsk., at pH 7.2. The slopes for AO bound to 1.0 pg. DNA, between pH 4.0 and 5.7, at 536 nm. and 604 nm., are practically equivalent to the slopes for AO bound to 1.0 pg. rRNA, $m = 4.0 \times 10^{-1}/pH$, at the same wavelengths. These circumstances imply that between a pH of 4.0 and 5.7

the binding of AO to DNA and rRNA macromolecules uniformly increases as a function of pH. This uniformity in the binding behavior of AO to DNA and to rRNA macromolecules, between pH 4.0 and 5.7, is offset by dissimilar DNA and rRNA conformations. The dissimilar conformations are reflected by the slope of the lines deviations from 4×10^{-1} /pH at pH 5.7 for DNA, and pH 7.2 for rRNA as a function of pH, and the quantity of AO bound to the DNA conformation in the monomer and aggregated forms averaged 1.6 times greater than the rRNA conformation at pH 7.2, compared to 4.9 times greater at pH 4.0. These results suggest that the DNA conformation has a greater structural stability and capacity to bind AO molecules in both molecular forms, than the rRNA conformation, especially at low pH values.

Also, in Figure 10, the relative fluorescence intensities of A0-gelatin protein complexes (3% pf. pgsk. only), at 536 nm. and 604 nm., rise as a function of pH. The fluorescence intensity, for 536 nm., at pH 8.4 is 10 times greater than the intensity at pH 4.0, and 6 times greater than the intensity at pH 4.0 for 604 nm. It appears that the fluorescence intensities begin to plateau at pH 8.4, and the slope between pH 4.0 and 7.2 is 2.9 x 10⁻¹/pH at 536 nm. The lower fluorescence intensities at pH 4.0 are due to molecular interferences produced by an increased positive charge concentration. However, at higher pH values the A0 molecules can freely bind to unobstructed carboxylic groups in or near hydrophobic regions of the gelatin protein conformation. The slope at 536 nm. for A0 bound to gelatin protein, between 4.0 and 5.7, averaged 28% less than the slopes for A0 bound to NA, and the fluorescence amounts of A0 bound to the gelatin protein at each pH are considerably less than the amount of A0 bound to rRNA and DNA. This suggests that

specific types and/or conformations of macromolecules have distinctive behaviors in binding AO molecules. The binding rates of AO, as a function of pH to NA, are greater than the rates for gelatin proteins and the highly ordered DNA conformation, and to a lesser extent, the rRNA conformation have higher potentials for binding AO molecules than has the gelatin protein conformation. The fluorescence intensities, at 536 nm., for AO bound to gelatin protein, are significantly greater, in comparison, than the intensities at 604 nm., demonstrating that AO predominantly binds to gelatin proteins in the monomer form.

The degree of dye aggregation on DNA and rRNA macromolecules changes as a function of pH; see Figure 11. The degree to which AO aggregates onto rRNA macromolecules decreased by 54%, from 0.35 at pH 4.0 to 0.19 at pH 7.2, and another 14% at pH 8.4. In addition, the degree of aggregation for rRNA macromolecules at pH 4.0 is 1.6 times larger than the value for DNA macromolecules. This indicates that lowering the pH disturbs the less stable rRNA conformation, thus changing the hydrophobic microenvironment of the helical regions capable of binding AO in the monomer form. (These regions may not necessarily have the same fine structure as the DNA double helix.) This lowers the number of binding sites on the rRNA conformation that ordinarily bind AO in the monomer form. Concurrently, the binding sites for AO in the aggregated form are undisturbed, thereby increasing the ratio for the degree of aggregation at low pH. The degree of aggregation for 1.0 pq. DNA increases by 27%, from 0.22 at pH 4.0 to 0.28 at pH 7.2, and is 1.5 times greater than the value for 1.0 pg. rRNA at pH 7.2. It then decreases to 0.22 at pH 8.4. In contrast, the hydrogen bonds in the hydrophobic interior of the DNA double helix are intact at pH values

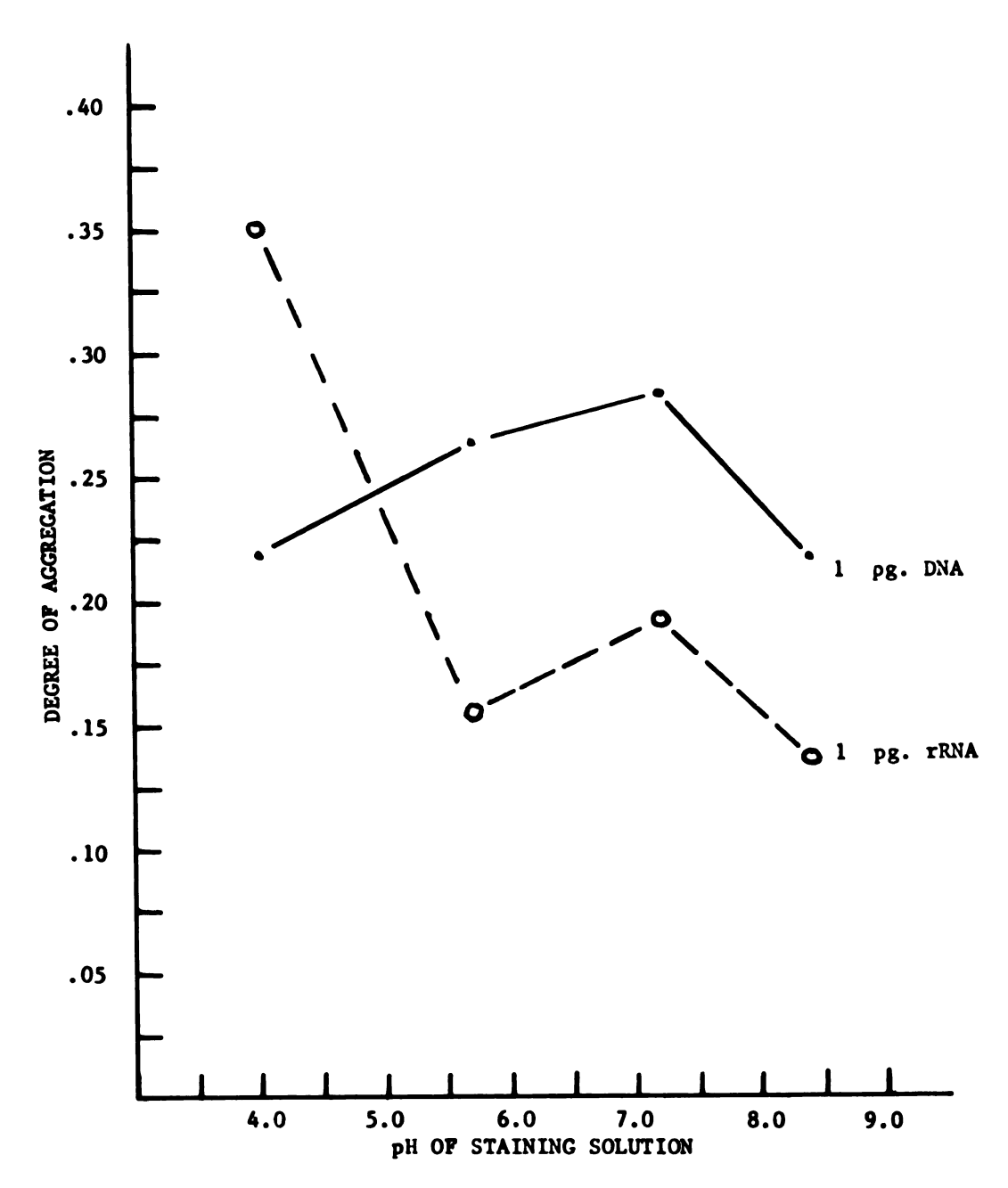


Figure 11. The degree of aggregation of AO onto 1.0 pg. DNA or rRNA in 3% pf. pgsk. for different acridine orange staining solution pH, AO staining concentrations 5 x 10^{-5} M, staining time 30 mins..

above 4.0 and are reversibly destroyed at pH values below 4.0. Therefore, between pH 4.0 and 8.4, the AO monomer binding sites on the more stable DNA conformation are unimpaired, and are located in similar microenvironments. Once the AO monomer binding sites in a NA conformation are filled, further binding of the dye molecules are in the aggregate mode of binding. Since the AO monomer binding sites were nearly all full, any variations in the binding of AO to the DNA conformation above pH 4.0 would be in the aggregated mode and would depend upon the ionic interactions of the dye molecules and DNA nucleotides, and less on hydrophobic interactions. Enhancing the positive charge concentration disrupts the binding of AO molecules to the DNA macromolecules, thus reducing dye aggregation. Enhancing the negative charge concentration favors the binding of AO to DNA, thus increasing the dye aggregation. The degree of aggregation, at each pH value, for 1.0 pg. DNA and 1.0 pg. rRNA is less than 0.36, indicating that AO preferentially binds to DNA and rRNA in the monomer mode.

Langridge et al [1957; West, 1969] reported that, for the living cell, the intranuclear pH is 7.6-7.8, while the cytoplasmic pH is 6.8. Digesting the microdroplet results, the author concludes that the intracellular pH values would allow for optimal binding of AO to NA in the living neuron. Along with the nuclear and cellular membranes, the binding of AO to the intracellular NA would greatly increase, resulting in a tremendous dye-to-nucleotide ratio. The amount of AO bound per NA macromolecule would make the degree of aggregation large enough to produce orange to red colors, provided the staining conditions are appropriate.

4. The fluorescence intensity changes of AO-NA complexes as a function of NaCl content.

The ionic strength of the molecular microenvironment should have profound effects on the binding behavior of acridine orange molecules to a NA macromolecule, since acridine orange not only binds to NA via hydrophobic interactions, but also by a strong ionic bond between the positive charged dimethylamino group of the acridine orange ring and the negative charged phosphoric acid group of a NA nucleotide. In order to study these effects, different amount of NaCl were embedded in gelatin microdroplets and analyzed along with 0.5 pg. DNA or 1.0 pg. rRNA. Each microdroplet was stained with 5 \times 10^{-5} M acridine orange for 30 mins. at a pH of 4.1. To avoid complications, the ionic strength and pH of all of the reaction solutions were held constant throughout the entire experiment. The emission spectrum of each microdroplet was recorded with the microspectrophotometer, while exciting at 400 nm. The average relative fluorescence intensities of AO-DNA, AO-rRNA, and AO-gelatin protein complexes, at 536 nm. and 604 nm., for a particular NaCl content, are tabulated in Table 5 and graphically displayed in a semilogarithmic plot in Figure 12.

Figure 12 demonstrates that the fluorescence intensity of AO bound to 0.5 pg. DNA and 1.0 pg. rRNA in 3% pf. pgsk., and to 3% pf. pgsk. only, at 536 nm. and 604 nm., is dependent upon the NaCl content within the microdroplet. The average fluorescence intensities of monomer AO-DNA complexes rapidly increased from 0.00 pg. NaCl to 98% of its maximum value at 29.5 pg. NaCl, having a slope equal to 4.0×10^{-2} /pg. NaCl. Above 29.5 pg. NaCl, the slope decreased dramatically to a plateau. Dissimilarly, the plots for AO-rRNA complexes never plateau. The

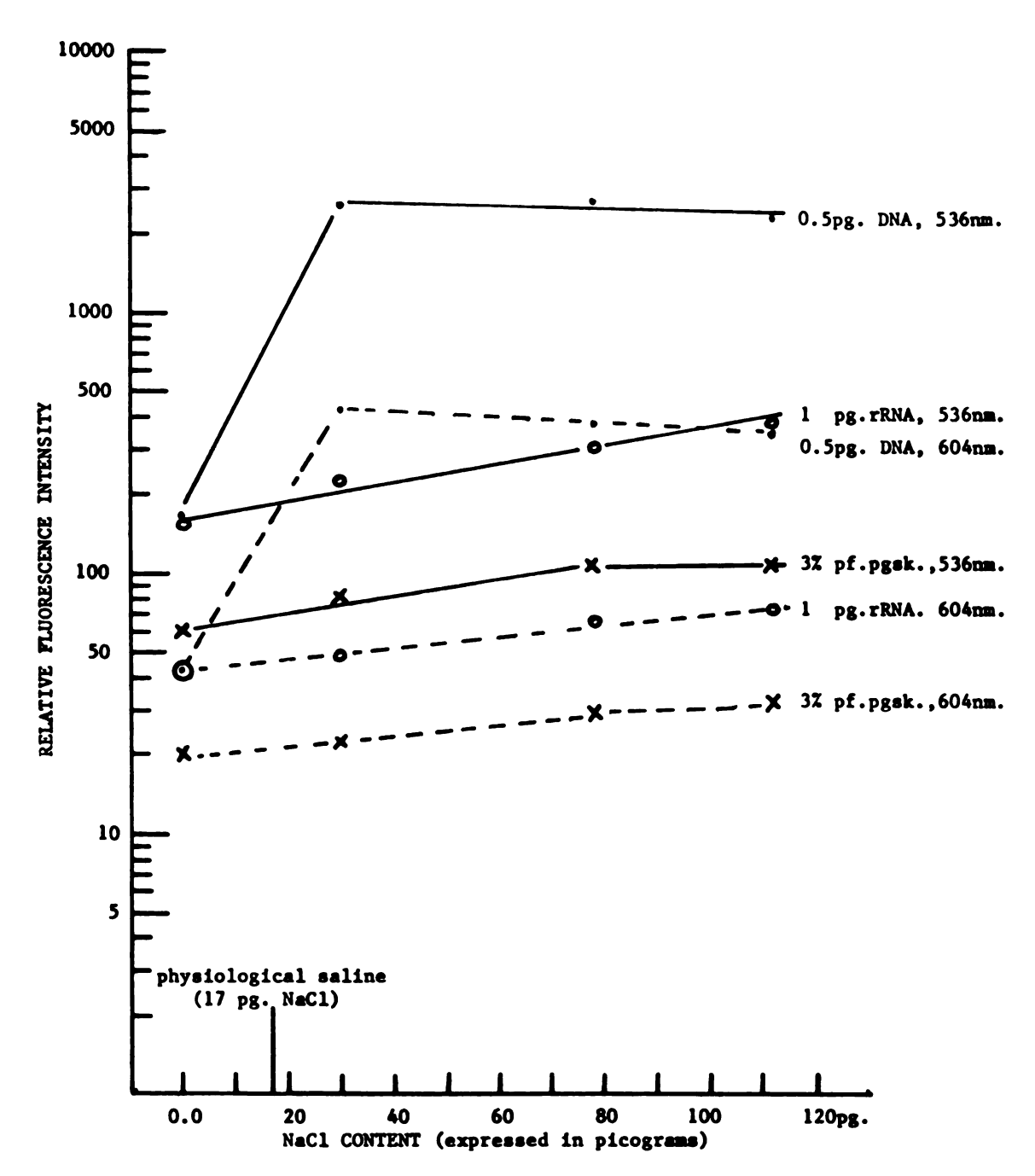


Figure 12. The average relative fluorescence intensities of 0.5 pg. DNA-AO and 1.0 pg. rRNA-AO complexes in 3% pf. pgsk. and gelatin protein AO complexes of 3% pf. pgsk. only, at 536 nm. and 604 nm., for various NaCl contents (expressed in picograms), AO staining concentration $5 \times 10^{-5} \text{M}$, staining time 30 mins., pli 4.1.

TABLE 5

The average relative fluorescence intensities of 0.5 pg. DNA-AO complexes and 1.0 pg. rRNA-AO complexes in 3% pf. pgsk. and gelatin protein-AO complexes of 3% pf. pgsk., at 536 nm. and 604 nm., for various NaCl contents expressed in picograms, AO staining concentration 5×10^{-5} M, staining time 30 mins., pH 4.1.

	NaCl Content				
	0.00 pg.	29.5 pg.	78.3 pg.	111.7 pg.	
3% pf. pgsk 536 nm.	61.2	81.5	105	106	
- 604 nm.	20.5	22.5	28.5	31.5	
1.0 pg. rRNA - 536 nm.	154	223	298	367	
- 604 nm.	42.5	47.5	65	71	
0.5 pg. DNA - 536 nm.	166	2580	2640	2220	
- 604 nm.	42.5	4 20	370	340	

average fluorescence intensities increased gradually from a minimum value. at 0.00 pq. NaCl, to a maximum value 2.4 times larger, at about 112 pg. NaCl, having a slope of 3.3 x 10^{-3} /pg. NaCl. These results suggest that increasing the NaCl content elevates the ionic strength within the external microenvironment of the NA macromolecules. This serves to fortify and enhance the hydrophobic interactions between the acridine and nucleotide base ring structures within the interior of the NA macromolecule, thus increasing the binding of AO to NA in the monomer form via hydrophobic bonding. Even though the DNA content was 50% less than the rRNA content, the binding of acridine orange, due to the differences in the two NA conformations, was still satisfactorily manifested by different fluorescence intensities and slopes. At equivalent amounts of NaCl. the fluorescence intensities for AO-DNA complexes were significantly greater than the intensities for rRNA, at 536 nm. and 604 nm., and the initial slope for monomer AO-DNA complexes was approximately 12 times larger than the slope for monomer AO-rRNA

complexes indicating that acridine orange discriminately binds to the DNA conformation over the rRNA conformation. The average fluorescence intensities of A0-gelatin protein complexes at 536 nm. gradually increased, as a function of the NaC1 content, from 0.00 to 78.3 pg. NaC1, having a slope equal to 3.2×10^{-3} /pg. NaC1. This implies that the increased binding of A0 to gelatin proteins, in the monomer form, may be due primarily to elevated interactions between the hydrophobic regions within the protein conformation and the ring structures of the acridine orange molecules. As reflected by similar initial slopes (3×10^{-3} /pg. NaC1), the binding behavior of A0 to gelatin proteins, as a function of the NaC1 concentration, is synonymous to that of rRNA, suggesting that there may be similarities in their structures while binding acridine orange in the presence of ions.

Since the degree of structural order of nucleic acids is decreased at low ionic strengths [Rigler, 1966], varying the ionic strength of the external environment of DNA and rRNA macromolecules would change their conformations and their internal microenvironments. The results displayed in Figure 12 show that the binding behavior of acridine orange to DNA, rRNA, and gelatin proteins relies heavily on the ions in the external environment of the macromolecules. Further, the lowest NaCl concentration that allows for the maximum binding of AO to each macromolecule is different. Note that the NaCl content of physiological saline is well below the plateau point for each macromolecule, and the DNA conformation is the lowest, at 29.5 pg. NaCl, suggesting greater stability, and structural order at lower ionic strengths.

The aggregation of AO molecules onto DNA and rRNA macromolecules depends on the ionic strength of the microenvironment (see Figure 13).

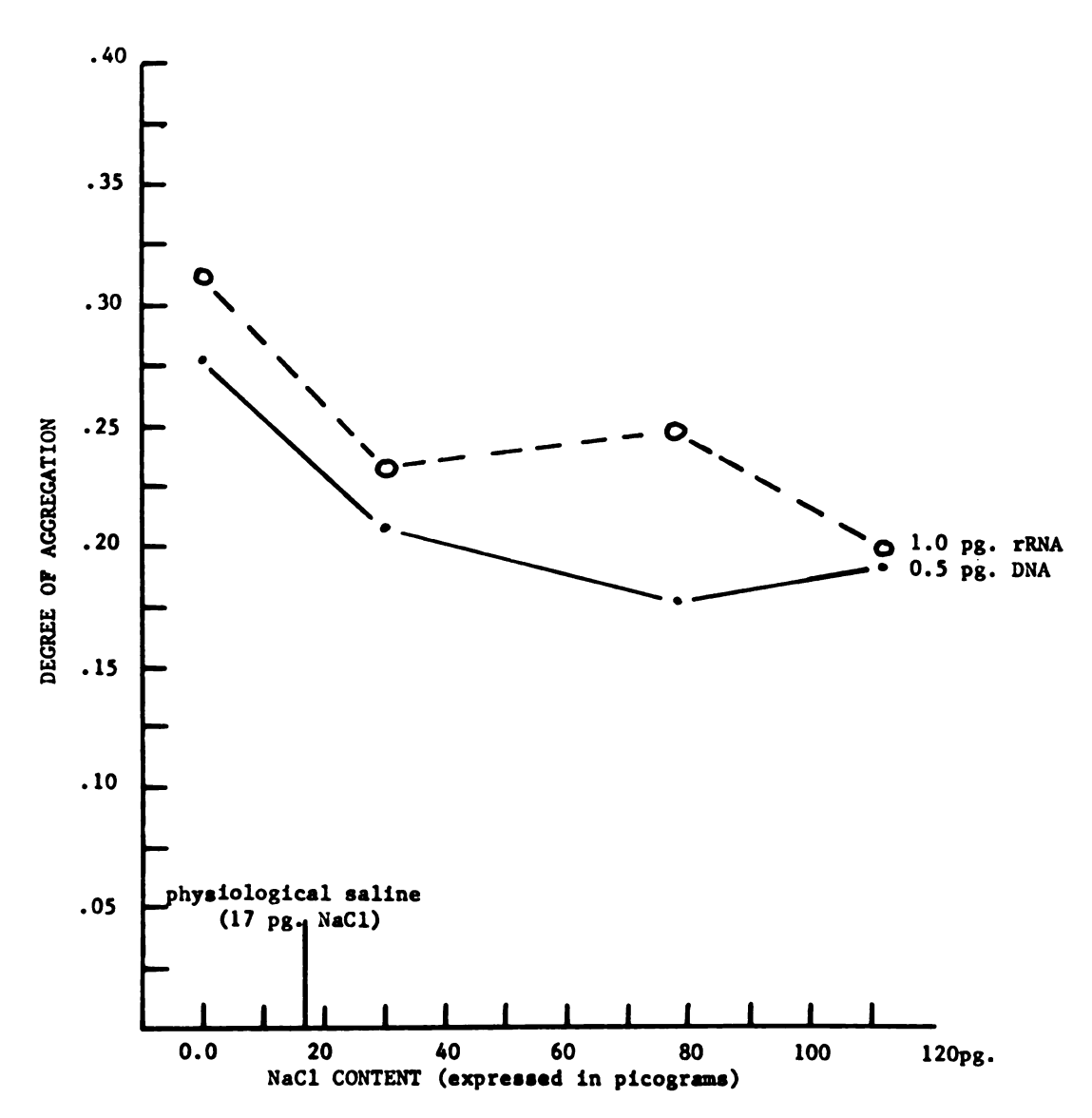


Figure 13. The degree of aggregation of AO onto 0.5 pg. DNA or 1.0 pg. rRNA in 3% pf. pgsk. for various NaCl contents, AO staining concentration 5 x 10^{-5} M, staining time 30 mins., pH 4.1.

The degree of dye aggregation on 0.5 pg. DNA and 1.0 pg. rRNA decreased as the NaCl content within the external environment increased. The degree of AO aggregation for rRNA decreased from 0.312, at 0.0 pg. NaCl, to 0.199. at 112 pg. NaCl. a reduction of 36%. The degree of AO aggregation for DNA decreased from 0.278 at 0.00 pg. NaCl to 0.192 at 112 pg. NaCl, a reduction of 31%, suggesting that the lower tendency of AO to aggregate, at a high ionic strength, on DNA and rRNA macromolecules may be induced by the increased interaction of ions with equal charge (NA⁺). The pattern of the degree of AO aggregation on rRNA as a function of the NaCl content is similar to the pattern for DNA, implying that AO aggregates on both macromolecules in similar regions and modes. However, the degree of dye aggregation on rRNA at each NaCl concentration averaged 17% larger than DNA, suggesting that AO has a slightly higher tendency to aggregate on the rRNA conformation than the DNA conformation. The aggregating behavior of AO onto DNA and rRNA, as a function of the NaCl content, is in contraposition to the binding behavior of AO to DNA and rRNA in the monomer form. This is evidenced when a 100-fold increase in the NaCl concentration produces a small decrease in the degree of dye aggregation on DNA and rRNA, versus a very large increase in the binding of AO to DNA and rRNA in the monomer form. The degree of dye aggregation on rRNA and DNA never exceeded 0.35, accompanied by significantly greater fluorescence intensities at 536 nm. than at 604 nm., concluding that the binding of AO to DNA and rRNA is predominantly in the monomer form and is sensitive to ions within the microenvironment.

Rigler [1966] examined the effects of the ionic strength of the reaction solution upon the degree of AO aggregation and fluorescence intensity, at 530 nm., of a mouse fibroblast cell. He found that an

increase in the ionic strength caused a rapid increase of the fluorescence intensity at 530 nm. and a simultaneous decrease in the degree of dye aggregation. Rigler's results were analogous to the author's, in that the aggregation of AO onto NA in mouse fibroblast cells and in gelatin microdroplets was inversely proportional to the ionic strength, and the binding of AO in the monomer from had an opposite behavior.

5. The fluorescence intensities of AO-rRNA complexes at various microdroplet forming solution temperatures.

The binding of AO molecules to a particular NA macromolecule depends upon the NA native and denatured conformations. Raising the temperature of the microdroplet forming solution results in the denaturation of the NA macromolecules contained in the solution. In this experiment, various microdroplet forming solutions containing rRNA were slowly raised to different denaturation temperatures. The solutions were held at a specific temperature for 3 mins.; immediately afterwards, the droplets were formed and cooled rapidly. The rRNA content analyzed in each microdroplet was 1.0 picograms. Each microdroplet was stained with 5 x 10^{-5} M acridine orange for 30 mins. at a pH of 4.1. The emission spectrum of each microdroplet was recorded with the microspectrophotometer, while exciting at 400 nm. The average relative fluorescence intensities of AO-rRNA complexes in 3% purified pigskin, at 536 nm. and 604 nm., for a particular forming solution temperature are tabulated in Table 6.

Table 6 shows that a relative large increase in the microdroplet forming solution temperature produced only a small increase in the fluorescence intensities of AO bound to 1.0 pg. rRNA in 3% pf. pgsk.,

TABLE 6

The average relative fluorescence intensities of 1.0 pg. rRNA-AO complexes in 3% pf. pgsk., at 536 nm. and 604 nm., for various microdroplet forming solution temperatures, AO staining concentration 5×10^{-5} M, at pH 4.1, staining time 30 mins.

			Forming	Solution	${\bf Temperatures}$
			55°C	82°C	100°C
1.0 p	g. rRNA	- 536 604	85 20	86 23	100 27

536 nm. and 604 nm. As the temperature increased from 55°C to 82°C, the fluorescence intensity increased only 1% at 536 nm. and 15% at 604 nm. Increasing the temperature further, to 100°C, increased the fluorescence at 536 nm. by 16% and at 604 nm. another 17%. In addition, the fluorescence intensities of A0-rRNA complexes at 536 nm. averaged 3.9 times greater than the intensities at 604 nm. These results suggest that a rRNA conformation of low structural order of a completely denatured rRNA macromolecule (at 100°C) has a slightly larger capacity to bind A0, preferentially in the monomer form, than a rRNA conformation of higher structural order having a less disarranged conformation (55°C). This was in contrast to the expectation that an ordered rRNA conformation should bind more A0 molecules in the monomer form than a random rRNA structure. Unfortunately, there is not sufficient data to give a comprehensive explanation.

6. The fluorescence intensity changes of AO-NA, gelatin-protein complexes during continuous irradiation.

Like many other fluorescent molecular probes, i.e. small planar dye molecules, the fluorescence emission of acridine orange slowly

diminishes during electronic perturbation of excitation wavelength. The concern of this experiment was the establishment of the fluorescence decay behavior of acridine orange bound to NA and gelatin proteins in the monomer and aggregated forms, as a function of excitation time. Since the emission maxima of acridine orange fluorescence spectra are invariable with respect to the irradiation time, the 536 nm. and 604 nm. wavelengths were chosen as the emission wavelengths at which a measurement of fluorescence emission amplitude was taken at various irradiation intervals. The excitation, 400 nm., was continuous throughout the course of the measurements. The contents analyzed in each microdroplet were either 0.5 pg. DNA in 3% pf. pgsk., 1.0 pg. rRNA in 3% pf. pgsk., or 3% purified pigskin only, and were stained with $5 \times 10^{-5} M$ acridine orange for 30 mins, at a pH of 4.1. The average relative fluorescence intensities of AO-DNA, AO-rRNA, and AO-gelatin protein complexes, at 536 nm. and 604 nm., as a function of the irradiation interval. are graphically displayed in Figure 14. The intensities are normalized to the instantaneous fluorescence emission amplitude at time zero.

The curves shown in Figure 14 exhibit that, as a consequence of an extended irradiation time, there is a decrement in the fluorescence intensities, at 536 nm. and 604 nm., of AO bound to DNA, rRNA, and gelatin protein macromolecules in 3% purified pigskin microdroplets. The two fluorescence molecular species of acridine orange, the monomer and aggregated forms, have different fluorescence decay behaviors as a function of the irradiation time: the fluorescence fading of AO-DNA, rRNA, and gelatin protein complexes at 536 nm. displays somewhat faster decay rates than the corresponding fluorescence fading at 604 nm., depreciating over 50% of the initial fluorescence intensities at time

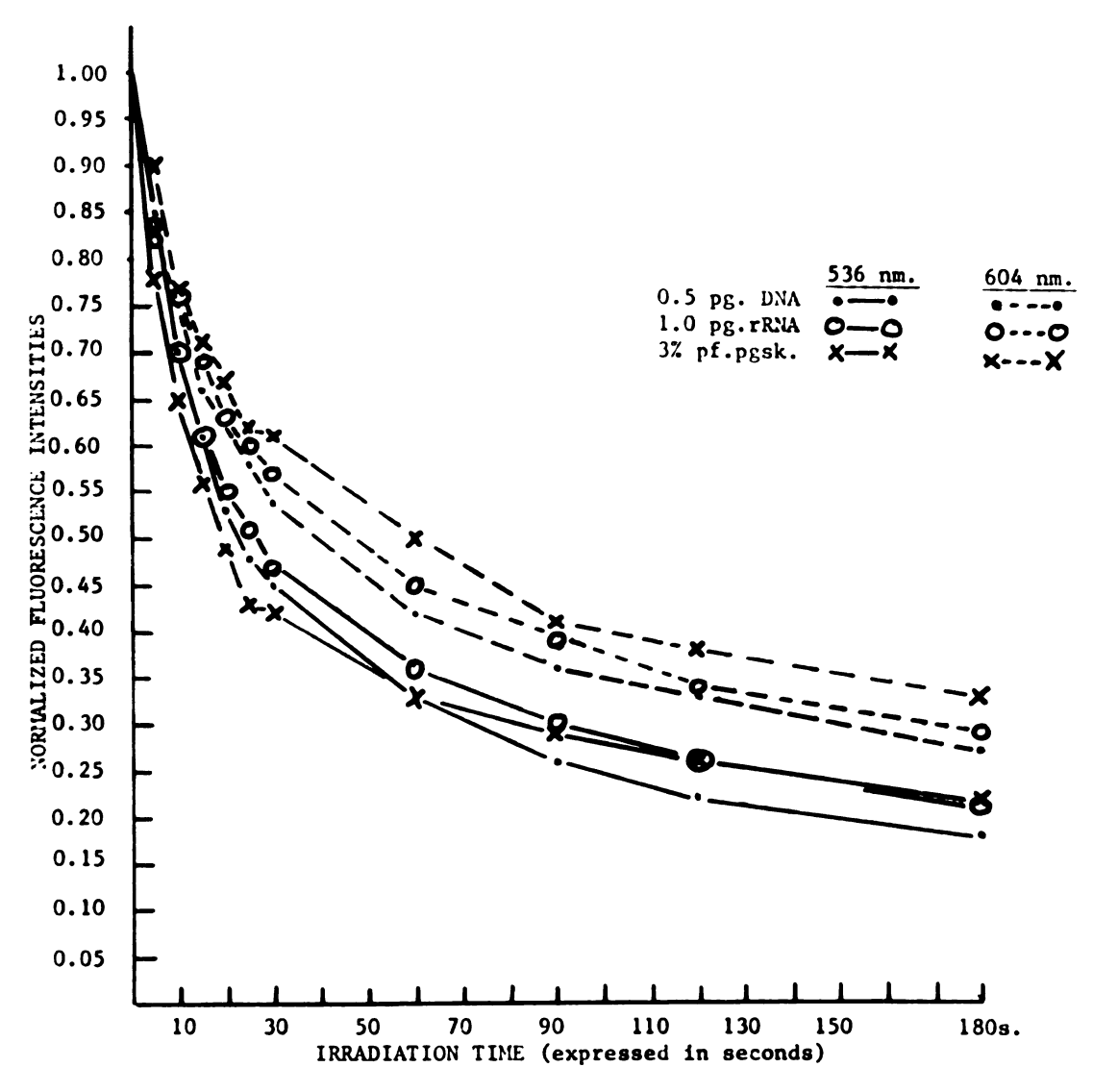


Figure 14. Fluorescence decay of AO-NA complexes, at 536 nm. and 604 nm., as function of the irradiation time, AO concentration 5 x 10^{-5} M, pH 4.1, staining time 30 mins., excitation wavelength 400 nm..

zero after 30 sec. of irradiation for 536 nm., versus 60 sec. of irradiation for 604 nm. The fluorescence decay behavior of AO-DNA complexes, at 536 nm. and 604 nm., resembles quite closely the fading behavior of AO-rRNA complexes at the same wavelengths. Where, after 10 sec. of irradiation, the fluorescence intensities of AO-DNA and A0-rRNA complexes rapidly decline from 1.00 to 0.70 at 536 nm., and to 0.76 at 604 nm., increasing the irradiation time to 30 sec., moderately decreased the emission, further, to approximately 0.46 at 536 nm. and to 0.56 at 604 nm. At a slower decay rate, the fluorescence intensities of AO-DNA and AO-rRNA complexes faded roughly to 0.35 at 536 nm. and to 0.44 at 604 nm. following 60 sec. of irradiation. Finally, after 3 mins. of continuous excitation, the fluorescence emission of AO bound to either DNA or rRNA macromolecules gradually decayed to nearly 20%, at 536 nm. and 28%, at 604 nm. of their original values at time zero. Similarly, the fluorescence decay behavior of AO gelatin protein complexes at 536 nm. and 604 nm. parallels that of AO-NA complexes at the same wavelength. These results suggest that the fluorescence decay behavior of AO molecules bound to a biopolymer, as a function of the irradiation time, is more dependent on the binding mode of acridine orange, the monomer or aggregated forms, than on the conformation or type of the biopolymer.

Comparatively, the results presented here are similar to the results obtained from single cells stained with acridine orange. West and Lorincz [1973] studied the fluorescence intensity changes of living human leukocytes, containing 1.05×10^{-14} moles AO/cell, at 540 nm. and 660 nm., as a function of the irradiation time. They found that the fluorescence fading at 660 nm., during irradiation with exciting

light, diminished at a slower rate than the fluorescence at 540 nm. The fluorescence intensities at 660 nm. and 540 nm. decline to almost 50% and 40%, respectively, of their original values at time zero, after 25 secs. of irradiation. Continuing the irradiation time to 50 secs. decreased the fluorescence emission roughly 5% at 660 nm. and 10% at 540 nm. The results of West and Lorincz were analogous to the author's, in that the fluorescent molecular species of acridine orange differed from each other on the basis of fluorescence fading. The fluorescent dacay behavior of A0 bound in the monomer form, as a function of time, fades at a faster rate than that of A0 bound in the aggregated form. From our results we infer that the two binding modes of A0 (the monomer and aggregated forms) are independent of each other and photochemically differentiable (i.e., fading), regardless of the microenvironment or the conformation of the biopolymer.

7. The fluorescence intensity changes of AO-NA complexes as a function of the nucleic acid concentration, and the quantitative determination of nucleic acids contained in a given microenvironment.

In collating the two molecular species of acridine orange, the monomer complex was found to be more sufficient as a fluorescent molecular probe for the detection of nucleic acids than was the aggregated complex. The previous experiments established that AO predominantly binds to DNA, rRNA, and Poly U in the monomer form with a small degree of aggregation. The AO molecules bound to a NA macromolecule in the monomer form are more stable and less sensitive to variations in the microenvironment, i.e. changes in the pH, temperature and ionic strength, than when the dye molecules are bound in the aggregated form. In this

experiment, gelatin microdroplets containing different amounts of rRNA and/or DNA were treated to identical staining conditions. The AO staining concentration was $5 \times 10^{-5} M$, and each microdroplet was stained for 30 mins. The pH of the staining and rediffusion solutions was 4.1. The fluorescence spectrum of each microdroplet was recorded with the microspectrophotometer, during irradiation with 400 nm. exciting light. The average relative fluorescence intensities of AO bound to DNA or rRNA in 3% pf. pgsk., at 536 nm. and 604 nm., for a particular DNA or rRNA concentration are tabulated in Table 7 and graphically displayed in a semilogarithmic plot, in Figures 15 and 16.

TABLE 7 The average relative fluorescence intensities of AO bound to DNA or rRNA, at 536 nm. and 604 nm., in 3% pf. pgsk. for various DNA and rRNA concentration, AO staining concentration 5 x 10^{-5} M, staining time 30 mins., pH 4.1.

		DNA and rRNA Concentration (exp. in pg.)					
	0.00	0.09	0.18	0.38	0.59	0.80	1.00
DNA - 536 nm. - 604 nm.	63.5 17.2	77.5 22.0	84 23.5	144 31.5	295 61.0	485 98.0	875 210
rRNA - 536 nm. - 604 nm.	68.3 18.3	58.5 16.0	61.5 16.0	73.5 19.5	96.0 27.5	134 32.5	115 25
	rRNA Concentration (exp. in pg.)						
	0.00	0.51	1.00	1.90	2.95	3.99	5.04
rRNA - 536 nm. - 604 nm.	53.2 16.2	86.0 22.5	121 30.0	197 41. 0	373 67.5	1160 210	1460 285

The relative fluorescence intensities, represented in Figure 15, of AO-DNA complexes in 3% purified pigskin, at 536 nm., were found to increase linearly as the DNA concentration increased from 0.00 pg. to

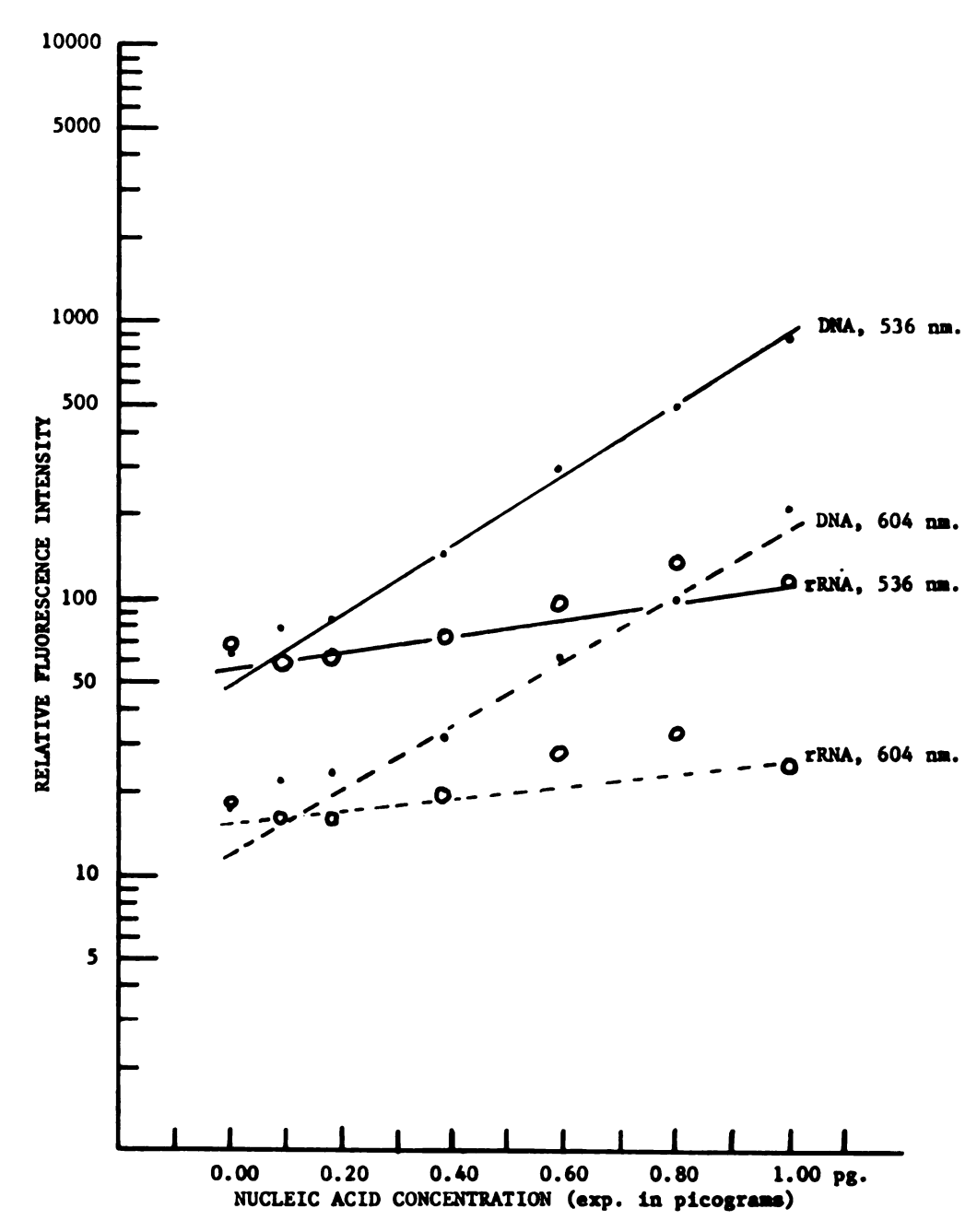


Figure 15. The average relative fluorescence intensities of AO bound to DNA or rRNA, at 536 nm. and 604 nm., in 3Z pf. pgsk. for various DNA or rRNA concentrations, AO staining concentration 5 x 10^{-5} M, staining time 30 mins., pH 4.1.

1.00 pg. The equation of the line, eq. 1, is as follows:

$$\log F_{536}^{DNA} = m_{DNA}(pg. DNA) + \log b$$
 (1)

where $\log F_{536}^{DNA}$ is the logarithm of the fluorescence intensity, at 536 nm., of a microdroplet containing only DNA; m_{DNA} is the slope of the line; (pg. DNA) is the quantity of DNA contained in the microdroplet expressed in picograms; and log b is the logarithm of the fluorescence intensity, at 536 nm., of the microdroplet containing no DNA. The line has a slope, m_{DNA} , equal to 1.26/pg. DNA. This means that the total amount of AO bound to the DNA macromolecules is proportional to the quantity of DNA available for binding the dye molecules, implying that a DNA macromolecule has a specific number of binding sites for AO molecules in the monomer form. As a function of the acridine orange concentration, the fluorescence emission of monomer AO molecules linearly increases until the polymerization of the dye molecules occurs, and, whenever bound to NA macromolecules, the fluorescence emission of monomer AO molecules are independent and unaffected by the emission of aggregated AO molecules [West, 1969]. In addition, since the effects of unbound excess dye molecules are eliminated from the system, equation (1) can be used to determine any amount of DNA contained in a 3% pf. pgsk. microdroplet, where the amount of DNA (in picograms) is equal to $(\log F_{536}^{DNA} - \log b)/m_{DNA}$. Displayed in Figure 15 are the fluorescence intensities of AO-rRNA complexes, at 536 nm. in 3% pf. pgsk. as a function of the rRNA concentration, where the fluorescence intensity proportionally increased 1.7 times as the rRNA concentration increased from 0.00 pg. to 1.00 pg. rRNA. In comparison, the fluorescence intensities of AO bound to 1.00 pg. DNA at 536 nm. and at 604 nm. averaged

eight times greater than the corresponding intensities of AO bound to rRNA at the same concentration, indicating that a DNA macromolecule has a significantly greater number of AO binding sites, in the monomer and aggregated forms, than does a rRNA macromolecule. These results suggest that with my methodology, the smallest amounts of nucleic acids, easily detectable, are about 0.38 pg. DNA and 0.8 pg. rRNA.

In Figure 16, the rRNA concentration was extended, permitting a more lucid portrayal of the binding behavior of AO molecules to rRNA, as a function of the rRNA concentration. The average relative fluorescence intensities of AO-rRNA complexes, at 536 nm., demonstrated a commensurable intensification, while the rRNA concentration enlarged from 0.00 pg. to 5.04 pg. This indicates that there exist a constant number of binding sites on rRNA macromolecules that bind AO in the monomer form. The equation of the line, eq. (2), is written as follows:

$$\log F_{536}^{\text{rRNA}} = m_{\text{rRNA}} (pg. \text{ rRNA}) + \log b$$
 (2)

where log F_{536}^{rRNA} is the logarithm of the fluorescence intensity of a microdroplet containing only rRNA, at 536 nm.; m_{rRNA} is the slope of the line; (pg. rRNA) is the quantity of rRNA contained in the microdroplet expressed in picograms; and log b is the logarithm of the fluorescence intensity, at 536 nm., of the microdroplet containing no rRNA. The slope of the line, m_{rRNA} , is equal to 0.272/pg. rRNA. Equation (2) can be used to calculate an unknown quantity of rRNA in a gelatin microdroplet, where the amount of rRNA (in pg.) is equal to (log F_{536}^{rRNA} - log b)/ m_{rRNA} . With respect to the NA concentration, the binding rate of AO molecules to DNA macromolecules is greater than the rate for rRNA macromolecules, since the slope m_{DNA} is 4.63 times larger than the slope

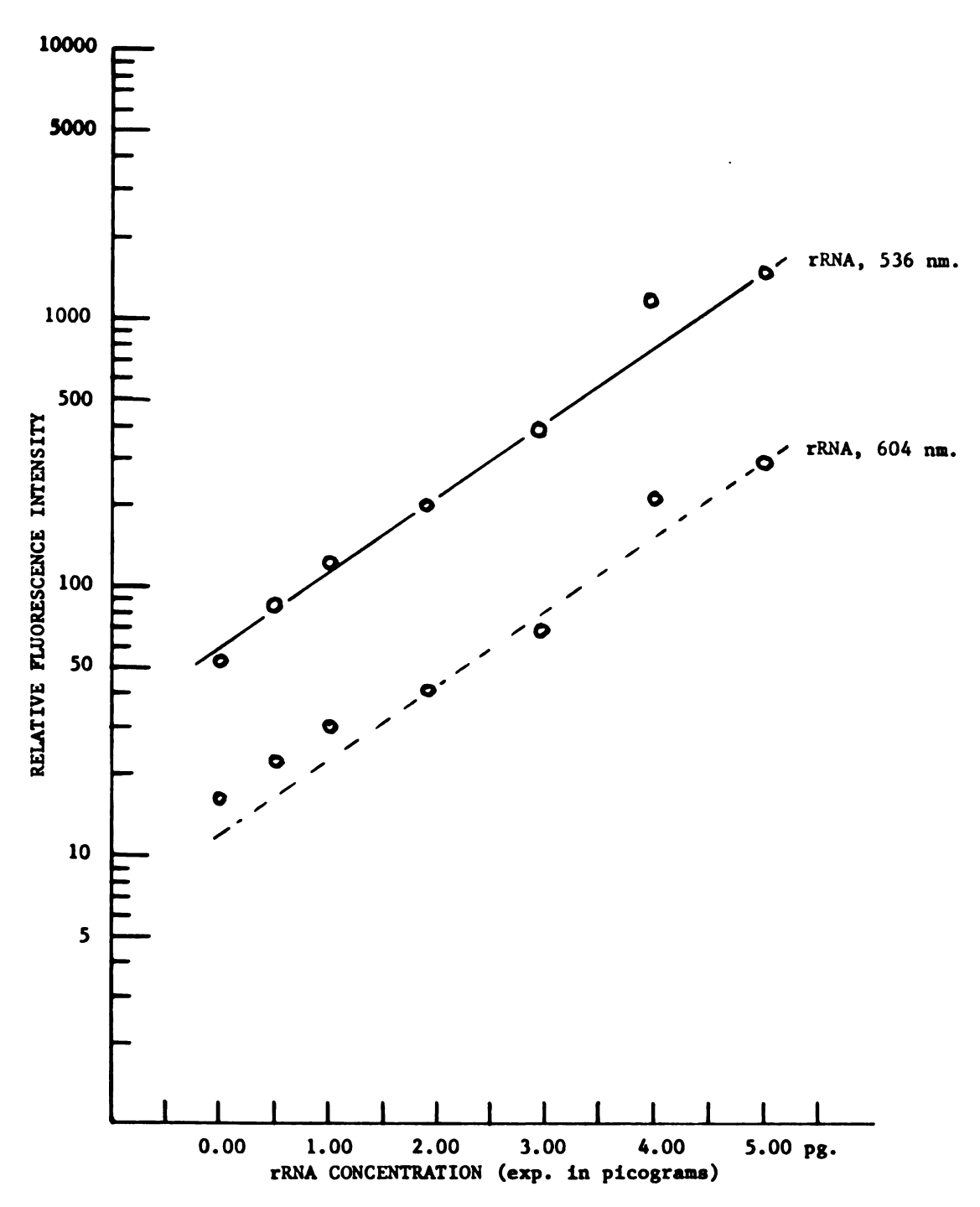


Figure 16. The average relative fluorescence intensities of AO bound to rRNA, at 536 nm. and 604 nm., in 3% pf. pgsk. for various rRNA concentrations, AO staining concentration 5 x 10^{-5} M, staining time 30 mins., pH 4.1.

m_{rRNA}. Therefore, after having identical fluorescence spectra, the binding of AO molecules to the DNA and rRNA conformations are only distinguishable by different binding affinities.

Throughout the course of the increments in concentration, the degree of dye aggregation on the DNA and rRNA macromolecules was, for all practical purposes, constant; the degree of AO aggregation on the DNA and rRNA conformations averaged 0.242 ± 0.016 at diverse NA concentrations; see Figure 17. (Because of sensitivity limitations, DNA contents below 0.38 pg. were not included in the average.) The aggregation mode of AO on the DNA and rRNA conformations was similar, inasmuch as each DNA and rRNA macromolecule had a specific number of binding sites for AO in the aggregate form, and their aggregate-to-monomer binding sites ratio was the same. At each NA concentration, the fluorescence intensities, at 536 nm., of AO-DNA and AO-rRNA complexes in 3% pf. pgsk., were 4.27 ± 0.62 and 4.81 ± 0.74 times larger, respectively, than their affiliated intensities at 604 nm., with a low degree of dye aggregation on the DNA and rRNA macromolecules, once more confirming that AO preferentially binds to NA in the monomer form.

The linearity between the fluorescence intensity of AO-NA complexes and the amount of NA available for binding the dye molecules suggests the possibility of determining the quantity of DNA and/or rRNA contained in a given microenvironment. If a gelatin microdroplet contains a mixture of DNA and rRNA macromolecules, a measurement of the microdroplet's monomer AO emission may be regarded as the sum of the fluorescence intensities characteristic for each constituent of the system. The logarithm of the fluorescence intensity at 536 nm. is then denoted as:

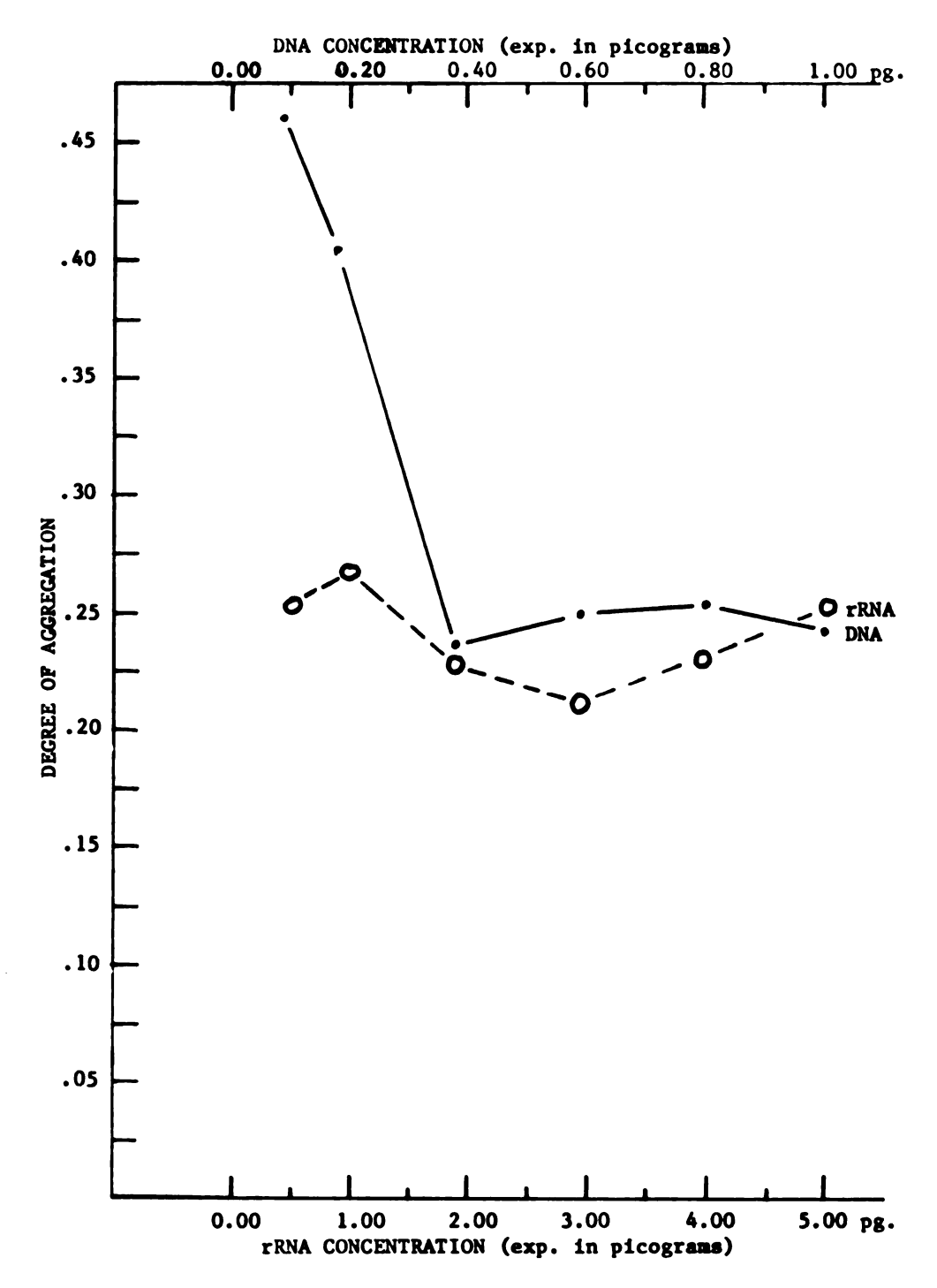


Figure 17. The degree of aggregation of AO onto DNA or rRNA in 3% pf. pgsk. for different NA concentrations, AO staining concentrations 5 x 10^{-5} M, staining time 30 mins., pH 4.1.

$$\log F_{536} = D(f.c.\frac{DNA}{536}) + R(f.c.\frac{rRNA}{536}) + \log b$$
 (3)

where log F₅₃₆ = the logarithm of the relative fluorescence intensity at 536 nm. of the gelatin microdroplet.

D,R = the quantity of DNA and rRNA contained in the gelatin microdroplet system given in picograms of nucleic acids,

f.c. DNA, f.c. rRNA = "fluorescence coefficients"; the slopes of the lines for the fluorescence intensities of AO-DNA and AO-rRNA complexes at 536 nm., as a function of the DNA and rRNA contents, respectively (see equations 1 and 2).

In simplifying equation (3) the total NA content of a system is given by:

$$R + \gamma D = \frac{\log F_{536} - \log b}{f.c._{536}}$$
(4)

where γ is a theoretical constant equal to the ratio of the DNA to rRNA fluorescence coefficients for any microenvironment, and is equal to 4.63.

Gelatin microdroplets containing different mixtures of known amounts of DNA and rRNA macromolecules were employed to test the validity of this equation. The value on the right side of equation (4) was compared to the value on the left side of the equation. For each microdroplet, the experimental (R and γD) value obtained from the [(log F₅₃₆ - log b)/f.c. rRNA] averaged 87% of the theoretical value derived from the known quantities of the embedded rRNA and DNA macromolecules. The results are tabulated in Table 8.

Since the validity of this methodology was based on only a few samples, these results should be regarded as a first approximation.

TABLE 8

The nucleic acid content of 3% purified pigskin microdroplets, derived from the sum of the embedded pg. rRNA + 4.63 (pg. DNA) on the left side of equation (4), is compared to its value on the right side of the equation, obtained from [[log F_{536} - log b)/f.c. F_{36} . The fluorescence spectrum and intensity, at 536 nm., of each microdroplet was obtained with the microspectrophotometer, while irradiating at 400 nm. The average relative fluorescence intensity of 3% pf. pgsk. microdroplets, containing no NA, at 536 nm. is equal to 54.5. The microdroplets were stained for 30 mins., with 5 x 10-5M AO, at pH 4.1.

NA Combinations in 3% pf. pgsk.	Micrd. #	The Theoretical Value for R + 4.63 (D)	F 536	The Experimental Value for (log F ₅₃₆ - log b)
0.38 pg. DNA + 1.9 pg. rRNA	۳. % ښځ	3.66 pg. 3.66 pg. 3.66 pg. 3.66 pg.	550 365 440 365	3.69 pg. 3.04 pg. 3.33 pg. 3.04 pg.
0.38 pg. DNA + 2.95 pg. rRNA	5. 7.	4.71 pg. 4.71 pg. 4.71 pg.	675 525 750	

However, a correlation does exist between the fluorescence intensities of AO-NA complexes, in the monomer form, and the quantity of NA available for binding the dye molecules. The application of equation (4) requires that the amount of AO bound by the NA in a given system must be proportional to the fluorescence intensity of the monomer AO molecules, and must be proportional to the quantity of the NA macromolecules in the system.

C. Neuron Analysis

With the recognition that the metabolic functions of nucleic acids are significant in the neuron to neuron interaction, it is postulated that the molecular events underlying neuronal activities are manifested in the cellular nucleic acid content during the development of nervous tissue. However, the intricate anatomical and cytoarchitectural design of the nervous system poses certain problems for the use of fluorescent molecular probes, in the study of a few intracellular components. Studying neurons in situ is complicated by the dense packing of nervous tissue, sheaths, glia, and blood-brain barriers. These problems may be obviated by means of dissociated cell cultures. Under various microenvironmental conditions, the binding behavior of acridine orange to nucleic acids has afforded investigators with information about the structure and function of the probed macromolecule [Rigler, 1966; West, 1969]. In association with my microdroplet results, these findings substantiate the concept that the utilization of acridine orange as a fluorescent molecular probe, in conjunction with dissociated neuron cultures, facilitates the microspectrophotometric determination of nucleic acids in single neurons.

The gross appearances of neurons grown in dissociated cell cultures are different than those <u>in situ</u> (i.e., the morphology in a normal developing animal). Therefore, if any meaningful correlations are to be realized from this investigation, it is of great importance that the nucleic acid determinations be made on specific neuronal types. In order to accomplish this, several neuronal types are identified in the cell cultures. The classification of these neurons were made with reference to their morphological descriptions. The neuronal types characterized are as follows:

- 1. <u>Canada, Type I neuron</u>. This cell has a large diamond-shaped cell body, having a length over 30% greater than its width. The cell body is customarily surrounded by perineuronal satellites [Jenkins, 1972, p. 59] see Figure 18. The nucleus is oval, generally located toward the center of the cell body, and contains several nucleoli. The nucleus comprises about 20% of the cell body. Each of the points on the diamond soma has a process that can measure up to several hundred microns. The cytoplasm is moderately filled with Nissl bodies, and is a little darker than the nucleus.
- 2. Canada, Type II neuron. These are very small cells, their somas being much smaller than that of the Canada, Type I neuron. The cell body exists in a polymorphic form with 3 to 4 processes; see Figures 20 and 26. The nucleus is round or oval-shaped, involving about half the area of the cytoplasm, and is usually located close to one side of the cell body. This cell is found in close association with other cells, particularly of the same type, and with astrocytes.
- 3. <u>Canada, bipolar neuron</u>. Distinguishing features of this neuron are the two primary processes, at opposite poles, of a round or spherically-shaped cell body. A bifurcation is regularly seen in one of the processes; see Figures 19 and 21. The nucleus is large, taking up most of the cell body, and conforms to the general shape of the cell body. The nucleus customarily contains at least one nucleoli.

A number of glial cells were found in situ, particularly the fibrous astrocytes (see Figures 19 and 22) which are spider-shaped cells [Jenkins, 1972, p. 59]. The neuronal type of a cell in culture is almost impossible to determine if the cell is in the process of redifferentiation (see Figures 22 and 23). The reader should note that

Figure 18. A photomicrograph of a living brain cell found in a dissociated monolayer cell culture, taken from the somatic sensory cortex I and II, of a 3 days old female albino rat. The cell was maintained 23 days in culture; at the time of photo, it has a diamond shape with a length of 130 microns and a width of 96 microns. The nucleus of the cell is centrally located, having an oval shape 30 microns long and 18 microns wide, with several nucleoli. This cell has been designated the Canada, Type I neuron. The scale for the photomicrograph is 14.4 microns per centimeter.

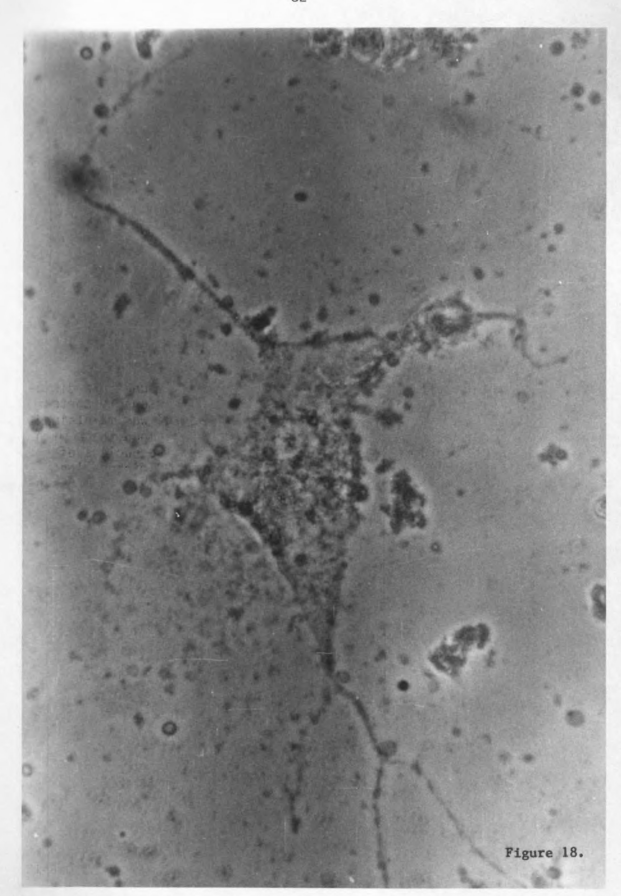
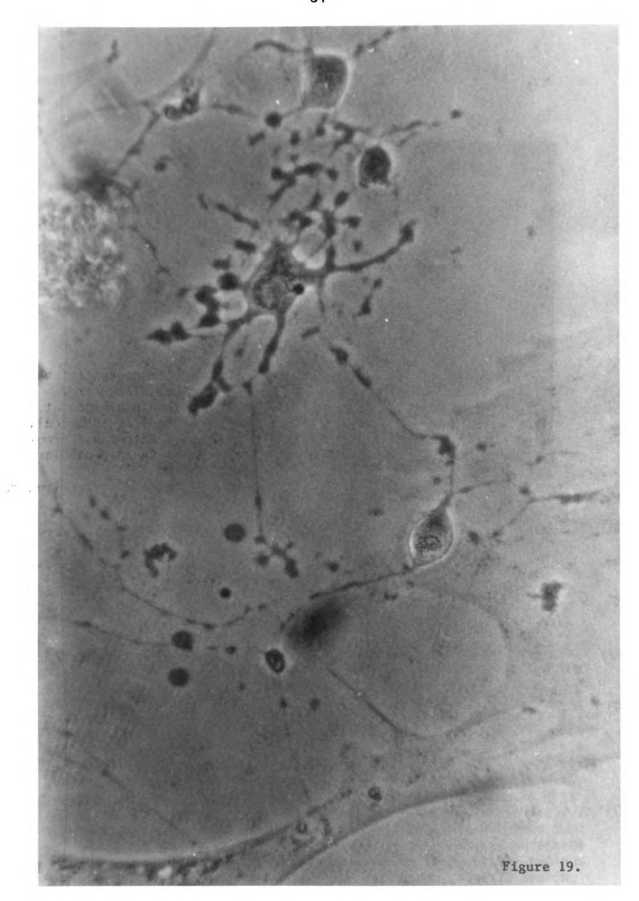


Figure 19. A photomicrograph of a living Canada, bipolar neuron (right of center) found in a dissociated monolayer cell culture, taken from the somatic sensory cortex I and II, of a 3 days old female albino rat. The cell was maintained 32 days in culture. The cell body is spherical, with a length of 26 microns and a width of 17 microns. Note the fibrous astrocyte above the center of the photomicrograph. The Canada, bipolar neuron is making a contact with a Canada, Type II neuron (bottom of center). The scale for the photomicrograph is 14.4 microns per centimeter.



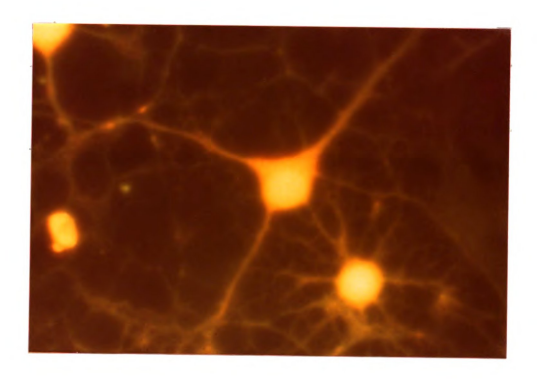


Figure 20. A photomicrograph of a Canada, Type II neuron found in a dissociated monolayer cell culture, taken from the brain of a 3 days old female albion rat. The neuron was maintained 96 days in culture, stained with $1\times 10^{-4} M$ acridine orange, at 22°C, for 30 minutes, at a pH of 4.1, and irradiated with 400 nm. light. The cytoplasm of the neuron is full of orange granules and the nucleus has a yellow-orange color, indicating that under these conditions the degree of aggregation of AO onto the NA macromolecules in the neuroplasm is very high and greater than that for the NA macromolecules in the neucleoplasm. The average soma area of the Canada, Type II neurons found in this culture was 179 sq. microns. Note that the processes of the cell in the bottom right corner appears to be making contacts with the soma and processes of the Canada, Type II neuron; the cell has an orange cytoplasm with a yellow-orange nucleus and its ratio of the nucleus to soma areas is greater than that for the Canada, Type II neuron.

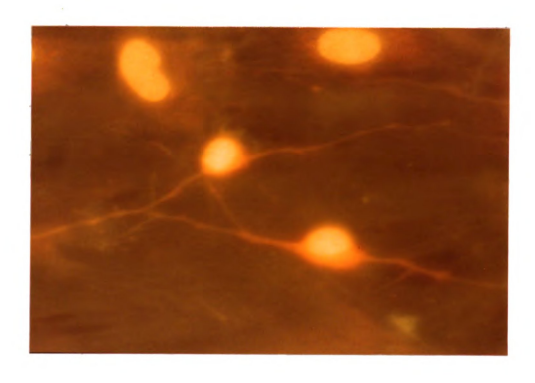


Figure 21. A photomicrograph of two Canada, bipolar neurons, found in a dissociated monolayer cell culture, taken from the brain of a 3 days old female albino rat. The cells were maintained 96 days in culture, stained with $1\times 10^{-6}\mathrm{M}$ acridine orange at $22^{\circ}\mathrm{C}$, for 30 minutes at a pH of 4.1, and irradiated with 400 nm. light. The average area of their somas is 112 sq. microns, having two processes at opposite poles, with a bifurcation in one of the processes. Both of their nuclei are large and round, taking up most of the soma, while stained a yellow-orange color. Their cytoplasm is orange in color. One of the Canada, bipolar neurons, with its bifurcated process, is making contact with a process of the other neuron.

Figure 22. A photomicrograph of living fibrous astrocytes during redifferentiation. The cells were maintained 23 days in a dissociated monolayer cell culture, and were taken from the somatic sensory cortex, I and II, of a 3 days old female albino rat. As it happens with cells in brain sections, these cells in culture may be confused with neurons.

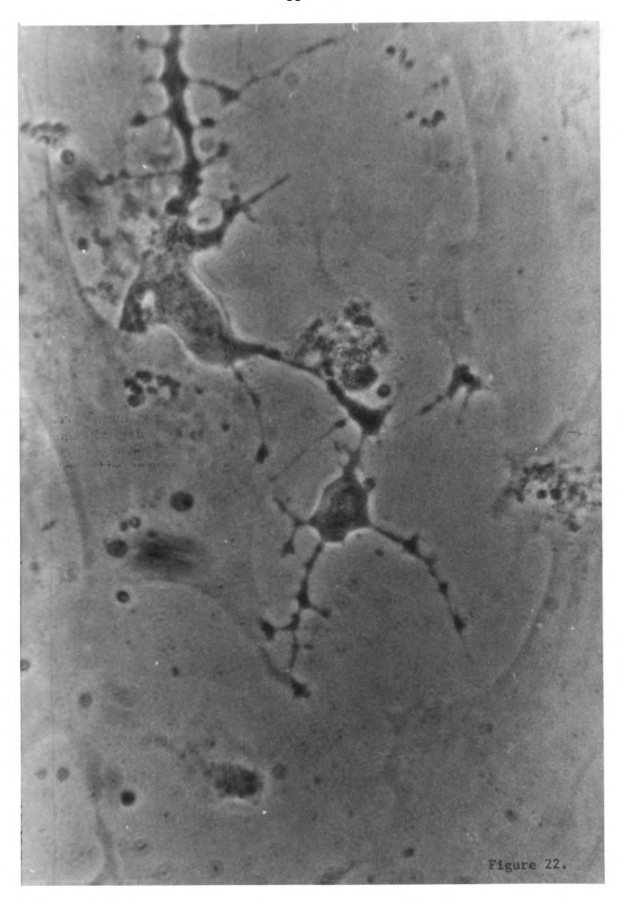
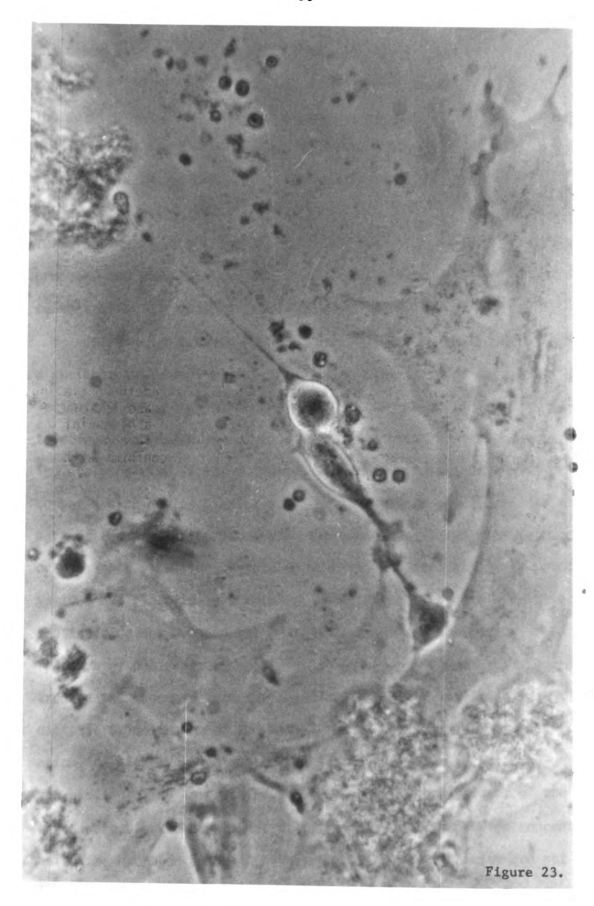


Figure 23. A photomicrograph of three living neurons redifferentiating, the cells were taken from the somatic sensory cortex, I and II, of a 3 days old female albino rat. They were grown 23 days in a dissociated monolayer cell culture. Note that there is a soma-somatic contact between two of the neurons. The nucleus of each cell conforms with the general shape of the cell body, having one or two nucleoli. The cytoplasm of each cell is dense with Nissl bodies. The cells in the surrounding environment are glia or connective tissue.



the names and characteristics of these neuronal types pertain to neurons taken from the rat cortex and maintained in dissociated cell cultures. The development of neurons in culture closely resembles the maturation of neurons in the natural state. A number of investigators have shown that changes in age can result in changes in the RNA content, establishing a differential growth rate in the development of neurons [Haltia, 1970; Sobkowicz et al, 1973]. It is for these reasons that the author's proposed technique was applied in the determination of the nucleic acid content of single neurons in culture, at two different ages.

Cellular or nucleic acids in the intact cell are usually found in a nucleoprotein complex; i.e. in vivo, nucleic acids are usually found intimately associated with proteins. The amphoteric nature of the protein fraction of the nucleoprotein complex elicits a slight problem during staining with acridine orange. The cationic portion of the protein competes with AO for binding sites on the nucleic acids, and the anionic part of the protein competes with the nucleic acid for binding acridine orange; both situations result in an emission spectral change for the various nucleic acid-AO complexes. A procedure was developed to minimize the interactions between the protein fraction and the nucleic acid fraction of nucleoproteins [Rigler, 1966]. The nucleic acids could be exposed and loosened from their nucleoproteins, by the blocking of the cationic amino groups of the proteins with acetic acid anhydride acetylation. A high hydrogen-ion concentration was found to halt the unspecific binding of AO to proteins. The anionic carboxyl groups of the proteins were blocked at a pH of 4.1, the maximum hydrogen-ion concentration which the hydrogen bonds in highly organized nucleic acids are not irreversibly destroyed. This causes the fluorescence spectra of

A0-nucleoprotein complexes to be identical to their free nucleic acid-A0 complexes emission spectra [Rigler, 1966].

In addition to water comprising approximately 70% of its total weight, a cell is also predominantly composed of proteins and nucleic acids which are about 22% of the total weight [Lehninger, 1970, p. 20]. During fixation, a neuron is dehydrated, reducing it essentially to a gelatin microdroplet. The internal microenvironment of a neuron is dependent upon its living condition and neuronal type. The neurons were stained for 30 mins., allowing the AO molecules to bind to almost all of the monomer binding sites on the NA conformations. Using an A0-staining concentration between 5 x 10^{-6} M and 5 x 10^{-4} M at a pH 4.1 permits equation (4), from the gelatin microdroplet experiments, to be directly applied to the fluorescence of neurons stained with AO, since the fluorescence coefficients of DNA and rRNA at 536 nm. are constant under these conditions (rRNA is the major type of ribonucleic acid found in the cell, comprising over 80% of total cell RNA) [Lehninger, 1970, p. 254]. The fluorescence spectrum of each neuron was recorded with the microspectrophotometer, during irradiation with 400 nm. exciting light. The pg. rRNA + γ (pg. DNA) content of the Canada, Type II and bipolar neurons' cell bodies, at 67 da. and 99 da. old are tabulated in Table 9. Except for neuron #10, the neurons at each age were grown in the same culture; and were taken from a 3 day old female albino rat. The age of a neuron, in days, is equal to the sum of the age of the rat at the time of sacrifice plus the number of days the neuron spent in culture before fixation.

The logarithm of the background fluorescence, log b, for each cell was equal to zero, even though the AO staining concentrations were

TABLE 9

The R + γD content in the cell bodies of Canada, Type II, and Canada, bipolar neurons, at 67 da. and 99 da. old, as determined microspectrophotometrically using equation (4), R + γD = (log F₅₃₆ - log b)/f.c. rRNA, where γ is equal to 4.63 and f.c. rRNA is equal to 0.272. Cells #1 through 7 were stained with 1 x 10-4M AO, and neurons #8 through 12 were stained with 5 x 10-5M AO for 30 mins., at a pH 4.1. All of the cells were taken from the cerebral cortex of a 3 da. old albino female rat and maintained in dissociated cell cultures. Neurons #8 through 12 are from the somatic sensory cortex I and II.

	Neuronal Type	Time Spent in Culture	Soma area (μ ²)	F ₅₃₆	Aperture Correction	R + γD in pg.
1	Canada, Type II	96 da.	179	7200	2.1	15.4
2	Canada, Type II	96 da.	179	5700	2.1	15.0
3	Canada, Type II	96 da.	179	5100	2.1	14.8
4	Canada, bipolar	96 da.	112	7650	3.4	16.2
5	Canada, bipolar	96 da.	112	6500	3.4	16.0
6	Canada, bipolar	96 da.	112	8000	3.4	16.3
7	Fibrous astrocyte	96 da.	116	7250	3.3	16.1
8	Canada, Type II	64 da.	89	436	4.3	12.0
9	Canada, Type II	64 da.	114	300	3.3	11.0
10	Canada, Type II	64 da.	108	600	3.5	12.2
11	Canada, bipolar	64 da.	119	1075	3.2	13.0
12	Canada, bipolar	64 da.	319	1900	1.2	12.3

different, since the fluorescence of the area surrounding each cell body analyzed was either nil or negligible for both of the AO staining concentrations. Because the neurons were found living either on the glass slide alone or on top of an glial cell, and the major subcellular components in the cytoplasm of most glial cells are made of proteins [Hyden, 1967, Chap. 4], the background area of the neuron contains no appreciable amount of nucleic acids, if any. The negligible background fluorescence intensities harmonize with results found by Rigler [1966]: after enzymatic extraction of the nucleic acids, the fluorescence emission, at 530 nm., of the protein residual of AO-stained cells at pH 4.1, amounted to about 2% of the total fluorescence intensity at 530 nm. of A0-stained cells containing nucleic acids. In this investigation, the fluorescence spectral patterns of the cells stained at 1 \times 10⁻⁴M AO were identical to the spectral patterns of the cells stained at 5 x 10^{-5} M AO. The degree of dye aggregation for the cells stained at 1 x 10^{-4} M averaged 0.29, and for cells stained at $5 \times 10^{-5} M$ it averaged 0.25. Visually, the cells stained at the higher AO staining concentration had orange cytoplasms and yellow-orange nuclei (see Figures 24 through 27). In contrast, the cells stained at the lower AO staining concentration were green all over (nucleus and cytoplasm) similar to the appearance of the gelatin microdroplets under the same staining conditions. These differences may be due to the older neurons' (99 da.) greater capacity to retain AO than the younger neurons (67 da.), resulting in a higher intracellular dye content for the older neurons. Since the amount of fluorescence light reaching the phototube is dependent on the slit size, aperture correction factors were introduced in Table 9 in order to correct for intensity differences caused by the smaller apertures used for the cell

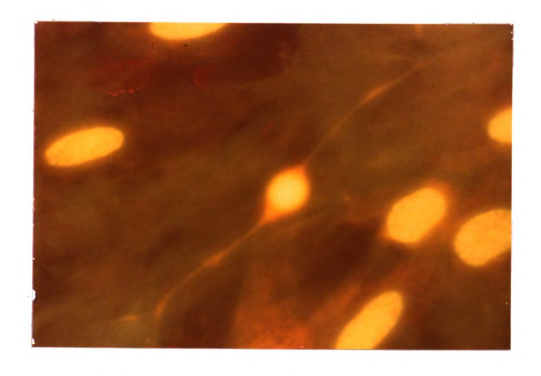


Figure 24. A photomicrograph of a single Canada, bipolar neuron found in the same culture and subjected to the same conditions as those in Figure 21. The average area of the soma is 112 sq. microns. The other large oval-shaped yellow-green objects are the nuclei of glia cells. Note the local accumulation of dye molecules at the orange thickenings in the bifurcated process, before and at the bifurcation, due to an increased aggregation of AO.

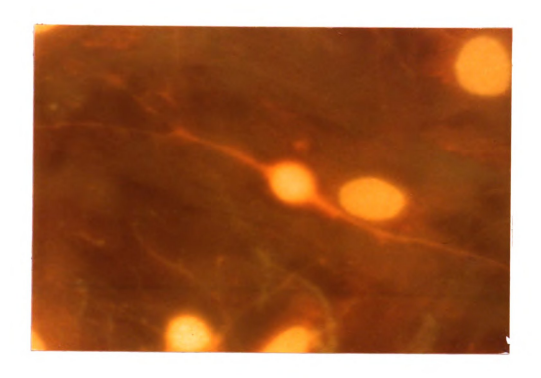


Figure 25. A photomicrograph of a Canada, bipolar neuron found in a dissociated monolayer cell culture, taken from the brain of a 3day old female albino rat. The cell was maintained 96 days in culture, stained with $1\times 10^{-4} \rm M$ acridine orange, at 22°C, for 30 minutes at a pH of 4.1, and irradiated with 400 nm. light. The average area of the soma is 112 sq. microns, having two processes at opposite poles, with a bifurcation in one of the processes. Note the neuron at the bottom of the photomicrograph is sending its process towards the bifurcated process of the Canada, bipolar neuron.

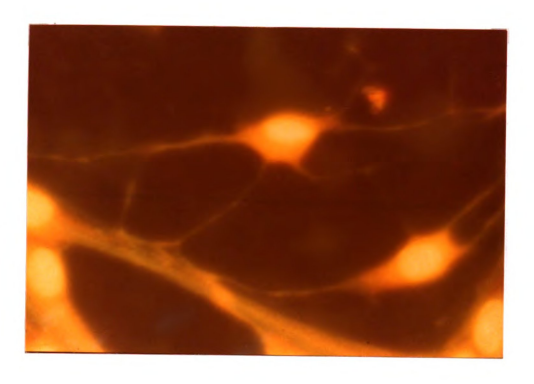


Figure 26. These two cells are Canada, Type II neurons. Canada, Type II neurons occur in polymorphic form, with 3 to 4 processes, in dissociated monolayer cell cultures of 3 days old female albino rat brains. Note that there is one contact between the two neurons and a contact with a common body. The cells were maintained 96 days in culture, stained with $1\times 10^{-4} \rm M$ acridine orange, at 22°C, for 30 minutes at pH 4.1. The photomicrograph was taken while exciting the cell with 400 nm. light. The average area of their soma is 179 sq. microns. The cytoplasm is stained orange. The yellow-orange nucleus is usually round or oval in shape, comprising about half the area of their somas.

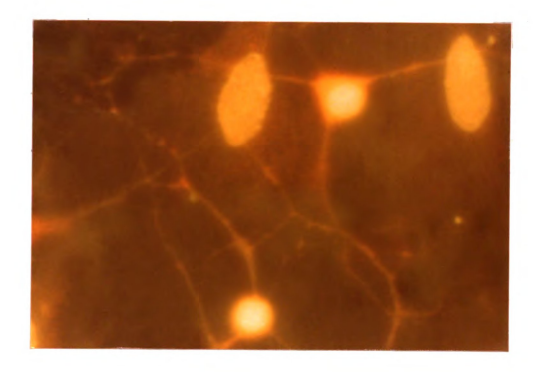


Figure 27. A Canada, Type II neuron, in upper section, found in the same culture and subjected to the same conditions as those in Figure 26. Notice the extensive network of fibers between this cell and the cell in the lower section. Two of the processes of the Canada, Type II neuron are making several contacts with the processes of other cells.

bodies. The fluorescence coefficients were determined for an aperture area of 380 sq. microns.

The average R + YD values for the Canada, Type II and the Canada, bipolar neurons demonstrated an increase as a function of neuronal age. where the $R + \gamma D$ value per neuronal type averaged 28% greater at age 99 da. than at age 67 da.; see Figure 28. The slopes of the line for the $R + \gamma D$ values of Canada, Type II, and Canada, bipolar neurons, as a function of time, are equal to 1.1×10^{-1} pg/da., suggesting that both neuronal types have identical growth rates in culture; between 64 da. and 96 da. in culture, the R + γ D value per neuron increased 0.1 pg. per diem. Since the $\gamma(pg. DNA)$ content per neuron is constant at each age, the slope can reflect the rate at which the RNA content of each neuronal type increases as a function of age. The low value for the slopes infer that neurons, grown in culture, grow at a very slow rate. This agrees with the results published by Sobkowicz et al in 1973, in which they reported that the RNA content of spinal ganglion neurons in culture increased at a much slower rate than when grown in vivo. Figure 28 also demonstrates that the amount of RNA contained in a given neuron in culture is dependent upon its neuronal type, inasmuch as the $R + \gamma D$ value of the Canada, bipolar neurons averaged 8% greater than the $R + \gamma D$ content of Canada, Type II neurons at each age.

Table 9 shows that the area of a neuron's cell body is dependent upon the neuronal age and type. The average cell body area of the Canada, Type II neurons increased 73%, as the neuronal age increased from 67 da. old to 99 da. old. In contrast, the average area of the Canada, bipolar neuron's cell body decreased as their neuronal age increased. However, in Figure 29, the $R + \gamma D$ content per neuron was not dependent upon the

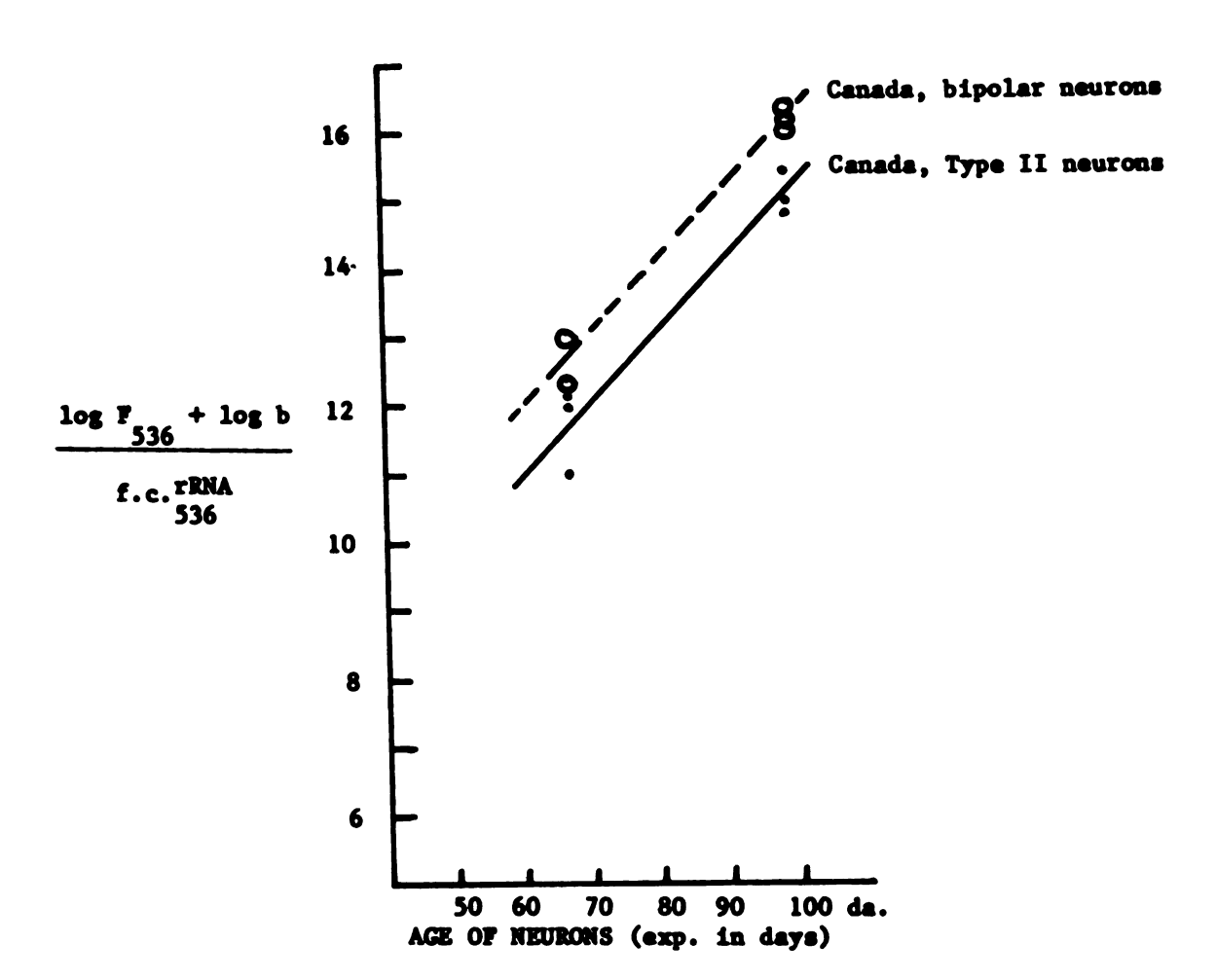


Figure 28. The $\{rRNA + \gamma(DNA)\}$ content, in picograms, per neuronal type for different neuronal ages.

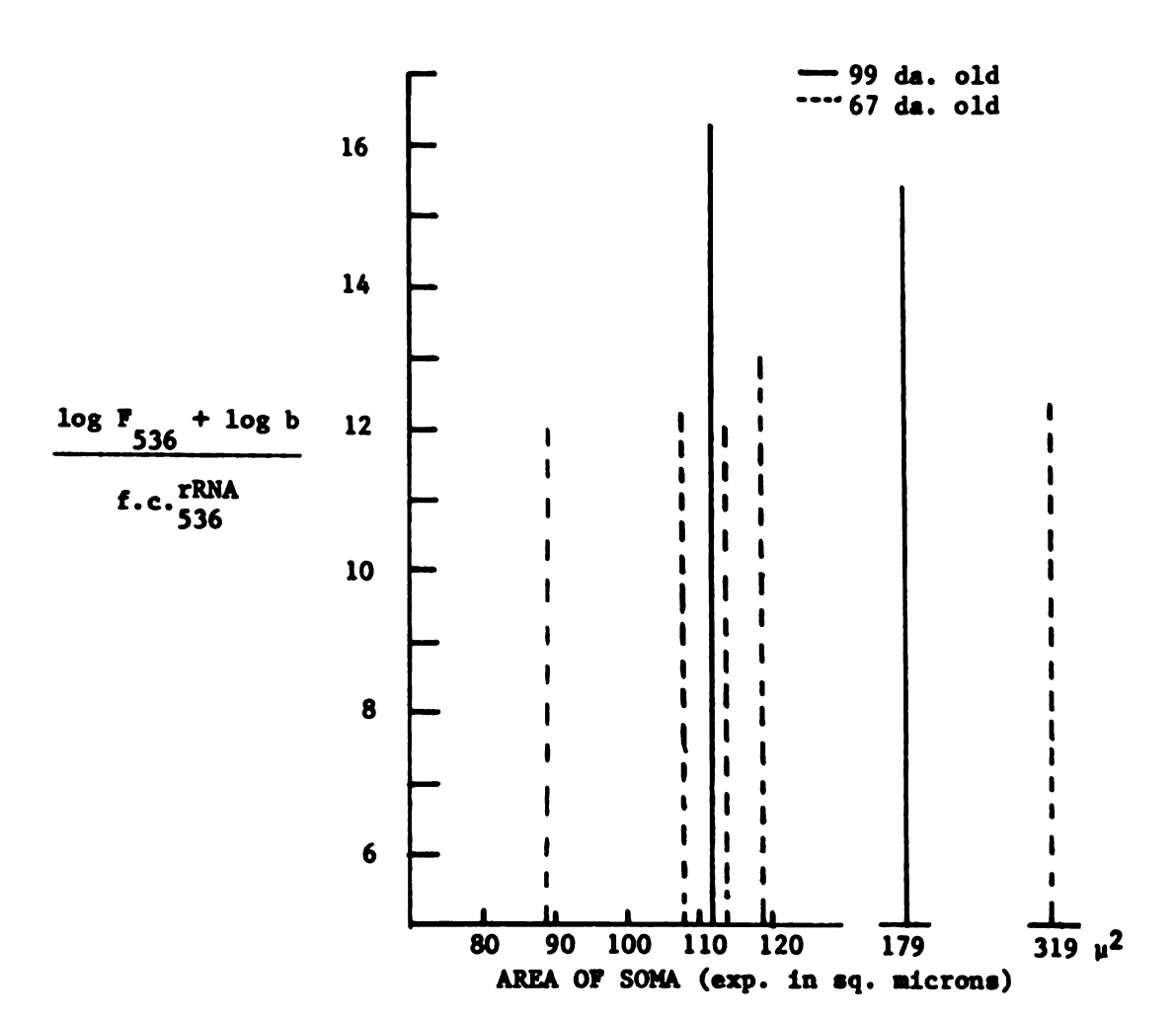


Figure 29. The $\{rRNA + \gamma(DNA)\}$ content, in picograms, per neuronal age for different soma areas of the neurons.

size of its cell body; the R + γD content per neuron presented no definite pattern as a function of the neuron's soma area. Clearly, these results suggest that during the normal development of neurons in culture their RNA content and the size of their cell bodies are highly correlated with age. The same is true in situ [Haltia, 1970. Sobkowicz et al, 1973].

No doubt, a better experimental design could be conceived for determining the NA content in single neurons. The ability of this modus operandi to yield the absolute value of the NA content in the soma of a single neuron must be questioned. Logically, the R + γ D value of each neuron is greater than the value of γD , but never less than the value of γD . However, the experimental R + γD value (<15.4 pg.) of each neuron was found to be less than the expected yD value of 30.1 pg. The theoretical yD value, 30.1 pg., was determined by multiplying the reported DNA content of a mammalian neuron, 6.5 pg. [Mahler, 1972] by the γ value of 4.63. The use of 4.63 as the value of γ was based on the assumption that a fixed cell was analogous to a gelatin microdroplet, whereby under similar staining conditions the binding behavior of AO molecules to NA macromolecules inside a fixed cell is identical to the binding behavior of AO molecules to NA macromolecules in a gelatin microdroplet. Obviously, this assumption was wrong, since the experimental YD value of each neuron appears to be considerably less than 30.1 pg. Therefore, the γ value of a fixed neuron must be less than the γ , 4.63, value of a gelatin microdroplet.

The fluorescence coefficients obtained from the gelatin microdrop-let experiments, f.c. $_{536}^{DNA}$ = 1.26/pg. DNA and f.c. $_{536}^{rRNA}$ = 0.272/pg. rRNA, cannot be used to calculate the absolute NA content within the soma of

a single fixed neuron. Evidence suggests that the fluorescence coefficients of the fixed neuron are different from the fluorescence coefficients of the gelatin microdroplet, in that the f.c. $\frac{\text{rRNA}}{536}$ and f.c. $\frac{\text{DNA}}{536}$ of the fixed neuron may be greater than the corresponding coefficients of the gelatin microdroplet, or the f.c. $\frac{\text{rRNA}}{536}$ of the fixed neuron is greater than its f.c. $\frac{DNA}{536}$, or both may be possible. (Note: $\frac{1}{7}$ = f.c. $\frac{DNA}{536}$) f.c. rRNA .) More importantly, Beer's law may not prevail at the staining concentrations used in the fixed neurons, as it does with regards to the gelatin microdroplets, resulting in an erroneous application of the fluorescence coefficients and equation (4) to the fixed neurons. Under these conditions, the fluorescence intensity of AO bound to the macromolecules in the monomer form, and the amount of the macromolecules in question are not proportional to the amount of AO inside the fixed neuron, as compared to the gelatin microdroplet. Consequently, experiments must be devised to determine the staining concentrations for which Beer's law holds true for a fixed neuron. An example of such an experiment might be the examination of the fluorescence emission properties of the Nissl bodies, contained in the cytoplasm of a specific AO-stained neuronal type, as a function of their staining concentrations.

The potential modification of the fluorescence coefficients, derived from the gelatin microdroplet experiments, can be created by the cellular and nuclear membranes and the dissimilar internal environment of the fixed neuron. As one might expect, unlike the nonmembranous gelatin microdroplet the nuclear and cellular membranes serve to concentrate the AO content within the fixed neuron by obstructing the diffusion of excesses outside the neuron. This enhances the binding of AO molecules

to the NA macromolecules. Also, the binding of AO molecules to NA macromolecules increases, as a function of the ion concentration in the microenvironment and, due to the higher ionic strength in the internal environment of the fixed neuron, the amount of AO molecules bound per NA macromolecule in a fixed neuron is greater than the amount of dye molecules bound per NA macromolecule in a gelatin microdroplet. This would cause the f.c. $\frac{DNA}{536}$ and f.c. $\frac{rRNA}{536}$ of the fixed neuron to be greater than the corresponding coefficients of the gelatin microdroplet. the gelatin microdroplet, the internal environment of the fixed neuron contains other AO binding biopolymers that are intimately associated with the NA macromolecules, such as the ribosomal proteins, histones, etc. [Rigler, 1966]. These biopolymers may serve to indirectly increase the amount of AO molecules associated with a NA macromolecule. Since they are not found in the gelatin microdroplets, the quantity of AO molecules bound per NA macromolecule in a fixed neuron is greater than the amount of dye molecules bound per NA macromolecule in a gelatin microdroplet, resulting in higher fluorescence coefficients for the fixed neuron. The conditions inside a fixed neuron can cause the f.c. $\frac{rRNA}{536}$ to be larger than the f.c. $\frac{DNA}{536}$. Due to a higher concentration of AO molecules in the neuroplasm, the amount of dye molecules bound per rRNA macromolecule in the neuroplasm is greater than the quantity of AO molecules bound per DNA macromolecule in the nucleoplasm. This is brought about by a greater ionic strength and concentration of AObinding biopolymers in the neuroplasm of the fixed neuron than in its nucleoplasm, and the obstruction by the nuclear membrane of the diffusion of dye molecules into and out of the nucleus. These circumstances are evidenced by the orange cytoplasm and yellow nucleus of the AO-stained

neurons in Figures 24 to 27. The orange cytoplasm indicates a high degree of dye aggregation, resulting from the high concentration of A0 molecules in the neuroplasm. The cellular and nuclear membranes and the higher ionic strength, along with the other biopolymers that bind A0 molecules, would cause the internal A0 concentration of the fixed neuron to be greater than the gelatin microdroplet, under the same staining conditions. The staining concentration that deviates from Beer's law for the fixed neuron would be lowered, thus preventing the direct application of equation (4). Since A0 obeys Beer's law up to a concentration that would cause its aggregation [West, 1969], at the staining concentration of 5 x 10^{-5} M and 1 x 10^{-4} M A0, the amount of A0 inside the fixed neuron may not be proportional to the fluorescence intensity of the monomer A0 molecules and the amount of the NA macromolecules in the neuron.

The aperture (area) correction factors may be a source of error in calculating the R + γ D value of each neuron. Although the thickness of the gelatin microdroplets and the neurons were about the same a volume correction factor would be more accurate to use than the area correction in correcting for the size differences between the gelatin microdroplet and the cell bodies. The different fixation processes of the gelatin microdroplet and the fixed neuron may be another source of error, resulting in different binding behaviors of AO molecules to the NA macromolecules. No doubt, there may be a need to introduce other correction factors; only further experimentation can yield this answer. Nonetheless, the quantitative aspects of this investigation may be regarded as a first approximation, since the fluorescence intensity of AO-NA complexes at 536 nm. is proportional to the amount of NA available for binding the

dye molecules, reflecting the quantity of NA in AO-stained neurons. The $R + \gamma D$ values can be used to calculate the growth rate in the RNA content per neuronal type, as a function of time, since only the RNA content of the neuron is changing.

The reliability of this technique to yield accurate data should be tested against other biochemical and biophysical-cytochemical methods for the determination of NA in single cells. The biochemical procedures developed by Edstrom [1953, 1958, 1964] and ethidium bromide fluorescence microspectrophotometry [LePecq, 1973] are suitable methodologies to examine the competency of this technique. Hyden [1967, p. 191] modified the Edstrom methods for the analysis of brain cell material, involving the extraction of RNA and its determination by a microphotographicphotometric procedure in which a single neuron is removed from brain tissue, placed in a special chamber under liquid paraffin, and incubated with ribonuclease to enzymatically break down the large molecules of RNA. The depolymerized RNA is dried as specks on a glass slide and redissolved in a glycerine solution, forming microdrops. The microdrops and a density scale are photographed with 357 nm. ultraviolet radiation. Curves showing the RNA content of each microdrop and the density scale are photometrically produced by scanning the images on the photographic plate with light while recording the responses with a photocell-amplifierrecorder. The method can determine at least 20 pg. of RNA with a variation coefficient of the whole procedure being about 5%. Hyden [1967, p. 197] employed this technique to study the motor neurons in man. Unlike many other cells whose RNA content increases during the prenatal period, the RNA content in the nerve cell increases during the postnatal period of development. After birth the RNA content in the motor neuron

increases significantly until the ages around 40. Between the ages of 0 and 20 years, the RNA content in each cell averages 402 ± 28 pg., and between 21 and 40 years it averages 553 ± 38 pg. Between 41 and 60 years of age, the RNA content in each cell is maintained at a high level, averaging 640 ± 55 pg. per neuron. After the age of 60 years, the RNA content in each cell decreases significantly. Between the ages of 61 and 80 years the RNA content per neuron averages 554 ± 31 pg. Over the age of 80 years the RNA content per neuron averages 460 ± 30 pg. [Hyden, 1967, p. 197]. The integrity of the Edstrom procedure [1953, 1958, 1964] is confirmed by the following investigators—Hyden [1967], Haltia [1970], and Sobkowicz et al [1973]—and used in the demonstration of a growth-curve relationship (a differential growth rate) between the RNA content and the age of the developing neuron.

The compound, ethidium bromide (Figure 30) is a fluorescent molecular probe of the NA structure, binding to the NA conformation in two different forms [Le Pecq, 1973]. Similar to the acridine orange molecule, ethidium bromide (EthBr) preferentially binds to the NA conformation in the monomer molecular form. In this form, the dye molecule is intercalated between two base pairs, forming a "sandwich complex." The plane of the dye molecule is parallel to the plane of the base pairs. The binding of EthBr to the nucleic acids increases the fluorescence quantum efficiency, 20 times greater than that of the free dye in aqueous solution, to a value of 0.14, and shifts the absorption spectrum to longer wavelengths, having an emission peak at 575 nm. The bound dye molecule has a fluorescence lifetime equal to 24 ns. [LePecq, 1973]. The intercalation of EthBr is specific for the double stranded regions in either the DNA, RNA, or DNA-RNA hybrid structures. The fluorescence intensity of the

Figure 30. Ethidium Bromide

dye is increased proportional to the amount of double stranded regions available for binding, and is negligible in the presence of single stranded structures. The fluorescence enhancement of the bound dye is due to the immersion of the dye molecule into the hydrophobic medium of the intercalation site [LePecq, 1973]. Unlike the acridine orange molecules, ethidium bromide molecules cannot readily bind to the NA conformation in the aggregated form. The stacking of the dye molecules, along the single stranded regions and on the outside of the double stranded regions in the NA conformation, is obstructed by the phenyl substituent, in the sixth position, the latter being oriented perpendicular to the main ring of the molecule. The fluorescence quantum efficiency of the dye molecule bound in the second sites is considerably less than the fluorescence quantum efficiency of the intercalation sites [LePecq, 1973]. The binding constant for DNA is less than that for RNA and the binding constant for both structures is dependent upon the salt concentration in the microenvironment. The binding constant of EthBr to the monomer binding sites (intercalation sites) of the NA conformation, at low ionic strength, is of the order of 1 x 10^6 M, and the binding constant decreases slightly as the ionic strength is increased. In contrast, the binding constant of EthBr to the NA conformation, in the aggregated form, is completely eliminated at high salt concentrations.

The conformation and the conformational changes of a NA macromolecule were studied, in vitro, using the fluorescence properties of EthBr bound to the macromolecule. The binding constant of EthBr for a naturally super-coiled DNA conformation is larger than that for a nicked circular DNA conformation [Bauer and Vinograd, 1968; LePecq, 1973]. The fluorescence intensity of EthBr bound to a given concentration of

supercoiled DNA is higher than the fluorescence intensity of EthBr bound to the same concentration of nicked circular DNA under identical conditions, thus demonstrating the affinity differences of EthBr for the two different DNA conformations. The binding of EthBr to naturally supercoiled DNA progressively releases (denatures) the superhelix into a relaxed circle because the intercalation process of EthBr induces a change in the torsion of the double helix. The conformational changes of the DNA superhelix is a function of the EthBr concentrations, whereby increasing the EthBr concentration gradually unwinds the naturally supercoiled DNA conformation, and the number of turns in the superhelix is proportional to the amount of EthBr bound by macromolecule [Bauer and Vinograd, 1968; LePecq, 1973]. The fluorescence intensity of the EthBr-induced circular DNA (covalently closed circular DNA), the DNA structure resulting from the increased binding of EthBr. is identical to the fluorescence intensity of EthBr bound to the nicked circular DNA conformation, under similar reaction and fluorescence measurement conditions. This means that the affinity of EthBr for the completely released superhelix is equivalent to the affinity of EthBr for the nicked circular DNA conformation. Increasing the EthBr concentration to excess induces the circular DNA to form a superhelix of the opposite sign, compared to the sign of the original superhelix. The affinity of EthBr for the supercoiled DNA conformation of opposite sign is less than that of the nicked circular DNA conformation under identical conditions. binding less ethidium bromide molecules, and it is less fluorescent than the nicked circular DNA conformation. These experiments can yield the number of dye molecules bound per macromolecule of circular DNA, and if the change in torsion connected with the intercalation process

is ascertained, the sign of the superhelix and the degree of superhelicity of the original supercoiled DNA conformation can be determined [LePecq, 1973]. The difference in affinity of EthBr for the supercoiled DNA and the nicked circular DNA conformation, at high dye concentrations, is used to investigate the conformational changes induced by an enzymatic reaction [Paoletti et al, 1971; LePecq, 1973]. In the presence of excess EthBr, a single nick is made on the supercoiled DNA conformation; the break in the nucleotide sequence is made by the enzymatic reaction of DNase. As the topological constraint limiting the binding of the dye molecules is eliminated, the nicked superhelix relaxes into the nicked circular conformation, accompanied by an increase in the fluorescence intensity. The reverse is true for the transformation of the nicked circular DNA conformation into the supercoiled DNA conformation. The enzyme, Ligase, is used to repair the break in the nucleotide sequence of the nicked circular DNA conformation. The result is a decrease in fluorescence intensity, associated with the conversion of the nicked circular conformation into the supercoiled DNA conformation. The fluorescence intensity changes accompanying the transformation of the DNA conformations provides the basis for studying the details of these enzymatic reactions [LePecq. 1973].

A conformational change in a macromolecule, involving a minor modification of the distance between two chromophores, can be perceived by measuring the changes in the energy transfer rate of the chromophores. The rate of energy transfer between a donor and an acceptor chromophore is inversely proportional to the sixth power of the distance between them, and proportional to their orientation factor [Forster, 1959; LePecq, 1973]. Minor variations in the intermolecular distance between

the base of phenylalanine t-RNA of yeast and EthBr bound to the strongest binding site were uncovered by Tao et al [1970; LePecq, 1973] who measured the variations of the energy transfer rate between the chromophores. They found that the rate of energy transfer, and thus the intermolecular space between the chromophores, change, as a function of the change in the salt concentration of the solution. This suggests that the degree of a conformational change in the t-RNA biopolymer is dependent on the ionic strength of the microenvironment.

Although the DNA macromolecule has a large molecular weight the fluorescence lifetime of the rigidly bound, intercalated EthBr molecules is of a sufficient duration to detect the dynamic structure of DNA [Kelly and Sinsheimer, 1967; LePecq, 1973]. The rotational relaxation time of a macromolecule can be determined by measuring the fluorescence depolarization of the bound probe [Stryer, 1968]. The decay in the fluorescence anisotropy of the bound EthBr monomer, as a function of time in the nsec. range, implies that the DNA macromolecule in solution has an internal oscillatory Brownian motion, possessing a relaxation time of 28 nsec. and an amplitude of 35° for the oscillation [LePecq, 1973].

The facility and limitations of using EthBr fluorescence microspectrophotometry to obtain detailed information on the structure and function of nucleic acids, in respects to the intact cell, can be examined in complicated systems of nucleoproteins like ribosomes, chromosomes, etc. [Bollen et al, 1970; Angerer and Moudrianakis, 1972; LePecq, 1973]. In the cell the nucleic acids are found intimately associated with proteins. The existence of proteins on the surface of the nucleic acids hinders the binding of EthBr to the NA macromolecule.

In experiments involving the reconstitution of the ribosome out of its protein and nucleic acid components, Bollen et al [1970; LePecq, 1973] investigated the binding behavior of EthBr molecules to rRNA macromolecules in the presence of ribosomal proteins. The fluorescence intensity of EthBr bound to rRNA was measured as the ribosomal proteins were serially added to the rRNA. When the concentration of the ribosomal proteins increased, the fluorescence intensity of the EthBr-rRNA complexes exhibited a drastic decline. The EthBr molecules were bound into the double stranded regions of the rRNA macromolecule, in the monomer form, and were expelled from the rRNA macromolecules during the formation of the ribosome. The reconstituted ribosome was contradistinctive to the native ribosome in that it binds some EthBr and the latter did not [Bollen et al, 1970]. Since fluorometry can be used to follow the reconstitution kinetics of ribosomes in vitro, the formation of Nissl bodies, i.e. polyribosomes, and the NA-dye-protein interactions may be investigated by EthBr fluorescence microspectrophotometry in the living neuron. The stimulation of a living neuron would result in an increase in the Nissl body content of the neuron, which would be accompanied by a decrease in the fluorescence intensity of EthBr bound to the free rRNA macromolecules in the neuron. In the dissociation and reconstitution of nucleohistones, and in the trypanosoma (which are parasitic flagellate protozoans that infest the blood stream of animals) the binding behavior of EthBr to DNA macromolecules in the presence of chromosomal proteins is similar to the binding of EthBr to rRNA macromolecules in the presence of ribosomal proteins [Angerer and Moudrianakis, 1972; LePecq, 1973]. The EthBr molecules can readily bind to a DNA

macromolecule that is free of proteins, in contrast, the binding of EthBr to DNA macromolecules in deoxyribonucleoproteins is limited by the close association of the chromosomal proteins with the surface of the DNA macromolecules. The binding of EthBr molecules to the DNA macromolecule may be further limited by the foldings in the DNA structure. The fluorescence characteristics of EthBr bound to the DNA of intact phages has been measured as a function of the folding constraint of the DNA macromolecules in the phage [LePecq, 1973]. The variations of the constraints imposed by the DNA folding which induces conformational changes in the DNA helix are produced by the smaller amount of DNA, packed in the same head volume, of different deletion mutants of the phage. As the amount of DNA is decreased in the mutants, the folding constraint of the DNA macromolecules is progressively released. The fluorescence characteristics of EthBr bound to the DNA tightly confined in the deletion mutants, gradually returned to the fluorescence characteristics of EthBr bound to DNA macromolecules free in solution. The constraints imposed by the increased DNA folding restricts the intercaltion of EthBr, but favors the binding of the dye molecules to the second binding site [LePecq, 1973]. The limitations in using EthBr fluorescence microspectrophotometry must be known before any meaningful interpretations of the results on its application to the neuron can be expressed, especially the restrictions put upon by the folding constraint of the native NA structures and the protein components of nucleoproteins. The facility of using EthBr on single living neurons is the detection of changes in the conformations of the DNA macromolecules in the chromosomes, and changes in the cellular pool of free RNA macromolecules, as the result of alterations in the internal and/or external

environment of the neuron. The fluorescence of EthBr can be quenched through the transfer of energy between EthBr and a non-fluorescent EthBr derivative, and through proper energy transfer experiments, this may facilitate the maping of superhelices, the measuring of inter-helix spacing, and the study of DNA packing in the chromosomes, provided the superhelices can be specifically labeled [LePecq, 1973], and may facilitate the study of the NA-dye-protein interactions, in the neuron. The energy transfer and the quenching of fluorescence can be measured, as a function of changes in the microenvironment of the bound probe, yielding information on the molecular interactions of the probe before, during, and after any microenvironmental change.

Acridine orange and ethidium bromide are suitable fluorescent probes to explore the details of the structures and functions of nucleic acids in the single neuron. The AO and EthBr molecules can selectively bind, in the monomer form, into the double stranded regions of the NA macromolecules. In a similar manner, both dye molecules are intercalated, in a "sandwich complex," between two adjacent base pairs causing a slight distortion of the double strands; the three ring structure of the dye molecule is immersed into the hydrophobic interior of the stacked bases, with the electrically charged phosphate groups that are bound to the hydrophilic sugar residues of the nucleotides being located on the periphery of the complex. The differences between the binding behavior of AO and EthBr to the NA, and the nature of the investigation, prescribes which fluorescent probe is to be used on the NA in the neuron. Dissimilar to EthBr, AO molecules can readily bind to the native ribosomes and chromosomes. The existence of proteins on the surface of the NA macromolecules does not prevent the binding of AO to the NA, in fact, the

anionic portions (carboxyl groups) of the proteins in the organized nucleoprotein compete with the negatively charged phosphate groups of the NA to bind the cationic AO molecules. Since the amount of AO bound by a NA is proportional to the amount of the NA, the greater sensitivity of AO infers that in experiments involving the microspectrophotometric determination of the quantity of rRNA in the some of single neurons, as a function of a neuronal parameter such as age; AO would be the better fluorescent probe to use than the employment of EthBr. The amount of EthBr bound by a NA is a measure of the amount of double stranged regions in the NA [LePecq, 1973]. Although the binding affinity of AO for nucleoproteins is greater than that of EthBr. EthBr would be preferred over AO, as a fluorescent probe, in investigations of the molecular interactions of rRNA macromolecules, during the initial phases of the restoration of the neuron to its resting state following neuronal excitation or inhibition. Since the expulsion of EthBr occurs in the association of rRNA macromolecules with ribosomal proteins, the fluorescence intensity of EthBr bound to free rRNA macromolecules would decrease when the free rRNA macromolecules are integrated into ribosomes, and when the ribosomes are aggregated into polyribosomes. Keeping adult rats in the dark for 3 days, and then exposing them to laboratory lights and sounds of 15 mins., has been reported to increase the polyribosome to monomer (i.e. a monomer ribosome) ratio by 83% in their cerebral cortex while nothing happens in their liver [Mahler, 1972]. Electroshock has been reported to decrease the polyribosome to monomer ratio, because it dissociates the polyribosomes [Mahler, 1972]. This suggests that when the state of aggregation of the ribosomes in the neurons, the polyribosome to monomer ratio, increases the fluorescence intensity of EthBr bound

to the rRNA macromolecules in the ribosomes would decrease, and vice versa.

If the binding behavior of AO to the NA, as a function of the folding constraint of the NA, is similar to that of EthBr, then increasing the folding of the NA conformation would progressively strengthen the constraint limiting the binding of AO to the NA in the monomer form. Then the constraint imposed by the folding of the NA in organized systems like Nissl bodies, i.e. polyribosomes of different degrees of aggregation, and chromosomes inside the living or fixed neuron can hinder the binding of AO to the NA. The amount of AO molecules bound, in the monomer form, by the NA macromolecules in a gene or a ribosome of the neuron, would be less than the quantity of monomer AO molecules bound to the same NA macromolecules free in a gelatin microdroplet. Since the fluorescence coefficient of a NA at 536 nm. is a measure of the amount of AO molecules bound per pq. of the NA macromolecules, in the monomer form. Possibly the f.c. $\frac{DNA}{536}$ and f.c. $\frac{rRNA}{536}$ for the fixed neuron may be really less than the corresponding fluorescence coefficients for the gelatin microdroplet, advocating that the lower γ value for the fixed neuron is actually due to the f.c. $^{\text{rRNA}}_{536}$ being greater than the f.c. $^{\text{DNA}}_{536}$. In addition, the folding constraint may favor the binding of AO to the NA in the aggregated form, and since the AO molecule does not have a phenyl group lieing perpendicular to the plane of the dye molecule like EthBr, the aggregation of AO on a NA macromolecule is greater and occurs faster than that of EthBr. Then the amount of AO molecules aggregated on a given NA macromolecule in the neuron would be greater than the amount of dye molecules aggregated on the same NA macromolecule in a gelatin microdroplet, under the same staining conditions. This suggest that

	•
	,
	;
	<i>*</i>
	;
	•
	•
	,

the staining concentrations where Beer's law prevails for the fixed neuron is less than that for the gelatin microdroplet. At the $5 \times 10^{-5} M$ and $1 \times 10^{-4} M$ AO staining concentrations, the fluorescence coefficients and equation (4) of the gelatin microdroplet experiments can not be directly applied to the fixed neuron, in determining its rRNA + $\gamma(DNA)$ content.

The RNA metabolism of a neuron is strongly correlated to the behavioral and physiological functions of the neuron. The existing functional state of the neuron establishes the RNA level in the neuron, where, at the time of observation, the RNA content of the activated or depressed neuron is greater than or less than, respectively, the proper quantity of RNA in a normal quiescent neuron of the same age and type. The external and internal environmental circumstances of the functioning neuron affects the synthesis of RNA in the neuron. The rate of RNA synthesis in the giant neurons of the abdominal ganglia in the sea hare Aplysia, in vivo, is increased significantly as the result of prolonged neuronal stimulation; the incorporation of radioactively labeled nucleosides into the RNA of excited neurons is greater than that of unstimulated controls [Mahler, 1972]. This is consistent with the effects of stimulation on the RNA synthesis in the rat Purkinje neurons, and the frog retinal ganglion and cat sympathetic ganglion neurons. The correlation between the functional activity of a neuron and the synthesis of RNA in the neuron, as influenced by the environment, is demonstrated in experiments investigating the effects of visual stimulation on the incorporation of orotate (pyrimidine derivative of RNA precursors) into the RNA of the visual cortex in rats [Mahler, 1972]; and the effects of strychnine sulfate and of marijuana on the brain RNA and DNA content,

and on the maze learning (consolidation of memory) of rats [McGaugh and Petrinovich, 1959 and 1965; Carlini and Carlini, 1965; John, 1967]. The rate of labeling of RNA in the visual cortex of a totally blind strain of rats is delayed and decreased, in comparison to the rate of RNA labeling in the visual cortex of normal sighted rats [Mahler, 1972]. The RNA labeling of the visual cortex in the sighted animals is more distinctive when using a flashing light rather than continuous illumination for the stimulation, and the labeling rate of RNA in the motor cortex of the blind rats is similar to that of the sighted rats. This phenomenon can be seen in animals that are kept in the dark from birth or blinded, in that, they exhibited a deficit in the RNA content of various cells in their visual system [Mahler, 1972]. The level of RNA in a neuron can influence its performance in behavioral functions like memory and learning. Strychnine can cause hyperactivity and increase the synthesis of RNA in a neuron by prolonging the action potential and producing repetitive spike discharge in the neuron [Washizu et al, 1961; John, 1967]. The injection of strychnine sulfate into rats before or after learning trials increased their speed of consolidation (of memory) and enhanced the brain RNA content of the rats, with no effects on the brain DNA content. However, marijuana can only facilitate learning in rats when administered before the training session; the marijuana increases the concentration of the brain DNA but not RNA. The facilitation of learning by marijuana may not be directly related to the consolidation process, but due to general factors [John, 1967]. These results suggest that the rate of learning for rats can be increased by increasing the level of RNA in their neurons, and possibly by raising the nuclear DNA level of other brain cells such as the neuroglia.

8-azaguanine is known to inhibit the synthesis of RNA in the rat brain, and rats injected with 8-azaguanine show significantly poorer retention in learning a maze than compared to controls [Dingman and Sporn, 1961; John, 1967]. To reiterate, clearly, there is a strong correlation between the RNA metabolism and the behavioral or physiological functions of the neurons. The existing functional activity of a neuron can set the amount of RNA present in the neuron. The continuous activity of neuronal aging effects the RNA content of a neuron much more slowly than transient activities like neuronal excitation. Therefore, in order to accurately calculate the differential accumulation rate of RNA for a specific neuronal type, as a function of time (postnatal), the experimental neurons at the time of fixation or observation must be in the same transient state.

The incorporation kinetics of radioactively labeled precursors of RNA into the RNA of an isolated neuron can express the various molecular species of the RNA (newly synthesized) in the neuron [Mahler, 1972]. The nuclear and nucleolar RNA become radioactively labeled immediately after the administration of the precursors to the neuron. The ribosomal precursors are first labeled in the nucleolus, having sedimentation coefficients of 45S, 35S, and 32S; a little later, a polydisperse species is labeled in the nucleus, this is not the direct precursor of the equally polydisperse mRNA, but it has sedimentation coefficients varying from 50S to 5S and is capable of effective hybridization with DNA. Several minutes after the nucleus is extensively labeled mRNA makes its first appearance in the cytoplasm associated with ribonucleoprotein particles. The labeling of the stable rRNAs, which are integrated into the ribonucleoproteins, follows the

cytoplasmic mRNA within 30 mins. to 1 hr., proceeding until an isotopic steady state is reached [Mahler, 1972]. In addition, in the adult rat, the rRNAs and the ribosomal proteins of the ribosome turnover as a unit in about 12 days [Mahler, 1972]. It would be nice if there were specific fluorescent molecular probes for each of the various molecular species of RNA and DNA. Then the metabolic changes of each NA species, in relation to the state of the neuron, could be studied by fluorescence microspectrophotometry. A thorough understanding of the molecular events associated with the various NA species during behavioral or physiological functions of the neuron may eventually lead to the cures of some neural disorders, i.e. paralysis, mental illness, etc., and the enhancement of some normal neural functions like memory and learning.

Although, at present, only the relative values for the NA concentration in the soma of neurons can be determined by the author's methodology, the utilization of the appropriate staining conditions in the method may yield the absolute amounts of rRNA and DNA inside the soma of living neurons. The application of equation (4) to the single neuron requires that the fluorescence intensity of AO-rRNA and AO-DNA complexes at 536 nm. be proportional to the amount of AO molecules, DNA, and rRNA macromolecules available for interaction. Therefore, the ratio of dye to neuron (intracellular dye content per cell) is very important, since AO obeys Beer's law up to a concentration that would cause its aggregation. The cellular framework of the neuron serves to concentrate the amount of AO inside the neuron; a high dye-to-neuron ratio would increase the aggregation of the AO molecules onto the rRNA and DNA macromolecules, causing the fluorescence intensity of the AO-complexes at 536 nm. to be non-proportional to the concentration of dye molecules and NA

macromolecules in the neuron. The utilization of a low dye-to-neuron ratio would eliminate the problem caused by the polymerization of the AO molecules, and may be accomplished by using low dye concentrations for the staining of the neuron. The results of the gelatin microdroplet experiments indicate that an AO staining concentration of 1 x 10^{-6} M should be low enough so that Beer's law is obeyed, and toxicity or damage to the living neuron is prevented. At this concentration, the amount of AO bound per rRNA macromolecule is equivalent to the amount bound per DNA macromolecule and proportional to the monomer AO fluorescence intensity at 536 nm., and the degree of aggregation of AO onto the NA macromolecules is very low (see Figures 7 and 8). (An experiment to determine the staining concentrations for which Beer's law holds true for the living neuron is the examination of the fluorescence emission properties of the rRNA in Nissl bodies and the DNA in chromosomes of a specific AO-stained neuronal type and age, as a function of low staining concentrations.) The staining time for the neuron should allow for the maximum amount of monomer binding sites on the NA macromolecules to be filled, and the equilibrium between the cell and dye molecules to be reached. A neuronal staining time of 1 hr. should permit the monomer binding sites on the DNA and rRNA macromolecules to be roughly 70% full with all of the binding sites in the outer regions of the macromolecules completely filled. In order to keep the neurons healthy and alive during the staining process, physiological saline can be employed as a solvent for the dve and rediffusion solutions. Unfortunately, the results from the microdroplet experiments involving the binding of AO molecules to NA macromolecules in the presense of ions cannot be directly applied to the neuron because there

is no valid way to measure the ion concentration in the microenvironment of the NA in the neuron. However, the results (Figures 12 and 13) do show that ions in the microenvironment of the NA can increase the binding of AO in the monomer form, and decrease the aggregation of the AO molecules. The physiological saline can be buffered to pH 7.2 with McIlvanine's citrate-phosphate buffer, minimizing the changes in the ionic strength. The pH 7.2 would allow for the optimum binding of AO to the NA, and the amount of AO bound per rRNA macromolecule is nearly equivalent to the amount bound per DNA macromolecule (see Figure 10; for the living cell the intranuclear and cytoplasmic pH average 7.3). Bear in mind that not only is the interaction of AO molecules and the NA macromolecules affected by the dye concentration, staining time, staining solution pH and ionic strength, but also by the temperature at which the reaction is taking place. The neuron could be incubated in the reaction solutions, of constant volume, in its incubator at 37° C with a humid $C0_{2}$ -air (5:95) environment. A preliminary experiment must be performed to ascertain the effects of the incubation and of the rediffusion time on the interaction of AO with the NA in the living neuron.

Ideally, it would be desirable to have the binding behavior of AO molecules to the DNA and rRNA macromolecules in the microdroplet identical to that in the living neuron. This implies that the NA microenvironment of the microdroplet may be made similar, as much as possible, to the microenvironment of the NA in the neuron. The cellular components, void of NA, that make up neurons can be employed as the material for the microdroplets. Also, the microdroplets may be subjected to the same circumstances as the neuron. In addition, the above staining condition

can be applied to the microdroplets to obtain the proper fluorescence coefficients. If, under these conditions, the binding behavior of AO molecules to the NA macromolecules is identical to that in the neuron, then as a possible check, the F_{536} of 6.5 pg. DNA in the microdroplet should be equal to the F_{536} of the nucleus of neurons, and other mammalian cells treated in the same manner. This suggests that γ ,(f.c. $\frac{DNA}{536}$ /f.c. $\frac{rRNA}{536}$), may be equal to 1 or less, and the f.c. $\frac{DNA}{536}$ and f.c. $\frac{rRNA}{536}$ are equivalent or the f.c. $\frac{rRNA}{536}$ is greater than the f.c. $\frac{DNA}{536}$.

The RNA content in the soma of single neurons can be obtained as a function of various parameters such as age, drugs, excitation, etc. As an example, the neuron may be stimulated ionophoretically for various periods of time at a specific frequency; after each period the NA content in the neuron could be determined. Before the staining process, the neuron should be permitted to rest and given a chance to respond to the parameter. Staining procedures such as that used in Figures 24 to 27 may be devised to delineate AO-DNA complexes in the nucleus from AO-rRNA complexes in the cytoplasm. Also, the NA content of isolated nuclei or ribosomes may be determined chemically and compared to that determined by this method.

The author strongly advocates that the identification of future neurons found in dissociated or reassociating cell cultures of the cerebral cortex of rats, fitting the morphological descriptions of Canada, Type I, Canada, Type II, and Canada, bipolar neurons be characterized as these neuronal types.

IV. CONCLUSIONS

In this investigation, the author examined the fluorescence characteristics of the binding of acridine orange to nucleic acids in different microenvironments. The fluorescence emission spectra of acridine orange molecules bound to deoxyribonucleic acids, ribosomal ribonucleic acids, and polyuridylic acids in gelatin microdroplets and in single fixed neurons were found to be the same under a number of different circumstances (polyuridylic acids were not examined in the cells). The fluorescence spectrum of AO bound to each NA had a maximum at 536 nm. and a secondary peak at 604 nm. The relative fluorescence intensity at 536 nm. and at 604 nm. was interpreted to reflect the amount of AO molecules bound to the NA macromolecules in the monomer form [Bradley and Wolf, 1960; Loeser et al, 1960; Rigler, 1966; West, 1969, 1973] and aggregated form, respectively. It was determined that AO has a specific binding affinity for each NA: the binding constant for a DNA macromolecule is greater than a rRNA macromolecule, which is greater than a Poly U macromolecule. The binding affinity of AO for gelatin proteins is less than that for the NA.

The binding behaviors of AO molecules onto DNA and rRNA macromolecules were found to be different, as a function of the AO staining concentration, dye-NA interaction time, staining solution pH, and the NaCl concentration. 1. In the presence of an increasing dye concentration the binding of the dye molecules onto the nucleic acids' macromolecules demonstrated a linear intensification; indicating that

the total amount of AO bound to the NA in the monomer form, depends proportionately on the quantity of free dve molecules initially available in the microenvironment for binding a NA macromolecule. 2. Increasing the interaction time of the AO molecules with the NA macromolecules enhanced the binding of the dye molecules to the NA macromolecule. The amount of AO bound to rRNA in the monomer form is proportional to the length of time, in minutes, the dye molecules were allowed to bind to the rRNA macromolecules. There were two phases involved in the binding of AO molecules to the DNA macromolecules in the monomer form; during the first 35 mins. of staining, there was a rapid uptake of dye molecules by the DNA macromolecules--approximately 3.4 times faster than that of the rRNA macromolecules, later, the uptake of dye molecules by the DNA macromolecules substantially decreases by more than 80% of the initial value. The majority of the monomer binding sites on the DNA conformation were completely filled, during the initial 30 mintues of interaction. and on the rRNA conformation they were only partially filled. 3. The binding of AO to the nucleic acids increased, as the pH increased from 4.0 to 8.4. The lower amounts of AO bound to DNA or rRNA at acid pH were due to an augmented positive charge on the AO molecules and on the negative phosphoric acid residues of the nucleotides; which leads to an enhanced molecular repulsion, along with the suppression of the binding sites, thereby decreasing the binding of AO molecules to the NA macromolecule. Decreasing the positive charge concentration in the environment to neutral pH maintains a relatively stable NA conformation and permits the phosphoric acid residues to become ionized, favoring the molecular attractions and hydrophobic interactions of the NA nucleotides and the dye molecules. This increases the binding of AO to the

- NA macromolecule. 4. The binding of AO to the nucleic acids increased in the presence of ions. Since the degree of structural order of nucleic acids is reduced at low ionic strengths, increasing the NaCl concentration in the microenvironment would serve to fortify and enhance the hydrophobic interactions between the acridine and nucleotide base ring structures, within the interior of the NA macromolecule. This increases the binding of AO to the NA in the monomer form via hydrophobic bonding. At low NaCl concentrations, the DNA conformation has greater sensitivity in binding AO in the monomer form than the rRNA conformation.
- 5. The denaturation of the rRNA conformation slightly increased the binding of AO to the macromolecule. The spectral distribution of AO molecules bound to the different denatured conformations of rRNA macromolecules are identical.
- 6. The two fluorescence molecular species of acridine orange, the monomer and aggregated forms, were found to have different fluorescence decay behaviors as a function of the irradiation time: the fluorescence fading of AO-DNA, rRNA and gelatin protein complexes at 536 nm. displays somewhat faster decay rates than the corresponding fluorescence fading at 604 nm.; the fluorescence fading is more dependent on the binding mode of acridine orange than on the conformation or type of the biopolymer.
- 7. It was established that the total amount of AO bound by DNA and rRNA macromolecules is proportional to the quantity of NA available for binding the dye molecules, in the monomer form. This implies that each NA macromolecule has a specific number of binding sites for AO molecules in the monomer form. Fluorescence coefficients, f.c. $\frac{DNA}{536} = 1.26$ and f.c. $\frac{rRNA}{536} = 0.272$, were procured and employed in the calculation of

the NA content in gelatin microdroplets. The equation

$$R + \gamma D = \frac{\log F_{536} - \log b}{f.c._{536}^{\text{rRNA}}}$$

can be used to calculate the total NA content of a given gelatin microdroplet system; $\gamma = (f.c. \frac{DNA}{536})/(f.c. \frac{rRNA}{536})$, and b = background fluorescence. With the author's methodology, the smallest amounts of nucleic acids, easily detectable, were about 0.38 pg. DNA and 0.8 pg. rRNA.

There were three neuronal types identified in dissociated cell cultures of female albino rat cortices: the Canada Type I, Canada, Type II, and the Canada, bipolar neurons. The NA content in the Canada, Type II, and Canada, bipolar neurons between the ages of 67 da. and 99 da. old demonstrated identical growth rates, 0.1 pg. NA per diem. The NA content in the Canada, bipolar neurons were always greater than that in the Canada, Type II neurons by 8%. The monomer form of AO is the primary mode of binding onto the NA macromolecules in the neurons and in the gelatin microdroplets, and the disposition of this AO formation depends heavily on microenvironmental conditions.

In recent years neuroscientists have gained valuable information anent the structure and function of macromolecules involved in neural systems during behavioral responses. This information is inadequate to fully understand the molecular interactions between the central nervous system and the mind. However, if the neuroscientists were able to determine the molecular events underlying the behavioral or physiological functions of neural systems, drugs which affect specific molecular mechanisms can be administered to organisms in order to facilitate specific functions of their neurons [Washizu et al, 1961;

McGaugh and Petrinovich, 1959 and 1965; Cameron et al. 1961 and 1966; John, 1967; Unger, 1970; Gaito, 1971; Mahler, 1972]. The application of this concept to the human organism would improve our potential for specific behavioral characteristics, such as better work performance, increased longevity, higher intelligence, better mental makeup (mental health), and other aspects [Gaito, 1971]. The administration of yeast RNA to senile and arteriosclerotic individuals is reported to improve their memories and alleviate their emotional problems; however, these improvements would diminish when the RNA is discontinued [Cameron and Solyom, 1961; Gaito, 1971]. This may be due to the yeast RNA being readily attacked by the highly active RNase of the aged patients, permitting more of their native RNA to be free from attack since the RNase activity in the blood of humans increases with age [Kral and Sved, 1963; Gaito, 1971]. If neuroscientists could ascertain the molecular mechanisms of the learning process, the appropriate chemical could be administered to intellectual retardates or normal individuals to increase their intellecutal potential and performance. A considerable amount of time in the life of a human being is spent engaged in the performance of work. Improving the work performance of the individual would be of great value to man. Specified drugs administered to individuals could improve their performance and productivity during the work experience, thereby raising the level of the human society. The environmental circumstances of an individual affects the development of his intellectual potential. The author concludes that the concept of regulating specific endogenous chemicals, which affect the molecular events of specific behavioral or physiological functions of the neural systems in the human, may allow the individual to approach or reach

his true potential under the existing internal and/or external environment. The chemical approach could supplement the current principles in maximizing the intellectual and physical performance of the individual [Gaito, 1971].

The metabolic modifications of the structural and functional characteristics of the nucleic acids due to neuronal aging affects the functions of the normal living neuron. The RNA content in the neurons of humans may tend to decrease when the individual reaches the twilight years of life, resulting in the decline of behavioral and physiological functions of the individual's neurons, and reflected by the deterioration of the individual's physical and mental capabilities [Gaito, 1971]. The prevailing metabolic circumstances might cause the diminuation of the RNA content and the functions of the neurons in the aging human. Kral and Sved [1963; Gaito, 1971] reported that the RNase activity in the blood of humans increased with age of the individual. They found that the enzymatic activity of RNase in the blood of individuals at 60 years of age was about 25% greater than that in individuals at age 20; and at 100 years old, about 50% greater. The enzyme RNase attacks the RNA and degrades it by hydrolyzing the ester linkage between the hydroxyl and phosphoric acid groups of the phosphodiester bonds of the RNA backbone [Lehninger, 1970, pp. 254-255]. Provided that the RNase activity in the blood is representative of enzymatic activity in the brain, the increased activity of RNase in aged individuals would reduce the amount of RNA in the neurons of their brains [Gaito, 1971]. The template activity of DNA for RNA synthesis is less effective with increasing age [Gaito, 1971]. This would decrease the quantity of RNA in the aged neuron; coupled with the increase in the RNase activity, they may cause

functional changes in the aging human. To consider another metabolic circumstance of aging, the hydrogen bonding in polyribosomes is significantly different in neurons of aged rats (24 months) than in neurons of young rats (3 months) [Gaito, 1971]. In the aged rats the larger polyribosomes of the neuron exhibited less hydrogen bonding, and the smaller polyribosomes, conversely, exhibited greater hydrogen bonding, than that in corresponding polyribosomes of the younger rats. change in hydrogen bonding in polyribosomes of the aged neuron is greater when the temperature is raised, than that of younger neurons [Gaito, 1971]. This suggests that the polyribosomes of aged neurons have markedly different internal structures, and are deficient in the capacity to synthesize protein, compared to polyribosomes of young neurons. The agealtered conformation of the RNA in the polyribosomes of aged neurons can be restored to the characteristics of the young normal state by the administration of the drug, diphenylhydantoin or NP-113 (developed by the Newport Pharmaceuticals, Inc., Newport Beach, California) to the aged animal [Gaito, 1971]. These drugs enhanced the synthesis of brain RNA and protein and improved the learning and memory functions of the aged animals. Therefore, if the neuroscientists were able to determine the affects of aging on the molecular mechanisms of behaviors, the proper chemicals could be administered to aged individuals to increase their functional capabilities.

The regulation of the molecular events underlying behavioral or physiological functions of the neuron would be of great value to man; it could raise the performance and productivity of individuals in the total human society. Obviously much research is needed before such an idea can be put into practice today. However, the use of acridine orange

fluorescence microspectrophotometry, in conjunction with dissociated neuron cultures, can facilitate the realization of this concept in the future.

Forthwith, biophysical cytochemistry, i.e., the use of fluorescent molecular probes in conjunction with neuron cultures, can be applied in the investigation of the effects of alcohol (C_2H_60) on the structure and function of nucleic acids and on the behavioral and electrophysiological functions of the single living and/or fixed neuron; this is a research proposal of the author. Is the RNA metabolism and the functional activity of neurons maintained in the presence of alcohol significantly different compared to neurons not under the influence of alcohol? Is the correlation between the RNA metabolism and the functions of the intoxicated neuron different from that of the sober neuron? The response to these and many more questions concerning the molecular phenomena of neuronal functions can be facilitated by this technique. The RNA content in specific neuronal types and ages, as a function of the alcohol concentration in the medium of the living neuron, can be determined by the application of acridine orange fluorescence microspectrophotometry to single neurons from the cerebral cortex and/or the substantia nigra of the rat brain. Assuming that the synthesis of RNA in the neuron is slowed or inhibited by alcohol, neurons maintained in a high alcohol content environment should have less RNA than neurons of the same age and type living in an alcohol-free environment. Due to the metabolic changes of aging, the RNA synthesis of aged neurons, chronically subjected to high doses of alcohol, should be less than that of younger neurons under the same conditions. The pulse rate and the RNA content of a specific neuronal type and age can be determined before, during,

and after stimulation of the neuron; the firing behavior correlated to the RNA content of the alcoholic neuron should be different than that of the nonalcoholic neuron. EthBr fluorescence microspectrophotometry may possibly be used to follow the kinetics of polyribosome formation and structural changes of the chromosomes in neurons influenced by alcohol. If the correlation between the RNA metabolism and the functions of neurons, in vivo, are similar to those of neurons in culture, when subjugated to the same alcohol concentrations, the behavior performance and synthesis of RNA of the intoxicated animal or neuron may be lower than that of the sober neuron or animal. The author's application of biophysical cytochemistry to single neurons in culture represents a model system that may provide salient answers concerning the molecular events engaged in neuron-to-neuron interactions.

LIST OF REFERENCES

LIST OF REFERENCES

- Angerer, L. M., and Moudrianakis, E. M., "Interaction of Ethidium Bromide with Whole and Selectively Deproteinized Deoxynucleoproteins from Calf Thymus," J. Mol. Biol., vol. 63, p. 505, [1972].
- Bauer, W., and Vinograd, J., "The Interaction of Closed Circular DNA with Intercalative Dyes. I. The Superhelix Density of SV40 DNA in the Presence and Absence of Dye," J. Mol. Biol., vol. 33, p. 141, [1968].
- Benjamins, J., and McKhann, G., "Neurochemistry of Development," <u>Basic</u>
 <u>Neurochemistry</u>, Albers et al eds., Little and Brown Co., Boston,
 p. 269, 11972].
- Bertalanffy, Ludwig von, "Acridine Orange Fluorescence in Cell Physiology, Cytochemistry and Medicine," Protoplasma, vol. 57, p. 51, [1963].
- Bollen, A., Herzog, A., Favre, A., Thibault, J., and Gros, F., "Fluorescence Studies on the 30S Ribosome Assembly Process," FEBS Leters, vol. 11, p. 49, [1970].
- Bradley, D. F., and Wolf, M. K., "Aggregation of Dyes Bound to Polyanions," Proc. Natl. Acad. Sci. U.S., vol. 45, p. 944, [1959].
- Bradley, D. F., and Wolf, M. K., <u>The Neurochemistry of Nucleotides and Amino Acids</u>, R. O. Brady and D. B. Tower, eds., Wiley, New York, [1960].
- Cameron, D. E., and Solym, L., "Effects of Ribonucleic Acid on Memory," Geriatrics, vol. 16, p. 74, [1961].
- Cameron, D. E., Kral, V. A., Solyom, L., Sved, S., Wainrib, B., Beaulieu, C., and Enesco, H., "RNA and Memory," Macromolecules and Behavior, J. Gaito, ed., Appleton-Century-Crofts, New York, [1966].
- Carlini, G. R. S., and Carlini, E. A., "Effects of Strychnine and Cannabic Satira (marijuana) on the Nuclei Acid content in Brain of the Rat," Med. Pharmacol. Exptl., vol. 12, p. 21 [1965].
- Chignell, C. F., "Fluorescence Spectroscopy as a Tool for Studying Drug Interactions with Biological Systems," Fluorescence Techniques in Cell Biology, A. A. Thaer and M. Sernetz, eds., Springer-Verlag, New York [1973].

- Crain, S. M. and Peterson, E. R., "Onset and Development of Functional Interneuronal Connections in Explants of Rat Spinal Cord-Ganglia During Maturation in Culture," Brain Research, vol. 6, p. 750, [1967].
- Crestfield, A. M., Smith, K. C., and Worthington-Allen, F., "The Preparation and Characterization of Ribonucleic Acid from Yeast," J. Biol. Chem., vol. 216, p. 185 [1955].
- Dingman, W., and Sporn, M. B., "The Incorporation of 8-Azaguanine into Rat Brain RNA and Its Effect on Maze Learning by the Rat," J. Psychiat. Res., vol. 1, p. 1, [1961].
- Dobbing, J., and Sands, J., "Timing of Neuroblast Multiplication in Developing Human Brain," Nature, vol. 226, p. 639, [1970].
- Edstrom, J. E., "RNA Mass and Concentration in Individual Nerve Cells," Biochem. Biophys. Acta, vol. 12, p. 361, [1953].
- Edstrom, J. E., "Determination of Organic Compounds Below the Microgram Range: RNA and Its Constituents," Microchem J., vol. 2, p. 71, [1958].
- Edstrom, J. E., "Microextraction and Microelectrophoresis for Determination and Analysis of Nucleic Acids in Isolated Cellular Units," Methods in Cell Physiology, D. M. Prescott, ed., vol. 1, p. 417, [1964].
- Ehrlick, P., Arch. Anat. Physiol. Abt., p. 166, [1879].
- Foster, Th., Fluoreszenz Organischer Verbindungen, Vandenhoeck und Ruprecht, Gottingen, [1951].
- Forster, Th., "Transfer Mechanisms of Electronic Excitation," Disc. Faraday Soc., vol. 27, p. 7, [1959].
- Gaito, J., "DNA Complex Therapy," <u>DNA Complex and Adaptive Behavior</u>, J. J. Jenkins, ed., Prentice-Hall, Englewood Cliffs, New Jersey, p. 92, [1971].
- Haltia, Matti, "Postnatal Development of Spinal Interior Horn Neurons in Normal and Undernourished Rats: A Quantitative Cytochemical Study," Acta Physiologia Scandinavia, Suppl. 352, [1970].
- Hyden, Holger, The Neuron, Elsevier Publishing Co., New York, [1967].
- Jenkins, T. W., <u>Functional Mammalian Neuroanatomy</u>, Lea and Febiger, Philadelphia, [1972].
- John, E. Roy, "Possible Mechanisms of Stable Information Storage: Experimental Evidence," <u>Mechanisms of Memory</u>. Academic Press, New York, Chap. VI, p. 93, [1967].

- Kelly, R., and Sinsheimer, R. L., "The Replication of Bacteriophage MS2. VIII. Fractionation of the Replicative Intermediate Using a BNC Column," J. Mol. Biol., vol. 29, p. 229, [1967].
- Kohen, E., Thorell, B., Kohen, C., and Michaelis, M., "Rapid Micro-fluorometry for Biochemistry of the Living Cell in Correlation with Cytomorphology and Transport Phenomena," Fluorescence Techniques in Cell Biology, Thaer and Sernetz, eds., Springer-Verlag, New York, [1973].
- Kral, V. A., and Sved, S. Clinical and Biochemical Remarks on the Ribonucleic Acid Treatment of Alzhemer's Disease. Paper presented in symposium entitled "Nucleic Aci-s and Behavior," Midwestern Psychological Association Meetings, Chicago, Illinois, [1963].
- Langridge, R., Seeds, W. E., Wilson, H. R., Hooper, C. W., Wilkins, M. H. F., and Hamilton, L. D., J. Biophys. Biochem. Cytol., vol. 3, p. 767, [1957].
- Lehninger, Albert, <u>Biochemistry</u>, Worth Publishers, Inc., New York, [1970].
- LePecq, Jean-Bernard, "Ethidium Bromide: A Fluorescent Probe of Nucleic Acid Structure and its Potential for <u>In Vivo</u> Studies," <u>Fluorescence Techniques in Cell Biology</u>, Thaer and Sernetz, Springer-Verlag, New York, [1973].
- Lerman, L. S., "Structural Considerations in the Interaction of DNA and Acridines," J. Mol. Biol., Vol. 3, p. 18, [1961].
- Lerman, L. S., "The Structure of the DNA-Acridine Complex," Proc. Nat. Acad. Sci., vol. 49, p. 94, [1963].
- Lerman, L. S., "Amino Group Reactivity in DNA-Aminoacridine Complexes," J. Mol. Biol., Vol. 10, p. 367, [1964].
- Levene, P. A. and Simons, H. S., J. Biol. Chem., vol. 65, p. 519, [1925].
- Loeser, Ch. N., West, S. S., and Schoenberg, M. D., "Absorption and Fluorescence Studies on Biological Systems: Nucleic Acid-Dye Complexes," The Anatomical Record, vol. 138, p. 163, [1960].
- MacInnis, J. W. and Uretz, R. B., "Organization of DNA in Dipteran Polytene Chromosomes as Indicated by Polarized Fluorescence Microscopy," Science, vol. 152, p. 689, [1966].
- Mahler, H., "Nucleic Acid Metabolism," <u>Basic Neurochemistry</u>, Albers et al eds. Little and Brown Co., <u>Boston</u>, p. 245, [1972].
- McConnell, J. V. and Shelby, J. M., "Memory Transfer Experiments in Invertebrates," Molecular Mechanisms in Memory and Learning, Unger, ed., Plenum Press, New York, [1970].

- McGaugh, J. L., and Petrinovich, L., "The Effect of Strychnine Sulphate on Maze Learning," Am. J. Psychol., vol. 72, p. 99, [1959].
- McGaugh, J. L., and Petrinovich, L., "Effects of Drugs on Learning and Memory," Intern. Rev. Neurobiol., vol. 8, p. 139, [1965].
- Nelson, P. G. and Peacock, J. H., "Acetylcholine Responses in L Cells," Science, vol. 177, p. 1005, [1972].
- Paoletti, C., and LePecq, J. B., Lehman, I. R., "The Use of Ethidium Bromide-Circular DNA Complexes for the Fluorometric Analysis of Breakage and Joining of DNA," J. Mol. Biol., vol. 55, p. 75, [1971].
- Rigler, Rudoff, "Microfluorometric Characterization of Intracellular Nucleic Acids and Nucleoproteins by Acridine Orange," Acta Physiologia Scandinavia, Suppl. 267, p. 67, [1966].
- Rosenblatt, F., "Induction of Behavior in Mammalian Brain Extracts,"

 Molecular Mechanisms in Memory and Learning, Unger, ed., Plenum
 Press, New York [1970].
- St. Pierre, N., Biophysics Dept., Michigan State University, East Lansing, Michigan [1972].
- Seeds, Nicholas W., "Biochemical Differentiation in Reaggregating Brain Cell Culture," Proc. Nat. Acad. Sci., vol. 68, p. 1858, [1971].
- Sobkowica, H. M., Hartmann, H. A., Morzain, R. and Desnoyers, P., "Growth Differentiation and Ribonucleic Acid Content of the Fetal Rat Spinal Ganglion Cells in Culture," J. Comp. Neurol., vol. 148, p. 249, [1973].
- Stevens, W., Lang, R. F. and Schneebeli, G., "Acridine Orange Fluorescence for Differentiating Clean Nuclei from Nuclei with Adherent Cytoplasm in Fractionated Cells," Stain Technology, vol. 44, p. 211, [1969].
- Stryer, Lubert, "Fluorescence Spectroscopy of Proteins," Science, vol. 162, p. 526, [1968].
- Tao, T., Nelson, J. H., Cantor, Ch. R., "Conformational Studies on Transfer Ribonucleic Acid: Fluorescence Lifetime and Nanosecond Depolarization Measurements on Bound Ethidium Bromide," Biochem., Vol. 9, p. 3514, [1970].
- Unger, G., "Role of Proteins and Peptides in Learning and Memory,"

 Molecular Mechanisms in Memory and Learning, ed. G. Unger, Plenum

 Press, New York, [1970].
- Vatter, A. E. and Seeds, N. W., "Synaptogenesis in Reaggregating Brain Cell Culture," Proc. Nat. Acad. Sci., vol. 68, p. 3219, [1971].

- Washizu, Y., Bonewell, G. W., and Terzuolo, C. A., "Effect of Strychnine Upon the Electrical Activity of an Isolated Nerve Cell," Science, vol. 133, p. 333, [1961].
- Welker, C., Sinha, M. M., "Somatotopic Organization of Sm II Cerebral Neocortex in Albion Rat," Brain Research, vol. 37, pp. 132-136, [1972].
- West, Seymour S., "Fluorescence Microspectrophotometry of Supravitally Stained Cells," Physical Techniques in Biological Research, A. W. Pollister, ed., vol. 3C, Academic Press, New York, pp. 253-321, [1969].
- West, S. and Lorincz, A., "Fluorescent Molecular Probes in Fluorescence Microspectrophotometry and Microspectropolarimetry," Fluorescence Techniques in Cell Biology, ed. A. A. Thaer and M. Sernetz, Springer-Verlag, New York, [1973].
- Zanker, V., "Uber den Nachweis definierter reversibler Assoziate ("reversibler Polymerisate") des Acridinorange durch Absorptions und Fluoreszenzmessingen in wassriger Losung, "Z. Phys. Chem., vol. 199, pp. 225-258, [1952a].
- Zanker, V., "Quantitative Absorptions--und Emissionsmessungen am Acridinorangekation bei Normal--und Fieftemperaturen im organischen Losungemittel un ihr Beitrag zur Deutung des Metachromatischen Fluoreszenzproblemes," Z. Phys. Chem., vol. 200, pp. 250-292, [1952b].
- Zanker, V., Held, M. and Rammensee, H., "Neuere Ergebnisse der Absorptions Fluoreszenz und Fluoreszenz Polarisationsgrad Messungen am Acridinorange Kation, ein weiterer Beitrag zum Metachromasie Problem dieses Vitalfarbstoffs," Z. Naturforschg, vol. 14b, pp. 789-801, [1959].
- Zeiger, K. and Harders, H., "Uber vitale Fluorochromierung des Nervengewebes," Z. Zelforsch. Mikroskop. Anat., vol. 36, pp. 62-78, [1951].

